



TÉCNICO
LISBOA

POLITECNICO DI TORINO

Department of Environment, Land and Infrastructure Engineering

Master of Science in Petroleum Engineering

**STOCHASTIC HISTORY MATCHING OF CORE FLOODING EXPERIMENTS
ON CARBONATE SAMPLES**

Supervisor(s):

Prof. Francesca Verga

Dr. Costanzo Peter

Candidate:

KAMA'AN GEOFFREY JALO

S252863

External Supervisors :

Prof. Leonardo Azevedo

Prof. Gustavo Paneiro

FEBRUARY 2019

Thesis submitted in compliance with the requirements for the Master of Science degree

DEDICATION

I dedicate this work to God Almighty and to my Father who always supports my dreams and

To my mother whose fervent/relentless prayers brought me till far.

ACKNOWLEDGEMENT

Firstly, I want to thank God Almighty for his grace and favour that gave me the ability to start and finish this thesis work in good health and vitality.

I would like to thank Politecnico di torino and Instituto Superior Tecnico (Lisbon) for giving me this opportunity to execute this project. I am grateful to my thesis supervisor in the person of Professor Verga Francesca and Dr Peter Costanzo my tutor for their guidance and contribution throughout the course of this work.

My profound gratitude goes also to Professor Leonardo Azevedo and Professor Gustavo Paniero at the Center for Natural Resources and Environment (CERENA), Instituto Superior Tecnico, Lisbon, Portugal, for providing me with this wonderful thesis opportunity to conduct the experimental work at the laboratory of the Institute. The precious gift of their time to answer my many concerns regarding the results was admirable and highly appreciated. They kept their office doors open at all time with so much interest and enthusiasm in my work. Thank you so much, i am very appreciate of this sacrifice.

A special thanks also goes to Mr. Rueben Nunes, a PhD student in Geostatistics who also coached me extensively on geostatistical modelling and took time to explain the Geostatistical History Matching one on one.

Many thanks goes to Mr Tosin Fabusuyi also a PhD student of reservoir Engineering for his enormous support and lectures on Reservoir Numerical Modeling, for the opportunity to attend the reservoir lectures and learn the basics of writing the numerical model data file and interpretations.

My thanks goes Mr Ferdinandes, the research scientist who was always present to assist me with cutting the core plugs for the experiment. Without his assistance and zealousness to readily proffer help when needed, this work would not have been a success.

Furthermore, I thank my Parents, Mr and Mrs Geoffrey Jalo who believed in me and always encouraged me throughout this Masters program, also, I am grateful to my fiancé Mr Yusuf Mshelia, for his encouragement to keep thriving, to my friends, Happy Aminu, Blessing Ogwuke, Nancy Adams, Anthony Ndackson, Falinyi Johnson, Braimoh Joshua and Homtapwa Raymond for their support, love and encouragement throughout the course of this thesis work. Their presence in my life always kept me going and pushing on to the finish point of this work.

Finally, I would also like to acknowledge the input of my mother, Mrs Miriam Geoffrey Jalo for her fervent and consistent prayers on my life to always succeed in my life endeavours, she has always been my anchor.

NOMENCLATURE

SYMBOLS

μ - Viscosity

α - dipping angle

θ - Interfacial angle

ρ_o - Density of oil

λ - Mobility

ρ_o - Oil Density

σ - Interfacial tension

ΔP - pressure difference across capillary tube

ΔL - Change in Length

E - Overall recovery efficiency

ABBREVIATIONS

K_{rw} - Relative Permeability to water

K_{ro} - Relative Permeability to Oil

P_c - Capillary Pressure

P_{nw} - Pressure of non-wetting fluid

P_w - Pressure of wetting fluid

Q -Volumetric Flow Rate

S_o - Oil saturation

S_w - Water saturation

S_{or} - Residual Oil Saturation

S_{wi} - Irreducible Water Saturation

T-Temperature

t - Time

V - Velocity

V_o - Volume of oil in rock

V_b - Bulk Volume

V_v - Pore Volume

OOIP - Original oil in place

EOR - Enhanced Oil Recovery

H - Height of the column

M - Mobility

PV -Pore Volume

PVT - Pressure, volume and temperature relation

API - American Petroleum Institute

IFT - Interfacial Tension

PSO - Particle Swarm Optimization Algorithm

RF - Random Forest

IOR- Improved Oil Recovery

FPR- Field Pressure

FOPR- Field Oil Production Rate

FWPR- Field Water Production Rate

Table of Contents

| | |
|--|------|
| DEDICATION..... | i |
| ACKNOWLEDGEMENT..... | iii |
| NOMENCLATURE..... | iv |
| SYMBOLS..... | iv |
| ABBREVIATIONS..... | iv |
| Table of Figures..... | vii |
| APPENDIX A..... | viii |
| List of Tables..... | ix |
| ABSTRACT..... | x |
| 1.0 INTRODUCTION..... | 1 |
| 1.1 Context and Motivation..... | 1 |
| 1.3 Thesis Organization..... | 3 |
| 1.4 Study Goals and Objectives..... | 5 |
| 2.0 LITERATURE REVIEW..... | 6 |
| 2.1 Background..... | 6 |
| 2.2 Geological properties of the Samples used..... | 6 |
| 2.3 Enhanced Oil Recovery (EOR)/ Improve Oil Recovery (IOR)..... | 7 |
| 2.4 Core Flooding..... | 8 |
| 2.4.1 Uncertainties and Constraints..... | 8 |
| 2.4.2 Reservoir Fluid properties..... | 9 |
| 2.4.3 Rock-Fluid Interaction..... | 10 |
| 2. 4.4 EFFECT OF WETTABILITY ON RELATIVE PERMESABILITY..... | 12 |
| 2. 4.5 Effect of Ageing on the coreflooding..... | 14 |
| 2.5. Numerical Simulations..... | 15 |
| 2.6 Assisted History Matching..... | 16 |
| 2.7 Particle Swarm Optimization (PSO)..... | 17 |
| 3.0 Methodology..... | 19 |
| 3.1.0 Experimental Coreflooding..... | 19 |
| 3.1.1 Materials and Set up..... | 20 |
| 3.1.2 Experimental Procedure..... | 22 |
| 3.1.3 Waterflooding..... | 24 |
| 3.1.4 Waterflooding with two weeks old ageing..... | 28 |
| 3.2 Fluid Flow Dynamics Simulations..... | 28 |
| 3.2.1 Reservoir Simulation..... | 28 |

| | |
|--|----|
| 3.3 Evolution of Pressure over time | 30 |
| 3.4 History Matching with Stochastic Adaptive Particle Swarm Optimization..... | 36 |
| 3.4.1 Homogeneous Reservoir Model:..... | 37 |
| 3.4.2 Heterogeneous Reservoir Model: | 39 |
| 4.0 Results and Discussions | 41 |
| 4.1 Laboratory Experiments Results..... | 41 |
| 4.1.1 Pressure versus time plot for all samples..... | 41 |
| 4.1.2 Results of the production rate versus time..... | 42 |
| 4.1.3 Recovery Factor..... | 42 |
| 4.2 MODEL DESCRIPTION..... | 43 |
| 4.2.1 STATIC MODEL..... | 43 |
| 4.2.2 Dynamic Model..... | 44 |
| 4.3.0 History Matching of the Homogeneous Reservoir Model..... | 45 |
| 4.4 History Matching of the Heterogeneous Reservoir Model. | 47 |
| 4.5 Spatial Distribution of Permeability..... | 52 |
| 4.6 Spatial Distribution of Porosity | 53 |
| 5.0 Conclusion and Recommendation..... | 56 |
| 5.1 Recommendation..... | 57 |
| <i>Works Cited</i> | 58 |
| APPENDIX A: Laboratory experiment results: | 62 |
| APPENDIX B: Production Rate for all the samples..... | 64 |
| APPENDIX C: FLUID FLOW SIMULATION PLOTS..... | 66 |
| APPENDIX D: History Matching Results for Homogeneous system..... | 68 |
| APPENDIX E: History Matching Results for Heterogeneous System..... | 71 |

Table of Figures

| | |
|--|-----------|
| FIGURE 1 : GEOGRAPHICAL LOCATION OF THE SAMPLE UNDER STUDY [6]. | 7 |
| FIGURE 2: PLANE VIEW, CROSS SECTIONAL VIEW AND FLUID DISTRIBUTION IN A HYPOTHETICAL WATER WET, OIL – WET AND FRACTIONAL – WET PORE | 11 |
| FIGURE 3: EFFECT OF WETTABILITY ON THE RELATIVE PERMEABILITY OF A ROCK/OIL/BRINE SYSTEM (FROM RAZA ET AL. [27]) | 13 |
| FIGURE 4: SHOWING THE METHODOLOGY FOR THE STOCHASTIC ADAPTIVE HISTORY MATCHING. | 19 |
| FIGURE 5: THE CORE DRILL | 20 |
| FIGURE 6: MATRIX FROM WHICH CORE PLUGS ARE DRILLED FROM | 20 |
| FIGURE 7: SHOWING ALL THE CORE PLUGS USED FOR THIS STUDY. | 21 |
| FIGURE 8: A DIGITAL CALIPER | 21 |
| FIGURE 9: HASSLER CORE HOLDER | 22 |
| FIGURE 10: INTERNAL VIEW OF THE HASSLER CORE HOLDER. | 22 |
| FIGURE 11: DCP50 PUMP | 22 |
| FIGURE 12: SCHEMATIC REPRESENTATION OF THE EXPERIMENTAL SETUP [48] | 25 |
| FIGURE 13: THE 3D MODEL OF K1 SAMPLE ALONG THE Z DIRECTION | 29 |
| FIGURE 14: PRESSURE EVOLUTION AT TIMESTEP 1. | 30 |
| FIGURE 15 : PRESSURE EVOLUTION AT TIMESTEP 2 | 30 |
| FIGURE 16: PRESSURE EVOLUTION AT TIMESTEP 3 | 31 |
| FIGURE 17: PRESSURE EVOLUTION AT TIMESTEP 4 | 31 |
| FIGURE 18: PRESSURE EVOLUTION AT TIMESTEP 5 | 32 |
| FIGURE 19: PRESSURE EVOLUTION AT TIMESTEP 6 | 32 |
| FIGURE 20: PRESSURE EVOLUTION AT TIMESTEP 7 | 33 |
| FIGURE 21: PRESSURE EVOLUTION AT TIMESTEP 8 | 33 |
| FIGURE 22: PRESSURE EVOLUTION AT TIMESTEP 9 | 34 |
| FIGURE 23: PRESSURE EVOLUTION AT TIMESTEP 10 | 34 |
| FIGURE 24: PRESSURE EVOLUTION AT TIMESTEP 11 | 35 |
| FIGURE 25: PRESSURE EVOLUTION AT TIMESTEP 12 | 35 |
| FIGURE 26: PRESSURE EVOLUTION AT TIMESTEP 13 | 36 |
| FIGURE 27 : THE PRODUCTION HISTORY FOR THE K1 SAMPLE | 38 |
| FIGURE 28: PRESSURE VERSUS TIME PLOT FROM LABORATORY EXPERIMENT. | 41 |
| FIGURE 29: PRODUCTION RATE VERSUS TIME FROM LABORATORY EXPERIMENT | 42 |
| FIGURE 30 : STATIC MODEL REPRESENTATION OF THE CYLINDRICAL CORE | 43 |
| FIGURE 31: A GRAPHICAL REPRESENTATION OF THE MODEL. | 44 |
| FIGURE 32: PRODUCTION HISTORY OF THE SAMPLE K1 | 45 |
| FIGURE 33: A GOOD HISTORY MATCH FOR THE K1 SAMPLE. | 46 |
| FIGURE 34: RESULTS OF THE MISFIT COMPONENT FOR BOTH THE FOPR AND THE FWPR | 46 |
| FIGURE 35: A PLOT OF PARAMETER (POROSITY AND PERMEABILITY) VERSUS ITERATION | 47 |
| FIGURE 36: A GOOD HISTORY MATCH FOR THE K1 HETEROGENEOUS MODE. | 48 |
| FIGURE 37: RESULTS OF THE MISFIT COMPONENT FOR BOTH THE FOPR AND THE FWPR | 48 |
| FIGURE 38: POROSITY VERSUS ITERATION FOR THE FIRST 3 VALUES. | 49 |
| FIGURE 39: POROSITY VERSUS ITERATION FOR 3- 5 | 49 |
| FIGURE 40: POROSITY VERSUS ITERATION FOR 6- 5 | 50 |
| FIGURE 41: POROSITY VERSUS ITERATION FOR 9 | 50 |
| FIGURE 42: PERMEABILITY VERSUS ITERATION FOR NUMBER 1 AND 10 | 50 |
| FIGURE 43: PERMEABILITY VERSUS ITERATION FOR 2-4 | 51 |
| FIGURE 44: PERMEABILITY VERSUS ITERATION FOR 5 – 7 | 51 |
| FIGURE 45: PERMEABILITY VERSUS ITERATION FOR 8- 9 | 51 |
| FIGURE 46: SPATIAL DISTRIBUTION OF POROSITY IN SAMPLE K1 | 52 |
| FIGURE 47: SPATIAL DISTRIBUTION OF PERMEABILITY IN SAMPLE K2 | 52 |
| FIGURE 48: SPATIAL DISTRIBUTION OF PERMEABILITY IN SAMPLE K3 | 53 |
| FIGURE 49: SPATIAL DISTRIBUTION OF PERMEABILITY IN SAMPLE K4 | 53 |
| FIGURE 50: SPATIAL DISTRIBUTION OF POROSITY IN SAMPLE K1 | 54 |
| FIGURE 51: SPATIAL DISTRIBUTION OF POROSITY IN SAMPLE K2 | 54 |
| FIGURE 52: SPATIAL DISTRIBUTION OF POROSITY IN SAMPLE K3 | 54 |
| FIGURE 53: SPATIAL DISTRIBUTION OF POROSITY IN SAMPLE K4 | 55 |

APPENDIX A

| | |
|--|----|
| FIGURE A 1: PRESSURE VERSUS TIME PLOT FOR SAMPLES | 62 |
| FIGURE A 2: PRESSURE VERSUS TIME PLOT FOR K2 SAMPLE..... | 62 |
| FIGURE A 3: PRESSURE VERSUS TIME..... | 63 |

APPENDIX B

| | |
|--|----|
| FIGURE B 1: PRODUCTION RATE VERSUS TIME FOR K1 SAMPLES | 64 |
| FIGURE B 2: PRODUCTION RATE VERSUS TIME FOR K2 SAMPLE | 64 |
| FIGURE B 3: PRODUCTION RATE VERSUS TIME FOR K3 SAMPLE | 65 |
| FIGURE B 4: PRODUCTION RATE VERSUS TIME FOR SAMPLE K4..... | 65 |

APPENDIX C

| | |
|--|----|
| FIGURE C 1; PRODUCTION HISTORY PLOT OVER TIME (FOPR, FPR AND FWPR) FOR K1 SAMPLE | 66 |
| FIGURE C 2: PRODUCTION HISTORY PLOT OVER TIME (FOPR, FPR AND FWPR) FOR K2 SAMPLE | 66 |
| FIGURE C 3: PRODUCTION HISTORY PLOT OVER TIME (FOPR, FPR AND FWPR) FOR K3 SAMPLE | 67 |
| FIGURE C 4: PRODUCTION HISTORY PLOT OVER TIME (FOPR, FPR AND FWPR) FOR K4 SAMPLE | 67 |

APPENDIX D

| | |
|---|----|
| FIGURE D 1: BEST FIT MATCH FOR SAMPLE K1 | 68 |
| FIGURE D 2: MISFIT COMPONENT OF THE FOPR AND FWPR FOR SAMPLE K1 | 68 |
| FIGURE D 3: PARAMETER (POROSITY AND PERMEABILITY) VERSUS ITERATION FOR SAMPLE K1 | 68 |
| FIGURE D 4: BEST FIT HISTORY MATCH FOR SAMPLE K2..... | 69 |
| FIGURE D 5: MISFIT COMPONENT FOR SAMPLE K2 | 69 |
| FIGURE D 6: PARAMETER (POROSITY AND PERMEABILITY) VERSUS ITERATION FOR SAMPLE K2 | 69 |
| FIGURE D 7: BEST FIT HISTORY MATCH FOR HOMOGENEOUS K3 SAMPLE | 70 |
| FIGURE D 8: MISFIT COMPONENT VERSUS ITERATION FOR HOMOGENEOUS K3 SAMPLE..... | 70 |
| FIGURE D 9: PARAMETER (POROSITY AND PERMEABILITY) VERSUS ITERATION FOR HOMOGENEOUS K3 SAMPLE | 70 |
| FIGURE D 10: BEST FIT HISTORY MATCHING FOR HOMOGENEOUS K4 SAMPLE..... | 71 |
| FIGURE D 11: MISFIT COMPONENT FOR HOMOGENEOUS K4 SAMPLE | 71 |
| FIGURE D 12: PARAMETER (POROSITY AND PERMEABILITY) VERSUS ITERATION FOR HOMOGENEOUS K4 SAMPLE | 71 |

APPENDIX E

| | |
|---|----|
| FIGURE E 1: BEST FIT HISTORY MATCHING FOR HETEROGENEOUS K4 SAMPLE | 72 |
| FIGURE E 2: MISFIT COMPONENT FOR HETEROGENEOUS K4 SAMPLE | 72 |
| FIGURE E 3: PARAMETER (POROSITY) VERSUS ITERATION FOR HETEROGENEOUS K4 SAMPLE..... | 72 |
| FIGURE E 4: PARAMETER (POROSITY) VERSUS ITERATION FOR HETEROGENEOUS K4 SAMPLE..... | 72 |
| FIGURE E 5: PARAMETER (POROSITY) VERSUS ITERATION FOR HETEROGENEOUS K4 SAMPLE | 73 |
| FIGURE E 6: PARAMETER (POROSITY) VERSUS ITERATION FOR HETEROGENEOUS K4 SAMPLE..... | 73 |
| FIGURE E 7: PARAMETER (PERMEABILITY) VERSUS ITERATION FOR HETEROGENEOUS K4 SAMPLE..... | 73 |
| FIGURE E 8: PARAMETER (PERMEABILITY) VERSUS ITERATION FOR HETEROGENEOUS K4 SAMPLE..... | 73 |
| FIGURE E 9: PARAMETER (PERMEABILITY) VERSUS ITERATION FOR HETEROGENEOUS K4 SAMPLE..... | 74 |
| FIGURE E 10: PARAMETER (PERMEABILITY) VERSUS ITERATION FOR HETEROGENEOUS K4 SAMPLE..... | 74 |

List of Tables

| | |
|--|----|
| TABLE 1: SHOWING THE PROPERTIES OF THE CORE SAMPLES. | 26 |
| TABLE 2 : THE PARAMETERS USED IN THE STOCHASTIC ADAPTIVE HISTORY MATCHING WITH THE PARTICLE SWARM OPTIMIZATION ALGORITHM.. | 39 |
| TABLE 3: THE PARAMETERS USED IN THE STOCHASTIC ADAPTIVE HISTORY MATCHING WITH THE PARTICLE SWARM OPTIMIZATION ALGORITHM. . | 40 |
| TABLE 4: CALCULATED PARAMETERS FROM ROUTINE CORE ANALYSIS (RCAL)..... | 43 |

ABSTRACT

History Matching and uncertainty quantification are two important aspects of modern reservoir engineering studies. Finding multiple History Matching models for uncertainty quantification with minimum/lowest misfit is one of the focus of this research in Assisted History Matching methods (AHM).

In this paper, the laboratory coreflooding analysis on representative reservoir rock samples (particularly carbonate rocks); and translating them into a real reservoir scenario through numerical modelling of reservoir coupling stochastic History Matching using the Laboratory results to reduce the uncertainty in porosity and permeability of the carbonate rocks was the key focus of this thesis.

The study goals and objectives of this research is to perform a laboratory experiment on carbonate rocks and find their fluid saturation and the residual oil saturation, permeability and porosity values, the pressure values which can be used in the numerical simulations. The potential of Improved Oil Recovery (IOR) on carbonate rock samples by low salinity (brine) coreflooding has been investigated through both the laboratory measurement and the fluid flow simulation. Results show that both investigations indicated that the potential is high as it can be seen from the Oil Recovery which was between 38% - 42% percentage and this is reasonable for a secondary recovery coreflooding with brine. Ageing done on sample K4 shows that ageing increases the oil recovery during water coreflooding and aged samples provided the best History match result with the best misfit. The Assisted History Matching (AHM) method used raven epistemy software which enabled a more fast and reliable process. The History Match parameters for the production history from numerical modelling and from the laboratory experiments of hours of pressure build up test produces nearly identical effective reservoir permeability of 0.01 - 0.02mD and 0.146mD, therefore, we can conclude that there is a presence of interconnected micro-fractures as the main contributing factors. Using the Particle Swarm Optimization Algorithm (PSO), a lower misfit provides a better match of the production history and also, the sampling behavior of the optimization algorithm has a direct impact

on the prediction/forecast. For a heterogeneous Model, using higher particle number and a higher iteration provides more realistic results and gives a better understanding of the result because the convergence can occur at a higher iteration. Uncertainty Quantification using stochastic - Particle Swarm Optimization Algorithm seems to be a good approach for predicting and forecasting models in the Reservoir modelling field.

Finally, the uncertainty quantification in porosity and permeability obtained from laboratory experiments where these uncertainties were optimized through a Stochastic History Matching using Particle Swarm Optimization Algorithm (PSO), also shows that given a heterogeneous system, the best misfit provided results of the spatial distribution of permeability and porosity of close range to the values from the laboratory results.

KEYWORDS: *Assisted History Matching (AHM), Carbonate rock, Coreflooding, Numerical Simulations, Particle Swarm Optimization Algorithm, Permeability, Porosity, Uncertainty quantification.*

CHAPTER ONE (1)

1.0 INTRODUCTION

1.1 Context and Motivation

The experimental work conducted in this thesis is a research and investigation on the secondary oil recovery by the process Waterflooding basically in carbonated (limestone) rocks. It was fully carried out in the laboratory at the Center for Natural Resources and Environment (CERENA), Instituto Superior Tecnico, Lisbon, Portugal. The experiments are performed on different Carbonate Rock core samples – a coreflooding experiment. Experimental coreflooding have shown to be a significant tool for decades of research in oil exploration and production. Accurate and high quality coreflooding results are integral part for reservoir performance prediction and effective reservoir management.

Apparently, it is not an easy task to achieve or obtain high quality coreflooding results in the laboratory. It is also very important to note that coreflooding is not cost effective at the same time it is time consuming - and most times, the results have uncertainties associated with it. These uncertainties can come from instrumental errors, manual errors, and lack of correct representation of the rock, fluid or reservoir conditions.

Reservoir simulation models can improve reservoir performance and enhance hydrocarbon recovery mechanisms [1]. Numerous mathematical methods have been developed for handling nonlinear problems and to solve critical reservoir simulation models. In field applications, most models assume linearized conditions and ignore the inherent reservoir complexities [2]. Also, to predict the behavior of a given Hydrocarbon, there is a need to understand how fluid flows within the reservoir rock and consistently integrate this information within the modelling procedures. Using the experimental data acquired, it is possible to build a numerical mathematical model for the core and hence use the model to perform a simulation in terms of History Matching and possibly predict future forecast production.

To adequately improve the hydrocarbon recovery from an existing field, the capability of the engineer to quickly and accurately perform reservoir simulations to evaluate different improved oil recovery scenarios is very vital. Notably, these numerical simulations require input parameters such as relative permeability's, capillary pressures, and other rock and fluid properties, porosity versus permeability trends. These parameters are typically derived from Routine Core Analysis (RCAL) tests carried out in the laboratory.

Upon completion of the Numerical simulation on Eclipse, there is need for a Stochastic History Matching. In this thesis an Assisted History Matching was conducted on all samples using Particle Swarm Optimization Algorithm. This part of the thesis was conducted using Raven Epistemy which retrieve information from Eclipse and optimize it for a better History Match reducing the uncertainty in the values of permeability and porosity both in the homogeneous and heterogeneous reservoir models being studied.

The oil industry worldwide is currently faced with the pressing challenge to increase well productivity as the demand for oil and gas is increasing. The consumption rate of petroleum and other liquid fuels across the globe is on a high rise and on the other hand, discovery of new oil fields is very limited [3]. EIA in 2016 reported that the global petroleum and other liquid fuel consumption averaged 96.9 million barrels per day and the consumption has increased by 1.6 million barrels per day in 2018 [3]. Most of the reservoirs are now at matured state with low well productivity. Some reservoirs or reserves are large with majorly heavy oil or Bitumen and thus can only be produced through enhanced oil recovery (EOR) mechanism while some have huge oil but the energy of the system (reservoir) cannot support the production of the oil, therefore, Secondary Recovery of Oil has to be employed to maximize the production [4].

Due to this high demand of petroleum and liquid fuels, Petroleum Engineers and researchers have been working to increase productivity using the most cost effective and most stable techniques. Concerning production, the recovery of oil is one of the major challenges encountered by reservoir

engineers. Most times, the primary recovery which involves production of Hydrocarbon under the natural driving mechanisms present in the reservoir (the energy of the system) without any support from injecting other fluids (gas, or water) is not sufficient enough to give a high recovery of oil during production. Thus, the use of the secondary recovery is initiated.

Secondary recovery involves the injection of water or immiscible gas in order to induce a pressure that can enhance the recovery of oil [4]. Waterflooding is one of the most common methods of secondary recovery. Thomas, Mahoney, and Winter (1989) pointed out that in determining the suitability of a candidate reservoir for waterflooding, the following reservoir characteristics must be considered, these factors includes reservoir geometry, depth, lithology, fluid properties (viscosity of the oil, the oil viscosity is important because it helps in determining the mobility ratio which in turn controls the sweep efficiency) and rock properties, fluid saturations [5]. Before any improved recovery production is carried, the engineers perform Reservoir simulations (as much as possible to ascertain the best model with the Highest Recovery). Reservoir simulation models can improve reservoir performance and enhance hydrocarbon recovery mechanisms [2]. Also, to predict the behavior of a given Hydrocarbon Reservoir, it demands understanding how fluid flows within the reservoir rock and consistently integrating this information within the modelling procedure.

The focus of this thesis is on the laboratory coreflooding analysis on representative reservoir rock samples (particularly carbonate rocks); and translating them into a real reservoir scenario through numerical modelling of reservoir coupling stochastic History Matching using the Laboratory results to reduce the uncertainty in porosity and permeability of the carbonate rocks.

1.3 Thesis Organization

Chapter one (1) investigates the background of Oil Recovery techniques and the overall background of the study. Here the reason for indulging in improved oil recovery is discussed and also, the importance of having several

simulations of the recovery before the field operation in order to avoid errors which can high risk on the organization if not done correctly. The core flooding experiment at the lab scale is discussed and the fluid flow was considered also.

Chapter two (2) deals with a Literature review on past works on some methodology involved in this Conventional Improved Oil Recovery (IOR), the numerical simulations and many more as reported in the various sections were considered. Specifically, sections 2.2 covered the Geological properties of the Samples used, 2.3 discussed extensively the goals of the Improved Oil Recovery. Section 2.4 Core Flooding: where the main objectives of core flooding was reviewed which are the measurement of saturation, absolute and relative permeability's of the rock samples and the interaction of the fluid or the rock fluid interaction. Section 2.4.1 Uncertainties and Constraints: the uncertainties associated with the coreflooding experiments are highlighted here also.

Section 2.4.2 Reservoir Fluid properties, are explored in this section and we also looked at the impact of temperature on the fluid properties during coreflooding.

Section 2.4.3 Rock-Fluid Interaction; this is where we analyzed the effect of wettability on the interaction of the rock and the fluids and we noted the impact of the change of fluid wettability through the change in viscosity or temperature. Few factors affecting the wettability during coreflooding test were also reported in this section.

Section 2.4.5 Effect of Ageing on the coreflooding, Section 2.5 Numerical Simulations; the importance of reservoir Numerical simulation models are explored here, and the particular method used in the Numerical Simulations. Section 2.6 Assisted History Matching; here the Particle Swarm Optimization Algorithm was reported and examined critically.

Chapter three (3) cover the main work done in this project and it includes the Methodology; experimental apparatus and procedure, including the fluids, chemicals and material used for the experimental setup. The Numerical

Simulation and Stochastic History Matching of the Laboratory experiment in the coreflooding are all incorporated in this chapter.

Chapter four (4) outlines the results of the laboratory experiments, the simulation results and the results from the Stochastic History Matching and discussions of those results all are discussed in this chapter.

Chapter five (5) lays conclusion on the work with some possible recommendations for future works.

1.4 Study Goals and Objectives

The study goals and objectives of this research is to perform a laboratory experiment on carbonate rocks and find their fluid saturation and the residual oil saturation, permeability and porosity values, the pressure values which can be used in the numerical simulations. Another objective of this study is to quantify the uncertainties in porosity and permeability obtained from laboratory experiments and also optimizes the uncertainty through a Stochastic History Matching using Particle Swarm Optimization Algorithm.

CHAPTER TWO (2)

2.0 LITERATURE REVIEW

2.1 Background

The oil industry worldwide is currently faced with pressing challenges to increase well productivity as the demand for oil and gas is increasing. The consumption rate of oil across the globe is on the high rise and on the other hand, the discovery of new wells is very limited. Hence mechanism for oil recovery was developed among which Low salinity water injection was explored under the Enhanced oil recovery [3].

More than two centuries ago, oil and gas industry developed and implemented diverse techniques for oil recovery in a nearly depleted or depleted reservoir. Amongst these are the primary (which is induced by the energy of the system), Secondary and the tertiary recovery [3].

2.2 Geological properties of the Samples used

All specimens used for this study belongs to an outcrop which lies in the Lusitanian Basin, placed in the Western Iberian Margin. The accommodation for the sediments in this specific basin was created due to the sequence of rifting events that generated the opening of the North Atlantic Ocean [6]. The outcrop selected for use in the experiment belongs to the Middle Jurassic. During the Bathonian (167M.y), the Lusitanian basin was a carbonate ramp depositional system [6]. Ferreira et al reported that the units were mainly deposited in the inner ramp, where the rock specimen used for this study belongs. The crop out topography is a bank of the valley, with an NW-SE fault coincident with a water table [6].

The boundaries where the rock emerges is delimited respectively by the following cities, Leiria, Ourém, Tomar, at North by Torres Novas in the East, by Alcobaça in the West and by Rio Maior in the South. As noted by Ferreira et al, the outcrop was retrieved in Serra dos Candeeiros. The rock is an analogous formation of the Brazilian pre-salt reservoir [6]. The rock is dated from the Middle Jurassic and belongs to Santo António and Candeeiros

Formation, Codaçal member [7]. The author identified three barrier shoreface lithofacies: the first level with oolitic and bio-intraclastic grainstones, second level coarser grained grainstones/rudstones and the third level with coral/algal biostones. Below is the geographical location of the sample used for this thesis.

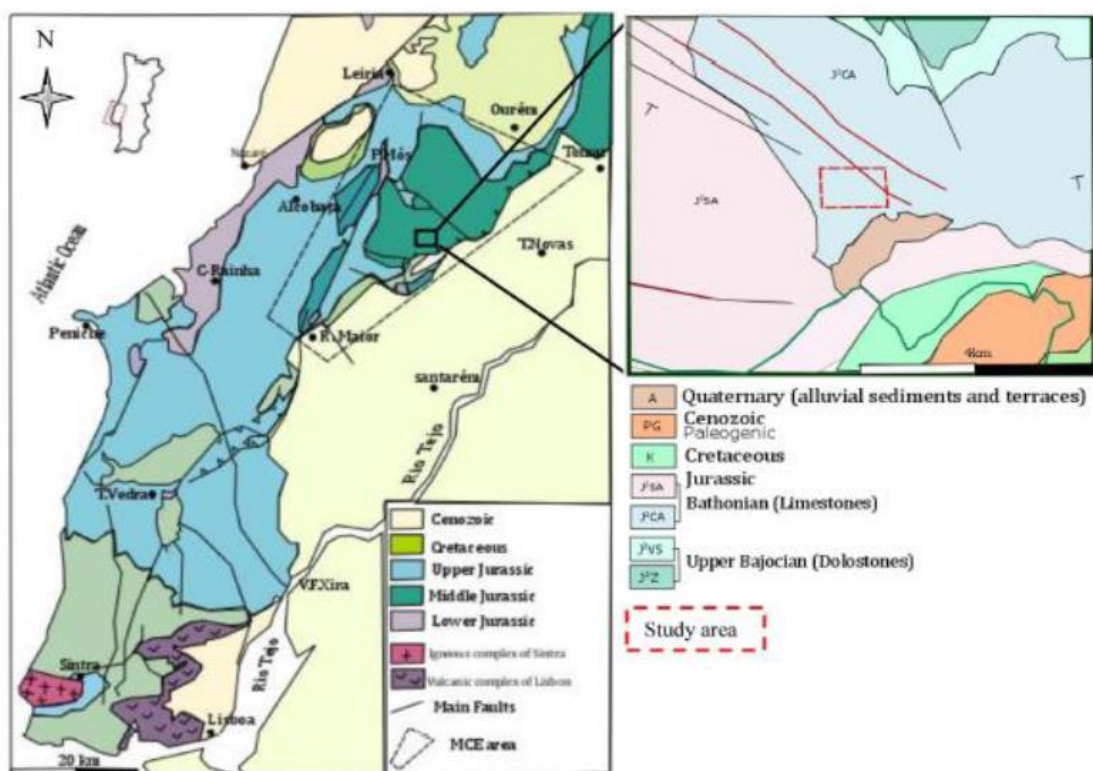


Figure 1 : Geographical location of the sample under study [6].

2.3 Enhanced Oil Recovery (EOR)/ Improve Oil Recovery (IOR)

The improved oil recovery (IOR) is also known as Enhance Oil Recovery (EOR) and also referred to as tertiary recovery. The EOR (tertiary recovery) has an ultimate goal of increasing final oil recovery and reducing the residual oil Saturation by altering the wettability which is a combined function of microscopic and macroscopic efficiencies. Several mechanisms play a major role in the primary production of oil. Primary production in general is known to be rather inadequate, as it only recovers less than 20 % of the original oil in place (OOIP) [8].

The modern Hydrocarbon production method, especially exploration of unconventional oil reservoirs makes the reservoir properties and fluid necessary to be known.

$$\text{Recovery Efficiency}(E_{ro}) = \frac{\text{Commulative oil Produced}}{\text{Original Oil in Place}} \quad (1)$$

The most important goal in Enhanced Oil Recovery (EOR) generally, the EOR processes involve an injection of gas or fluids into the oil reservoir, displacing crude oil from the reservoir towards a production well. The injection processes supplement the natural Reservoir drive present in the reservoir.

2.4 Core Flooding

A Core is a piece of rock from the reservoir under study. The cost of acquiring a rock sample from the reservoir rock is high therefore an outcrop of the reservoir rock is used. These plugs are cut in various shapes but mostly cylindrical shapes and are approximately 1.5inch in diameter and 3.125 inch in length [3]. Core flooding is a laboratory experiment done on reservoir rock plugs (cores) to ascertain the petro physical properties of the oil reservoir rock under study. Main objectives of Coreflooding test is the measurement of saturation, absolute and relative permeability of the Rock sample and also the interaction of the fluid or the rock fluid interaction [2]. Those experimental results is simulated for a large scale of the reservoir in order to determine the expected result for the real low salinity water injection into the reservoir to optimize the production.

2.4.1 Uncertainties and Constraints

Mahesh [9] identified many uncertainties associated with the core flooding. These uncertainties can be

- 1). Condition of the In-situ rock: This can occur during extraction or transportation: the core's petrophysical properties might be modified. Secondly, the evaporation of light components or asphaltenes precipitation will change fluid properties. Also, the cleaning of the plugs and aging can alter rock-fluid interactions (like wettability)

2). Limitations in up-scaling to reservoir level: High geological-variability inside reservoirs increases uncertainty of petrophysical properties extracted from core to large geological area in the reservoir. Also, Up-scaling of EOR methodologies is limited with many external parameters like raw material availability, government rules, economic profitability, on field consistency etc. Finally, there is a huge difference in modeling scale from core to reservoir possesses technical challenges.

3). Experimental Errors: Minor errors from lab setup create high impact on results due to small size of plugs [9]

2.4.2 Reservoir Fluid properties

Afinogenov, suggested that the decrease in Permeability (k), with increase of temperature might be caused partly by a “change in the petro physical properties of the fluid” [10]. It is important to note that by definition, the absolute permeability of a rock is independent of the fluid flowing through it - In reality, obviously there are exceptions in gas flows or clay well swelling during flow of fresh water (Klinkenberg effects) [11]. It is reasonable however, to expect that the temperature sensitivity of fluid properties affect the petro physical parameters describing the multiphase flow of the reservoir. Furthermore, considering the rock fluid interaction, there is possible [12] changes in chemical composition of the fluids as increased temperature, increases the oil – water interfacial tension (σ) and the viscosities of the fluid (oil/water). Since, the interfacial tension of oil-water decreases with increased temperature, the Capillary pressure(P_c) needed to force oil droplet out from the pore neck through a radius (r) during imbibition should decrease, based on the famous relationship of capillary pressure and the radius below [11].

$$P_c = \frac{2\sigma\cos\theta}{r} \quad (2)$$

Where θ is the oil – water –rock contact angle, so therefore if r and θ remains unchanged, the lowering of σ should reduce the volume of trapped oil at the end of the imbibition [11]. Also, Okandan, observed a lower imbibition capillary pressures (at relatively higher water saturation) at elevated

temperatures, but at lower water saturation values, the situation is reversed (that is, P_c is higher at higher temperature) [13].

Now, considering that σ has to be reduced at higher temperature to considerably lower value before any effective oil displacement is observed [14]. Benzagouta on the other hand observe that at a constant effective pressure, the permeability reduction becomes significant at a temperature of 50°C compared to the one obtained at 25°C. This reduction is in a continuous trend up to 100°C but at a lower rate with regards to the previous interval [15].

Notably, Benzagouta added that the reduction in porosity occurred at a different effective pressure levels until reaching the value of 3.75% at a pressure of 4000psi (275.8bar) [8]. Therefore, the reservoir fluid properties also need to be considered before and during a coreflooding experiment.

2.4.3 Rock-Fluid Interaction

It is important to understand the rock fluid interaction between the fluid used and also the rock. Wettability is one interaction that will be considered. Wettability can be defined as the tendency of a fluid to preferentially adhere to, or wet the surface of a rock in the presence of the other immiscible fluids [16]. It is important to note that wettability is used for the wetting preference of the rock and does not necessarily refer to the fluid that is in contact with the rock at any given time. Wettability concept and the locations of oil and connate water in the layer pores can be illustrated with a simple diagram

below.

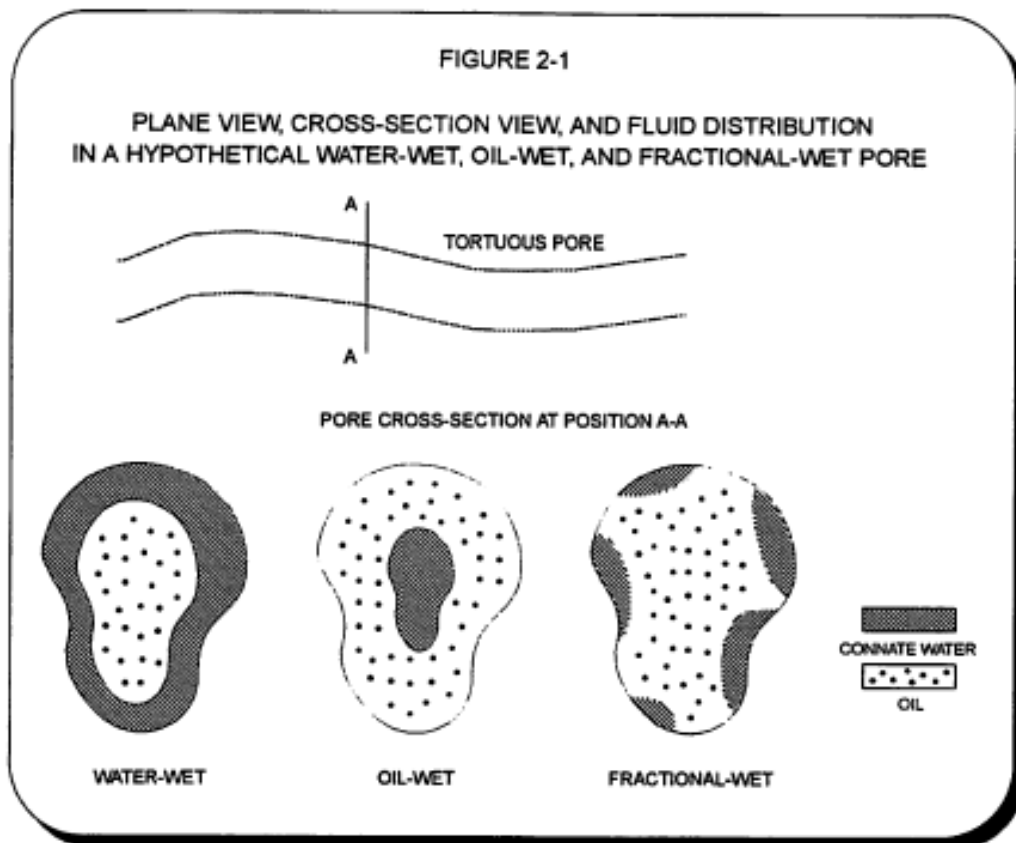


Figure 2: Plane view, cross sectional view and fluid distribution in a hypothetical water wet, oil – wet and fractional – wet pore

It is known that certain polar- nonpolar component of crude oil may get absorbed on rock surfaces and render them Oil-wet. Since such absorbed are thermodynamically unstable, they may be desorbed at elevated temperature and the rock may become water wet [17]. Marsden. S.S., and Ramey H.J. [18], observed that the importance of the change of wettability of a rock fluid system in explaining the observed temperature effects seems to have been over-emphasized in the literature. The importance of the change in the fluid Viscosity or rock matrix properties with temperature has to be considered in this regards [18]. It is generally accepted that the greater water wetness cause greater irreducible water saturation during the displacement studies [18]. If the aforementioned is true, Sinnoket et al, concluded that the sandstone (Carbonate) they studied becomes more water wet at high

temperature. That such a situation becomes possible is reinforced by the work of Poston et al [19] , Okandan [13] and Lo and Mungan [14] who found out that the oil-wet solid contact angle (on a flat surface) which is often taken as a measure of wettability decreases with temperature increase. All these studies reported a contact angle of $9^{\circ} - 46^{\circ}$, with the temperature effect being less than 22°C in all cases [18].

Craig defined Wettability as the tendency of one fluid to spread on or adhere to a solid surface in the presence of the immiscible fluids [20]. However, Anderson defined the wettability for crude oil/brine/rock system as the measure of the preference that the rock has for either the oil or the water [21, 22]. It is very important we understand the wettability of any rock/fluid system because it is the major factor that controls the location, flow and distribution of fluid in the reservoir. It is important to note that wettability is one of the major factors that affect the relative permeability of the brine. Most times, for simplicity sake, we assume the reservoir is uniformly wetted, but in reality it is not. Ugar and Suat, revealed that many reservoir rocks have heterogeneous wettability, where portion of the rock is water –wet while others are Oil – wet, this non-uniform state is called Fractional wettability and is more common to the uniform wettability state [23].

There are some factors that affect the wettability during the core flooding test and are reported as; Properties of the test fluids (salinity), test temperature, ageing time and temperature, and established initial water saturation [24] [8] [25].

Tang and Morrow studied the effect of each parameter and concluded that an increase in the rate of water imbibition translates to increases in water wetness, whereas a decrease in the same parameter results in an increase in oil wetness [25]. JAdhunandan and Morrow conducted 50 slow-rate laboratory waterflood to study the effect of wettability on oil recovery [8].

2. 4.4 EFFECT OF WETTABILITY ON RELATIVE PERMESABILITY

Wettability has an effect on the relative permeability of any reservoir rock. Ugar and Suat mentioned that it affect s the relative permeability by

controlling the flow and spatial distribution of fluids in a porous medium [23]. In strongly wetted rock, the relative permeability of the non-wetting phase is dependent on the saturation path, whereas the relative permeability of the wetting phase is often independent of the path [26]. The relative permeability of the wetting phase is a function only of its own saturation and is not influenced by the direction of saturation change or the nature of the non-wetting phase. At any given saturation, as the degree of rock preferential water wettability decreases, the relative permeability to oil decreases and the relative permeability to water increases, as shown in Figure 2 below [27] .

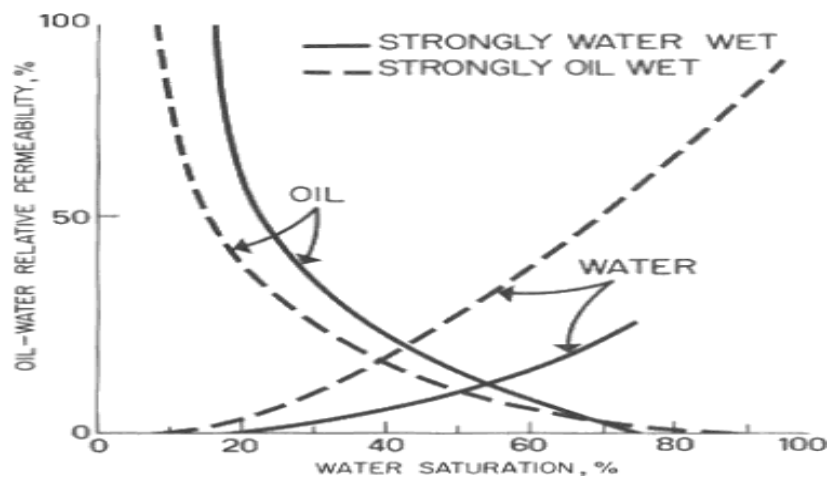


Figure 3: Effect of wettability on the relative permeability of a rock/oil/brine system (from Raza et al. [27])

Dullien et al [22] noted that, although macroscopic- to megascopic reservoir heterogeneities affect waterflood performance, oil displacement occurs at the pore level, and the microscopic displacement mechanisms must be determined. The microscopic efficiency of oil recovery is primarily influenced by the wettability, the saturation history, the viscosity ratio, and the pore structure [22]. It is generally accepted that a waterflood in a strongly water-wet rock is more efficient than that in an oil-wet rock. However, there is less agreement concerning the comparison of the waterflood performance of water-wet and intermediate-wet systems. Some researchers (such as, Owens and Archer [16] and Donaldson and Thomas [28]) noted that oil recovery was reduced as the wettability was changed toward less-water-wet conditions. However, other researchers (such as Graue et al., [29] Ma et al., [30] and Morrow [31]) reported that oil recovery increases as water-wetness decreases

and passes through a maximum when the system has intermediate wettability. Decreasing water - wetness, decreases the value of the end points of the relative permeability curves of the oil significantly [23]

A waterflood in a strongly oil-wet rock is much less efficient than that in a water-wet rock. When the waterflood begins, the water will form continuous channels or fingers through the centers of the larger pores, pushing the oil in front of it, and early water breakthrough occurs [29] [30] [31]. Oil recovery before breakthrough is relatively small, with most of the oil being produced after breakthrough.

The residual oil after the waterflood is found (i) filling the smaller pores, (ii) as a continuous film over the pore surfaces, and (iii) as larger pockets of oil trapped and surrounded by water [8]. Because much of this oil is still continuous through the thin oil films, it may still be produced at a very slow rate. The residual oil saturation is not well-defined. In contrast to the water-wet case, oil recovery is strongly dependent on the volume of water injected [15] [28] [8]. As previously described, a mixed- wettability system has continuous oil-wet paths through the larger pores, whereas the small pores are water- filled. Such a system combines the best aspects of water- wet and oil-wet systems. Compared with a water-wet system, trapping is reduced in the large, oil-wet pores. According to Anderson [14] and Ma et al. [27], in an oil-wet system, trapping is reduced because the small pores in a mixed-wet system are water-filled. When mixed-wet cores are water flooded, film drainage causes very low residual oil saturations. After the injection of many pore volumes (PVs) of water, a small but finite permeability to oil exists, even at very low oil saturations [14] [27].

2. 4.5 Effect of Ageing on the coreflooding

According to Xianmin et al, Oil recovery by waterflooding increases with increase in aging time that leads to a decreased in water wetness for crude oil/brine/rock group [32]. Also it was established that for core plugs with zero ageing time, the water breakthrough was earlier. Initial water saturation is also affected by ageing time- as ageing decreases the initial water

saturation [32]. Another important discovery by Xianmin et al is that recovery by waterflooding and recovery at breakthrough are affected by the ageing time in a direct proportional relationship. Ageing has been carried out in electronic world as can be seen from the works of Kulkarni and Somasundaran where they reported the effect of aging on zeta potential of quartz in aqueous solutions as obtained by streaming potential measurements. Significant changes were observed for as long as about 8 days [33]. Kittaka and Morimoto also showed an increase in surface conductivity with time for silica/aqueous solution systems [34].

However, in the petroleum industry, the common practice of wettability restoration is to clean the reservoir core sample. Jadhunandan stated that the purpose of cleaning is to make the core sample strongly water-wet which is believed to be the initial wetting condition before oil migrated into the reservoir [35]. Grist et al reported that - 19 - prolonged soaking in brine, before flow of oil, made the cores more water-wet. Many scholars have validated the effect of aging on interfacial tension of brine-crude oil systems [36]. The aging effect has shown over the years to be a significant factor in establishing the equilibrium contact angle or adhesion for silica/brine/oil systems [37] [38] [39]. The time factor for equilibration has long been considered in restoring the original wetting condition of reservoir core samples. After establishing the initial water saturations, the core samples were then aged at the reservoir temperature.

2.5. Numerical Simulations

Reservoir simulation models can improve reservoir performance and enhance hydrocarbon recovery mechanisms [1]. Numerous mathematical methods have been developed for handling nonlinear problems and to solve critical reservoir simulation models. In field applications, most models assume linearized conditions and ignore the inherent reservoir complexities [40] [41] [42] [43]. Also, to predict the behavior of a given Hydrocarbon behavior demands understanding how fluid flows within the reservoir rock and consistently integrating this information within the modelling procedure.

Using the experimental data acquired, it is possible to build a numerical mathematical model for the core and hence use the model to perform a simulation in terms of History Matching and possibly predict future forecast production.

Reservoir and pore modelling have same modeling equations, though there are few differences between the pore level simulation and the reservoir simulations model equation. [12]. Currently, there are many pore scale simulators that have been developed worldwide, but the practical use of these simulators is limited due to extreme complexity at micro-scale and difficulties in obtaining data to calibrate these models [9].

In this section, we shall derive basic petro-physical equations used by simulators. Most of the equations are simplified just to oil-water system at isothermal conditions and the eclipse 100 was used which is based on Black composite oil.

2.6 Assisted History Matching

History Matching is an iterative process used to modify a reservoir model to reproduce field behavior. Stochastic optimization most especially the population based algorithm like Particle Swarm Optimization are good for solving History Matching problems because they adaptively search for multiple good models and are less likely to get trapped in local minima [44]. Most case scenarios, uncertainty occurs due to the scarcity of data so the true distribution of facies, porosity and permeability in the system is observed [45]. History Matching entails tuning the properties of the reservoir model in such a way that computer simulations reproduce the observed production rate or pressure measurements available from the wells [44]. As an iterative process, it has a global framework based on minimizing the objective function which quantifies the mismatch between history data and the stimulated data. Also, History Matching is an Inverse problem [44] in which we use the known solution – that is our production data and we try to find the porosity and permeability of the system [45]. History Matching has been one of the most research topics in recent years. Goncalo et al mentioned

that the spatial pattern of porosity and permeability affects the flow response therefore, it is important to consider heterogeneity which is a very key in History Matching [45].

According to Mario et al, multiple History Matched reservoir models are used to quantify uncertainty of future Hydrocarbon production from a field. [46].

2.7 Particle Swarm Optimization (PSO)

The Particle Swarm Optimization (PSO) is a stochastic optimization technique inspired by the social behavior of the bird flocking or fish schooling. A schematic representation of the Assisted History Matching is shown in the figure below. The assisted history Matching is done by creating a project and a new study where we setup the study name and the simulator which is the Eclipse100 to ensure that the model and the files are compatible with each other. Then we proceed to set up the file for history Matching and the optimization, we then configure the model by importing the main data for our reservoir model. In the data file imported the main parameters (permeability and Porosity) values are replaced with dollar sign followed by the name (\$b and \$a respectively). The defined parameters (porosity and permeability) are given a range of uniform distribution for the sampling algorithm. Next is to set up the history data and we use the "OBS"- the JAVA extension and the file is imported into Raven and the sigma is also set up. An objective function specifies the response of each model as a mathematical measure of how close the model output is to the observed production data and they are the variables used for the optimization or misfit calculation. The single objective problem was used because the multiple objective function is complex for this case study. At the initial stage of the particle swarm optimization, there is a random initialization of a swarm of particles in the search space. PSO memorizes the best previous solution and the particles are positioned at initial parameter values by random generation. We set 500 iterations in the Raven software for a homogenous system and for heterogeneous system, we used 1500 iterations. Once, the second iteration produce better misfit than the previous locations or the overall, the PSO memorizes that new locations and the next iterations continues. The particle

keep moving to the new locations until there is a convergence over the defined iterations and generate the best misfit value which is then used to input into tNavigator for the final assessment of the overall reservoir model in terms of porosity and permeability values, the evolution of water saturation and pressure throughout the system over the entire time steps are all analyzed from tNavigator using the best misfit results.

There are different algorithm used in History Matching, these includes Ant Colony Optimization, Differential Evolution, Particle Swarm Optimization and the Neighborhood Algorithm.

CHAPTER THREE (3)

METHODOLOGY

3.0 Methodology

This chapter focuses on the methods followed throughout the entire period of this thesis work from the laboratory experiment of the water coreflooding down to the stochastic History Matching. Below is a summary of the process followed throughout the thesis. The first step is the laboratory experiment of the coreflooding in order to get the prior knowledge about the reservoir for the model creation.

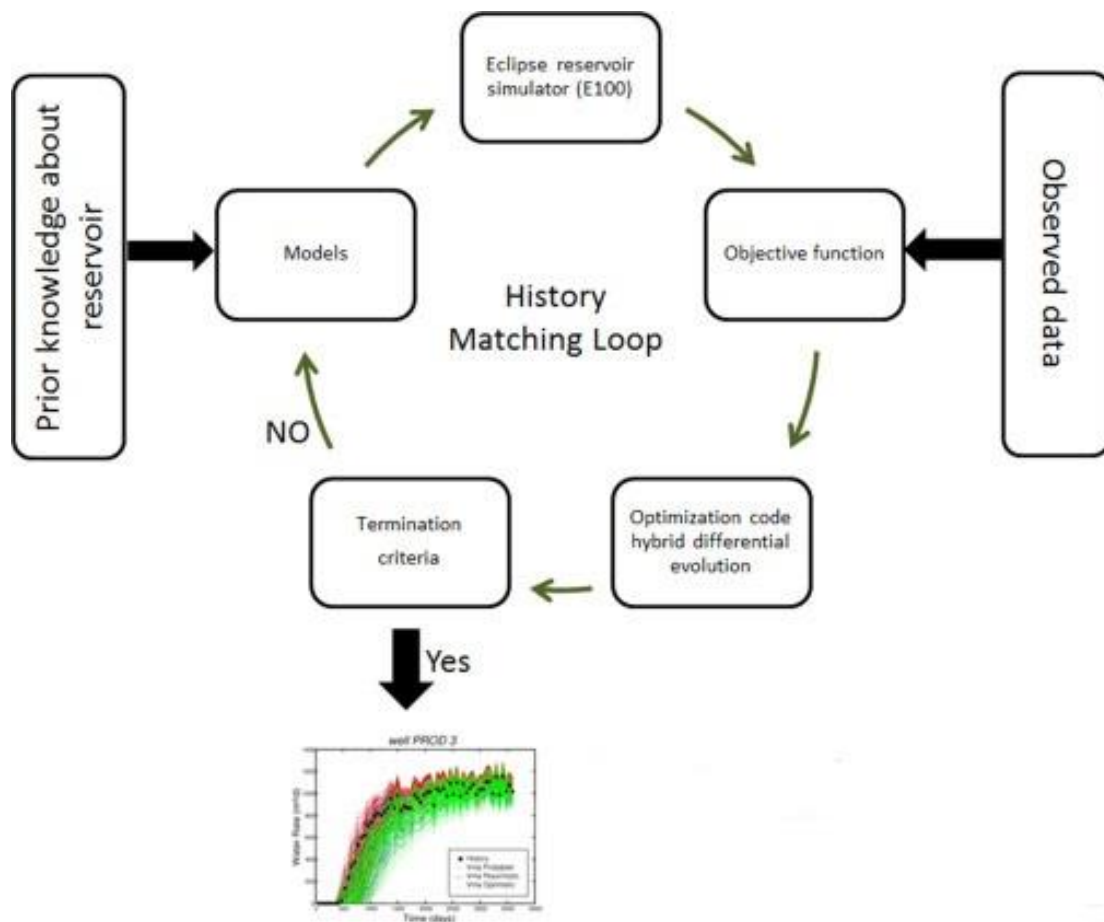


Figure 4: Showing the Methodology for the stochastic adaptive History Matching

3.1.0 Experimental Coreflooding

To perform core-flooding, three main steps are mandatory: core drying, core saturation, and water-flooding. The Core drying and saturation was done based on “International Society for Rock Mechanics suggested method for determining porosity, density, and water content”. The core drying process is performed by a conventional oven. The saturation process was achieved

using a desiccator. Finally, the water-flooding process was completed by the displacement pump, core holder, and automated weighing system.

3.1.1 Materials and Set up

All the materials used in this study are outline here and also the setup. The apparatus for experimental core-flooding composes of core holders, displacement pump, oven, desiccator, hydraulic pump, an automatic arduino-based weighing system and secondary tools like desiccator, caliper, a scale, coreflooding apparatus, the Eclipse simulator, Raven (Epistemy) simulator and Matlab software.

3.1.1.1 Core Drill

As mentioned earlier, the samples are cut out from a parent rock to a specific size for the core holder. These plugs are cut using a core drill as shown below.



Figure 5: The Core drill



Figure 6:Matrix From Which Core Plugs are Drilled From

A rule of thumb was followed which states that the core plug should have a length corresponding to one or two times the plug diameter. For this thesis, a total of four core plugs were used (K1, K2, K3, K4).



Figure 7: Showing all the core plugs used for this study

3.1.1.2 Digital Caliper

This is an instrument used for measuring the length and the diameter of the cylindrical core plugs. This caliper is very precise and has a resolution of 0.01mm. With the digital calipers, we are able to minimize visualization errors and the reliability of results is optimized.



Figure 8: A digital caliper

3.1.1.3 Core Holder

This apparatus is used for measurements of permeability, relative permeability, saturation change, formation damage caused by fluids injection or interactions between the rock and the injected fluids (ageing), but mostly used for Enhanced Oil Recovery (EOR) through core flooding. Core holders differ in terms of geometry (vertical or horizontal core holders and also it differs in the way stresses are applied (biaxial and triaxial). In this thesis, the

Hassler core holder was used as seen in the figure below. Schematic representation of the Core Holder used for this study



Figure 9: Hassler Core holder

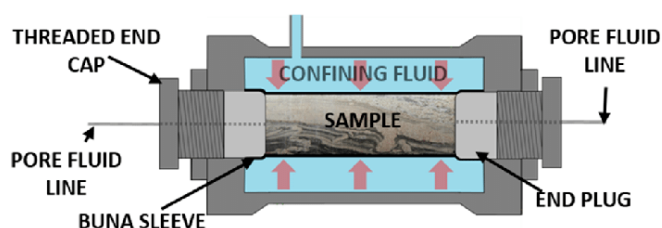


Figure 10: Internal view of the Hassler Core holder

3.1.1.4 High Precision Pump

The High precision pump has the function of injecting fluids at a given constant injection flow rate into the core holder, aiming to simulate the conditions of the reservoir during water injection. The pump selected for conducting this study was Pharmacia DCP50, which have a flow rate range of 1-499ml/hr and it varies in steps of 1 ml/h. It allows an operating pressure of 4.0 Mpa (40 bar). It achieves a flow rate precision better than 1 % over 8 hours at 6ml/hr with the same solvent and temperature.



Figure 11: DCP50 Pump

3.1.2 Experimental Procedure

The experiment was performed on core plugs extracted for the parent limestone rock acquired from the Reservoir site with similar characteristics

as the Brazilian Pre-salt. The core plugs samples which are cut in a cylindrical shape are measured for length and diameter using a digital Caliper. An averaged of several readings for each dimension (mm³), then weighed on the weighing balance to obtain the mass of the plugs with its water content. The plugs are then oven dried at a temperature of 105°C for 24 hours in order to obtain the Grain mass. After 24 hours of oven drying, a cooling process is done in an airtight lid container and placed in a desiccator for another 24 hours. The cooled samples are then weighed again to get the mass of the Oven-dried specimens. Now, for the calculation of Bulk volume, the buoyancy method was used from the ISRM suggested methods [47]. This method involved using Archimedes principles, the cylindrical specimens are 70% immersed in brine for 1 hour after which, the specimens are fully (100%) immersed in brine and left under vacuum pressure for 24 hours, the pressure was set up at 0.35 Bar. The specimens are removed from the immersion bath and surface dried with a moist cloth, care was taken to remove only surface water and to ensure that no rock fragments are lost. Its saturated-surface-dry mass is determined to an accuracy of 0.1 g. These specimens are now reweighed to get the mass of the saturated specimens. This is done in order to calculate the bulk volume of each specimen even though it can be obtained through a digital caliper.

The sample Pore Volume is calculated as

$$PV = \frac{M_{sat} - M_{dry}}{\rho_b} \quad Eq. 3 [47]$$

Where

PV is the pore volume

M_{sat} is the mass of the saturated sample

M_{dry} is the mass of the dry sample

ρ_b is the bulk density of the sample

The buoyancy method is the best method for obtaining a more accurate measurement of the bulk Volume. This stage is very important because it enables us to calculate the effective porosity.

The porosity is calculated as

$$n = \frac{V_v}{V} \times 100 \quad \text{Eq. 4 [47]}$$

Where

V is bulk sample volume

n is porosity

V_v is the volume of the void space.

Once the saturation process is completed, the process for estimating Permeability by measuring the pressure drop through the core length for a known flow rate is carried out through the Waterflooding process.

3.1.3 Waterflooding

Water flooding is the most widely used fluid injection process of Oil recovery worldwide today. In this process of water flooding, we used the falloff method to quantify the fluid passage through the rock specimens. In this method, the sample is at atmospheric pressure while the fluids are at a higher pressure when releasing into the inlet. Throughout this experiment, the pressure drop is only part observed here is the pressure build up during the Waterflooding and during this period we keep the outlet pressure at the production well constant at the atmospheric pressure (1atm) and all experiments have been performed at room temperature of 24°C

A schematic of the experimental apparatus used for the waterflooding studies is shown below.

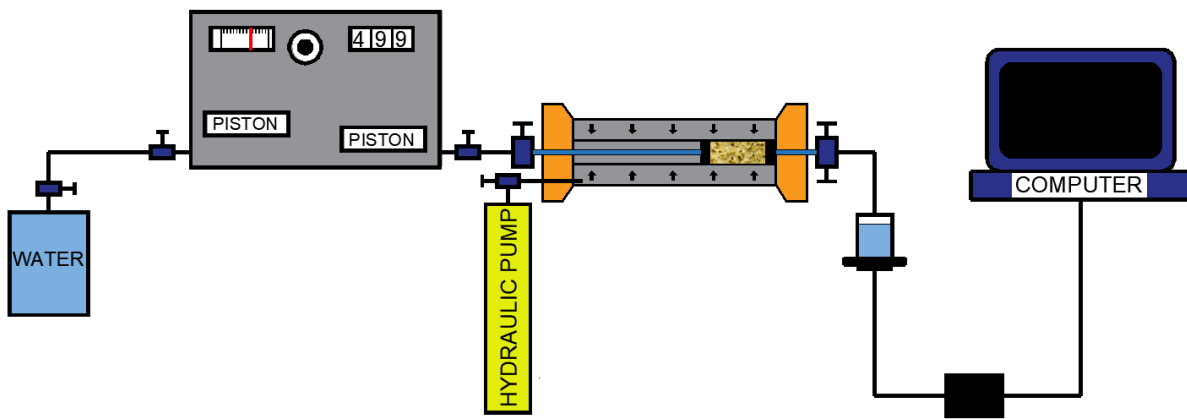


Figure 12: Schematic representation of the Experimental Setup [48]

In this experiment we started by taking the fully saturated core plugs and placing each in a core holder.

Preceding the Waterflooding test, some mandatory step had to be followed. First thing is the logistics of placing the core sample into the Hassler core holder. The core holder is opened carefully and put the core sample (which is inside a cylindrical rubber container) into it, then the core holder compartment is filled with Hydraulic Oil for the appropriate confinement pressure. It is very important to always be careful not to allow air bubbles in the core holder before the start of the experiment; therefore, a bleeding is done in order to remove all air bubbles with a vacuum pump. Next is to close the core holder at both end and apply a confinement pressure of 50bars. Prior to this stage the pump has been cleaned using the recommended procedure from Hassler Company.

After this, the following step is to set up the desired flow rate on the DC50 pump. The properties of the core samples are provided in the table below. The brine (water with 5% NaCl by Volume) was used as a saturating and as a displacing fluid while Isooctane is used as the Oil which is being displaced and its viscosities at room temperature of 24°C are 1.05cP and 0.51cP respectively.

Below is the table showing the properties of the core samples used in this work.

Table 1: showing the properties of the core samples.

| Samples | Length (cm) | Diameter (cm) | Moist-Dry Weight (g) | Oven-Dry weight (g) | Weight of saturated (g) | Weight of Brine (g) |
|---------|-------------|---------------|----------------------|---------------------|-------------------------|---------------------|
| K1 | 10.107 | 3.779 | 263.9 | 261.44 | 276.33 | 14.89 |
| K2 | 10.082 | 3.774 | 264.43 | 262.7 | 277.12 | 14.42 |
| K3 | 12.537 | 3.774 | 318.21 | 318.04 | 336.69 | 18.65 |
| K4 | 11.745 | 3.772 | 303.03 | 302.85 | 318.91 | 16.67 |

For this specific experiment, for stage one (1) which is the saturation stage with brine, we used an injection flow rate of 6ml/hr with the confining pressure of 50bars. The effluent from the cores is collected in a fraction collector and the pressure at the outlet was assumed to be 1atm while the system pressure is read from a pressure gauge connected to the inlet. Experiment was stopped when we have attained a steady state, where the pressure values become constant. Result obtained was used to calculate the absolute permeability of the Core Plug.

The second Stage of the flooding is to mimic reservoir generation and production where the Isooctane is injected till no more brine is collected at the effluent in order to obtain irreducible water saturation (S_{wi}). The Isooctane (synthetic Oil) is injected through the high precision Pump at a constant injection flow rate of 6ml/hr and production was done, samples of the brine was collected first, before the samples of oil (the production of oil) was collected. The experiment is stopped when we reached a steady state condition (Pressure reading become constant and the production rate at the effluent from the core equals the injection rate. At the end of this stage, we are able to calculate the relative permeability to oil through the application of Darcy Law expressed below.

$$k = \frac{Q\mu\Delta L}{A\Delta P} \quad \text{Equation 5. Darcy Equation}$$

Where

K is the permeability of the formation

Q is the flow rate of the injected fluid

μ is the viscosity of the fluid

ΔL is the length of the core

ΔP is the change in pressure

A is the cross sectional Area.

The final stage of the coreflooding is the recovery stage where the core which is fully saturated with Isooctane is now being flooded. In all the three stages were perform on each core samples with different injection flow rate but same confinement pressure. Selection of the injection flow rate was used based on the flood front stability criteria [49] such that for cylindrical short cores the front is unstable whereas for long square cross section core, it is stable.

During these displacement tests, the fraction of brine and isooctane are collected at the outlet in the fraction collector. From the measured isooctane and brine collected, the relative permeability ratio $\frac{K_{rw}}{k_{ro}}$ was calculated.

Since the carbonate rock sample used is a tight rock, we had a challenge of long acquisition time. As fluid flows through the porous medium, the pressure in the inlet rises due to geometric complexity of the porous framework. This is physical constraints implies a limitation in the range of possible flowrate use for this rock specimen. Also, one other key challenge with the experimental method is the use of ambient temperature rather than the typical reservoir temperature. All these could be a factor to a less perfect result.

Three out of the four (4) samples used, were conducted without consideration of the effect of aging on the Waterflooding experiment. However, for the last sample K4, an ageing of two (weeks) was carried out on the sample, under same condition of temperature and pressure.

At the end of the two weeks of aging, the flooding experiment was carried out on the sample K4 and results were obtained at a steady state condition.

3.1.4 Waterflooding with two weeks old ageing.

After the normal core preparation and saturation, we inserted the core into a Hassler core holder. The confining pressure was 50 bars. The absolute permeability was measure from the first stage of the experiment which is the saturation stage done with the brine. We established Initial Water Saturation, (Swi) by flowing oil (Isooctane) through the confined core. The isooctane injection flow rate was in the range of 6ml/hr. The initial water saturation obtained by this method was about 23%. After establishing initial water saturations with the designated crude oil, we shut the system down from production and close all valves and outlets. Confinement pressure used was 50bars and the temperature was room temperature of 25°C. Aging periods was for fourteen (14) days and at the end of the ageing time, the valves were opened and the third (3rd) stage which is the recovery stage is perform on the sample in order to obtain the result of the recovered isooctane. And we calculated the recovery factor from this result.

3.2 Fluid Flow Dynamics Simulations

The fluid flow Dynamic simulation was carried out with the Schlumberger software Petrel® - Eclipse® and RFD tNavigator® mostly for the numerical modelling and RAVEN® (Epistemy) was used for stochastic optimization. Several simulations were carried out considering different situations and conditions and results were obtained. Results (porosity and permeability, irreducible water saturation, and the pressure of the system) obtained from the laboratory experiments are imputed in the dynamic simulations. The data file was prepared and we used the Eclipse100 which is a Black composite oil model.

3.2.1 Reservoir Simulation

To produce a dynamic model, it is imperative to create a static model first and that was done using information of the core plugs used for the laboratory experiment. The fluid flow Dynamic simulation was carried out with the Schlumberger software Petrel® - Eclipse® and RFD tNavigator® mostly for

the numerical modelling and RAVEN® (Epistemy) was used for stochastic optimization.

Firstly, a 3D static model of the core plug was created by defining the grid Dimension of the core plug with $10 \times 1 \times 1 = 10$ cells which has various length as can be seen in table 1.0 above. The grid is done this way in order to show the true representation of the laboratory experiment, we have just a single injection well with only one cell in the vertical direction, so we don't have to select the cell of injection or production. The model has two vertical wells (an injection and production well) drilled at both ends of the core. Below is a schematic representation of the static 3D model of K1 from tNavigator. For the fluid flow simulation, both homogenous and heterogeneous systems were taken into consideration. The observed production data from the laboratory experiment were used to see the similarities for the laboratory results which were plotted on an excel sheet with the simulated plots of the field oil production, field Pressure, the field water cut, the production and injection rate were all observed during the simulations. Now, for each core samples, several simulations were done under different conditions- changing the grid size, considering heterogeneity and homogeneity etc. Below is the three Dimensional (3D) model of the reservoir model from eclipse. The two wells graphically represented are the Luanda which is the injector and the Braga which the producer.

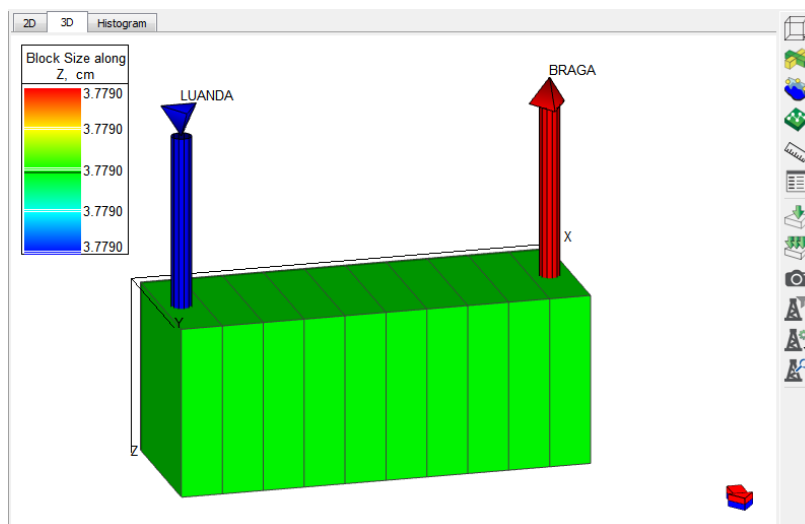


Figure 13: The 3D Model of K1 sample along the Z direction

3.3 Evolution of Pressure over time

Overtime, during the course of the experiment, the pressure evolution was simulated in order to see if the system represents the real scenario in the laboratory. Same is applicable to the water saturation in the core plug. Below are the graphical representations of the evolution of Pressure and Water saturation over time in the reservoir.

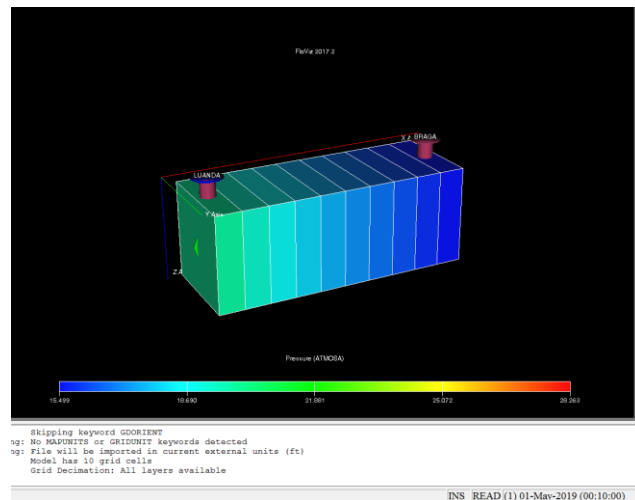


Figure 14: Pressure evolution at timestep 1

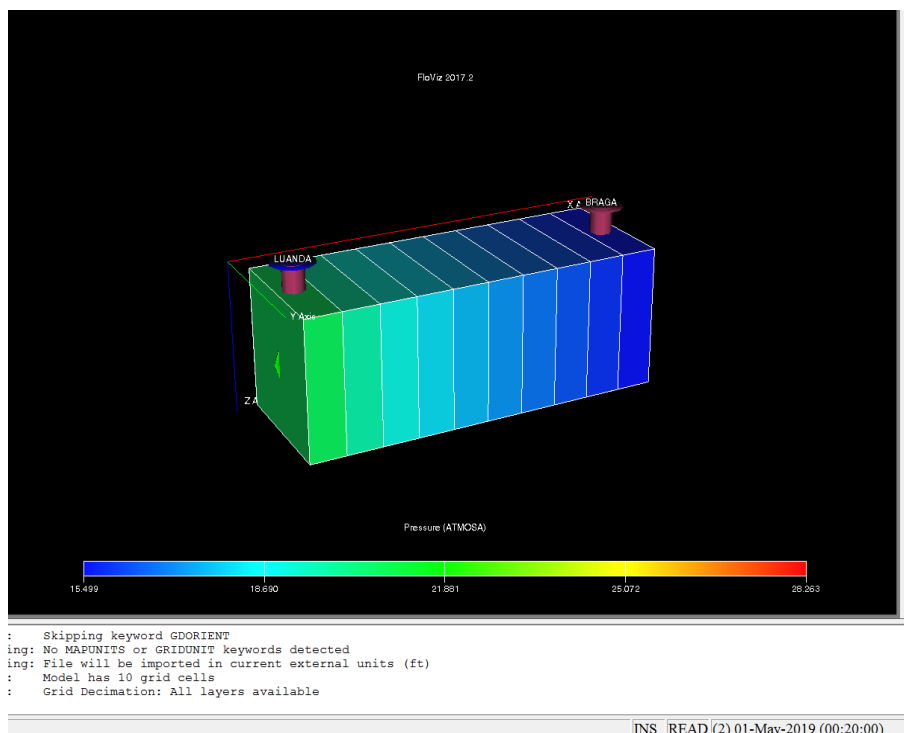


Figure 15 : Pressure evolution at timestep 2

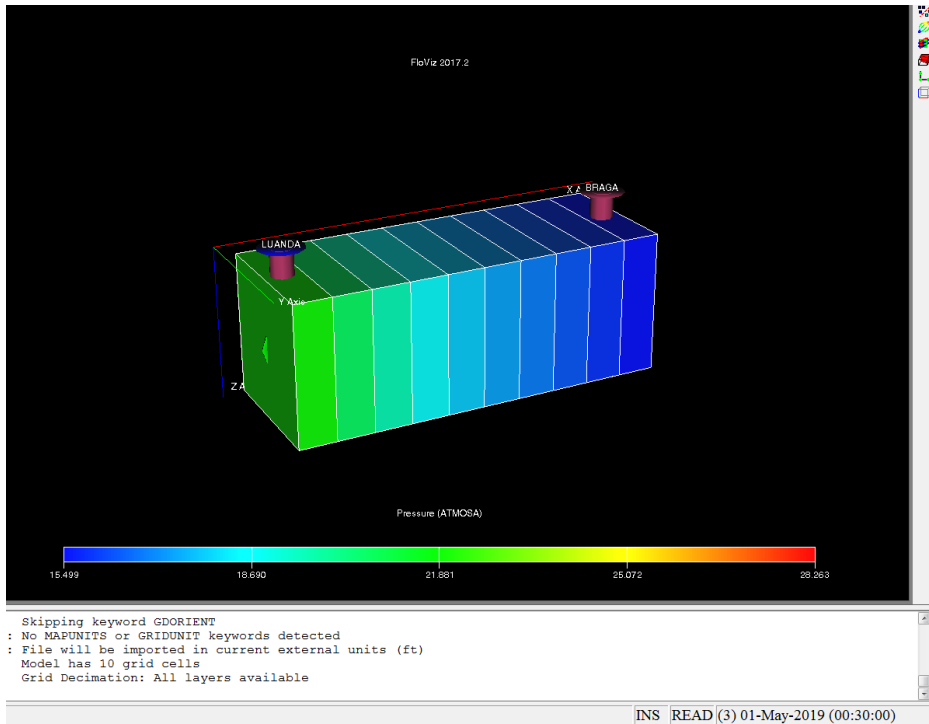


Figure 16: Pressure evolution at timestep 3

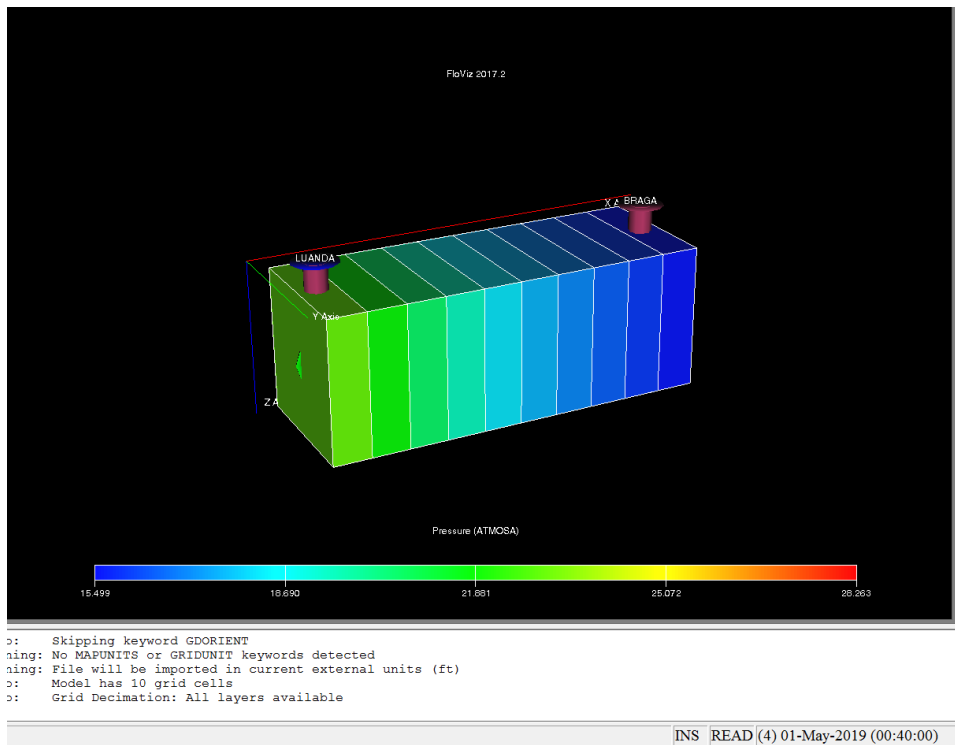


Figure 17: Pressure evolution at timestep 4

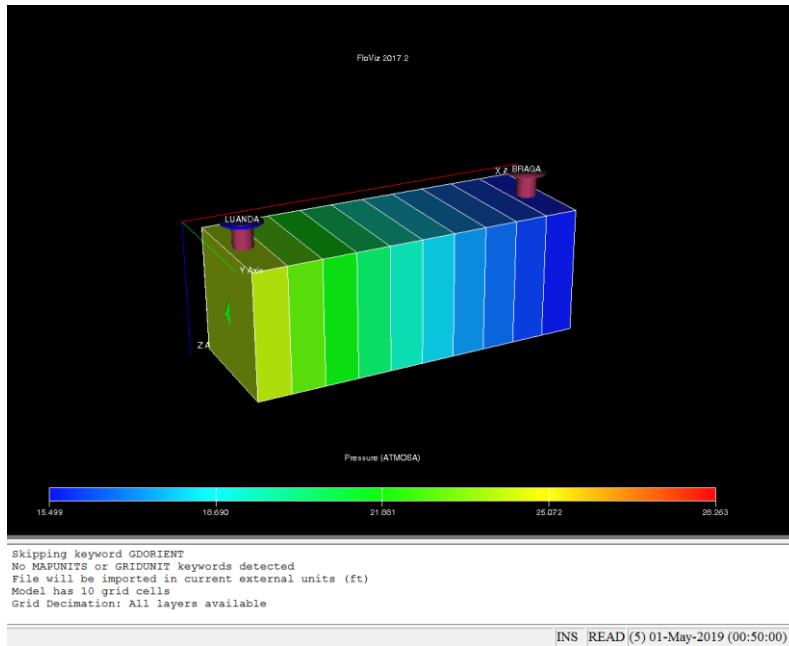


Figure 18: Pressure evolution at timestep 5

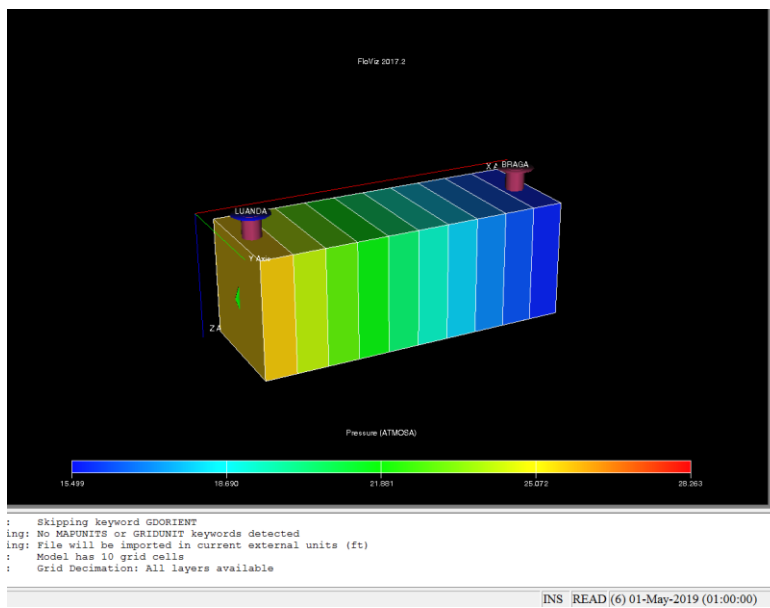


Figure 19: Pressure evolution at timestep 6

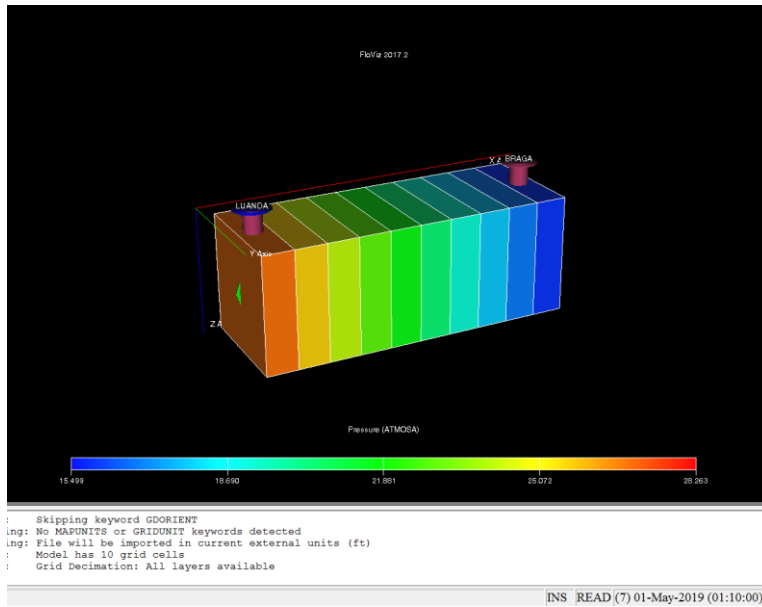


Figure 20: Pressure evolution at timestep 7

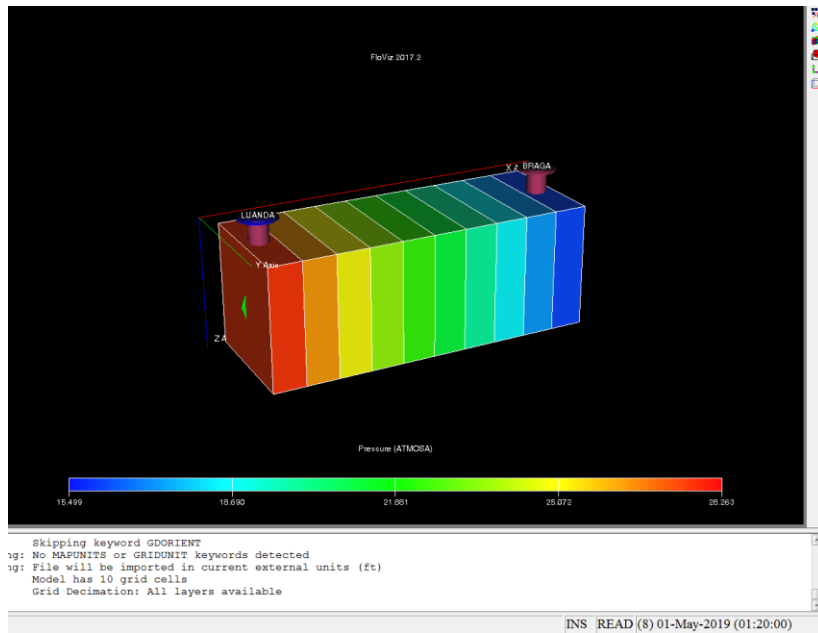


Figure 21: Pressure evolution at timestep 8

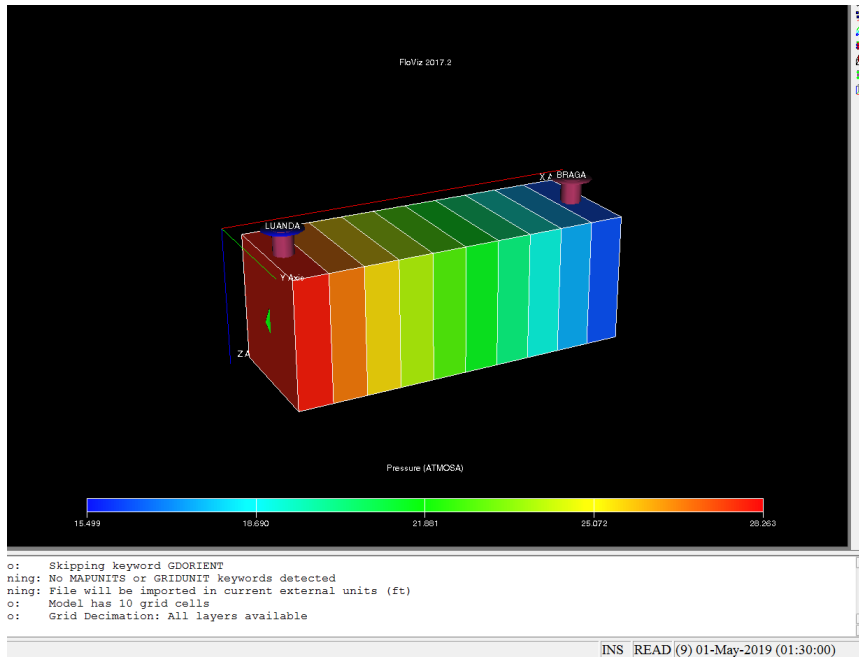


Figure 22: Pressure evolution at timestep 9

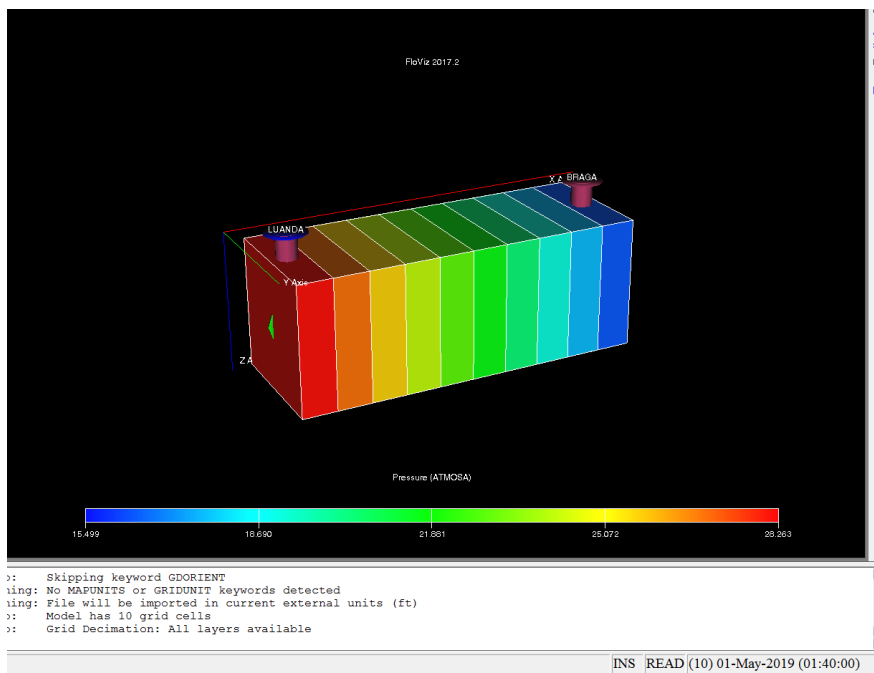


Figure 23: Pressure evolution at timestep 10

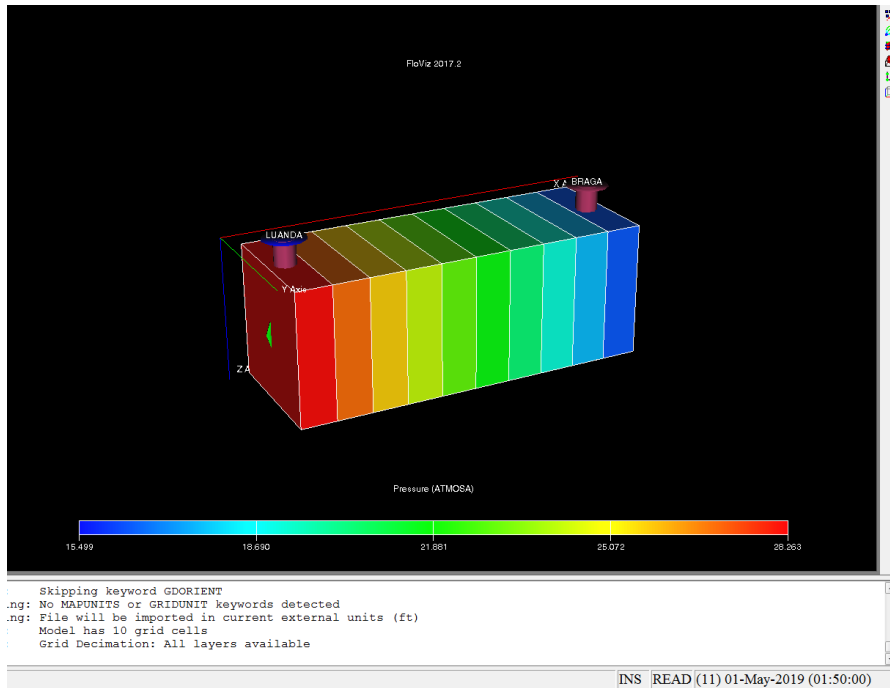


Figure 24: Pressure evolution at timestep 11

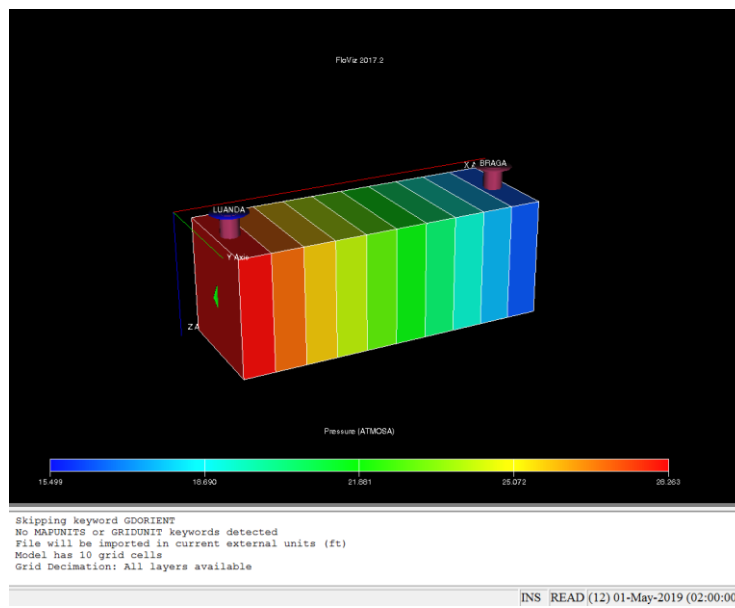


Figure 25: Pressure evolution at timestep 12

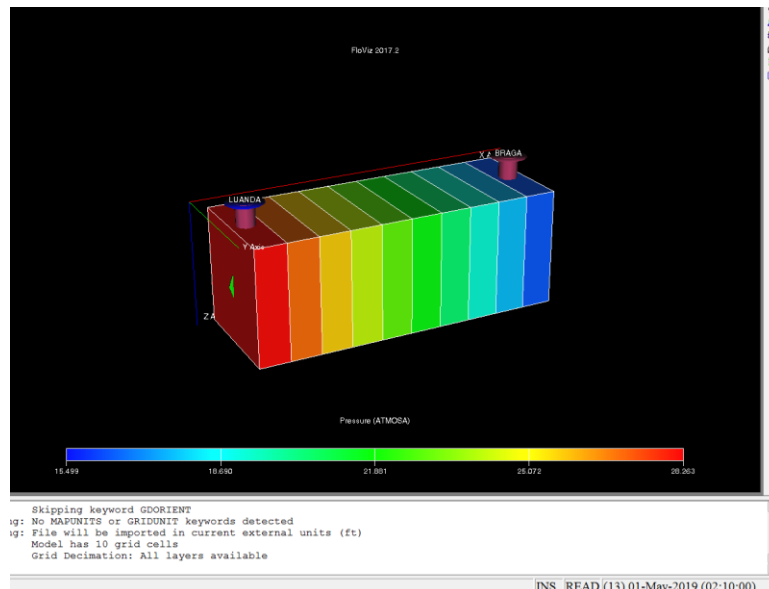


Figure 26: Pressure evolution at timestep 13

The simulated result for the evolution of pressure is coherent with the laboratory result where there was a gradual buildup of pressure over time at the injector well.

3.4 History Matching with Stochastic Adaptive Particle Swarm Optimization

We consider two reservoir models in this chapter. In History Matching, simulation model are calibrated to reproduce the historical observations from the oil and gas fields. This aspect of the thesis was carried out using RAVEN® (Epistemy) which is connected to Eclipse® and RFD tNavigator®. Eclipse® generate some results during the numerical simulation process using the result gotten from the laboratory experiments, these results are then used by RAVEN® (Epistemy) and optimize the result to acquire the best misfit possible using the objective functions and the appropriate optimization algorithm. In this thesis, the Particle Swarm optimization algorithm was used. Since a single simulation model takes hours or even days to run, it was necessary for the application of an effective adaptive Optimization algorithm to produce a possible combination of reservoir models properties that will obtain a good History Match.

The Homogeneous Reservoir model and the Heterogeneous Reservoir model, both with simple structure with 2 vertical wells which are the production and

injection well. These two models are both synthetic problem (based on the data from the laboratory experiment done on the core plugs under study). Both models have simple geological structure and the History Matching is based on multivariate data. The methodology adopted for the stochastic History Matching is in the

3.4.1 Homogeneous Reservoir Model:

The homogeneous Reservoir model is setup on a 10x1x1 block grid, the production history of the reservoir consisting of production rate of oil and water, etc are shown in the figures below.

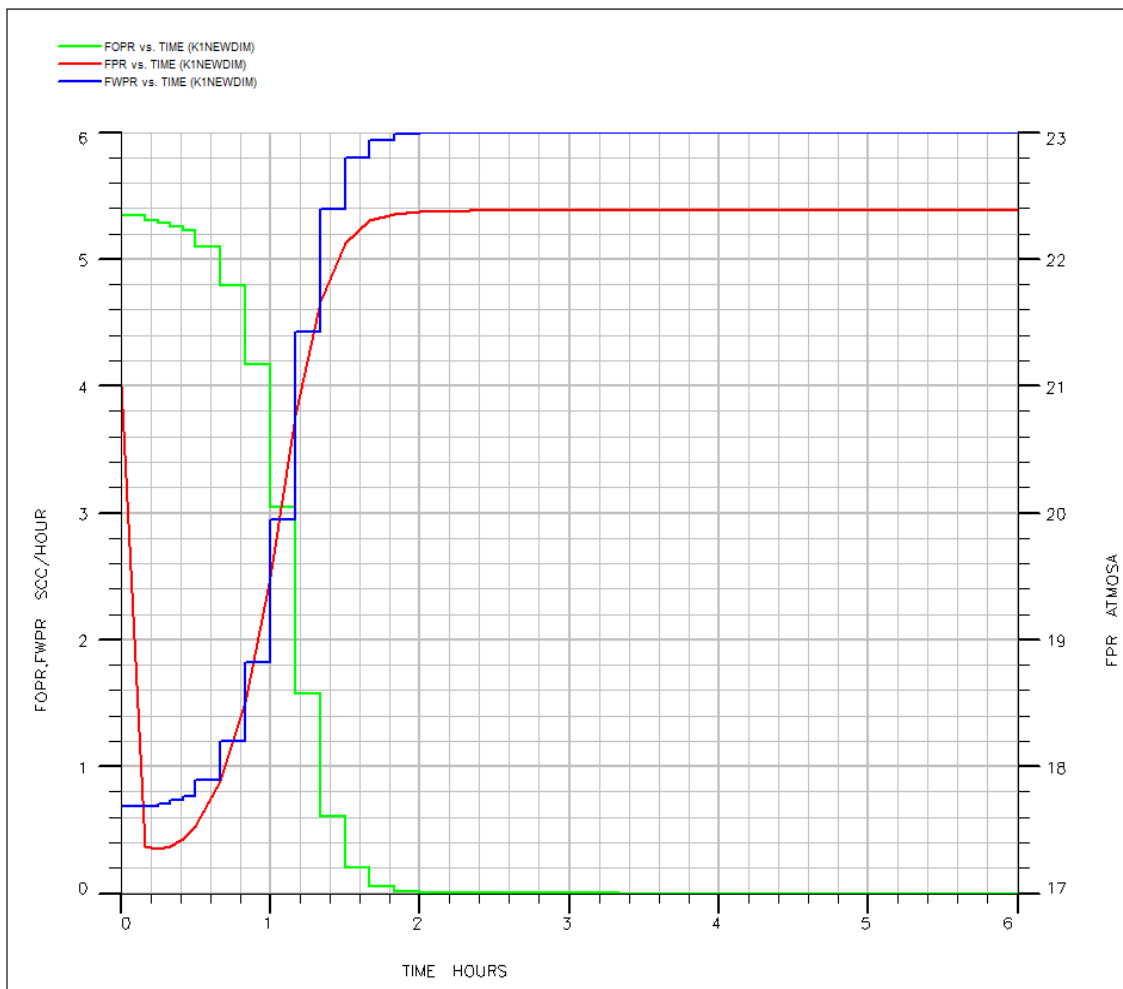


Figure 27 : The Production History for the K1 SAMPLE

In the homogeneous reservoir model, there is only one layer with uniform properties. The unknown parameter for the History Matching is the Permeability and the Porosity. History Matching is only done on field production rate. For the Homogeneous reservoir model, several different parameters are used and the permeability/porosity priori range was informed from the laboratory analysis of the core plugs to estimate and minimize the uncertainty in the permeability and porosity of each sample. For the 2 variables that we are considering (permeability and porosity), the values in the models are represented with “\$a and \$b” for porosity and permeability respectively. A minimum of 1000 iterations was used with a particle size of twenty (20). By estimating the porosity and permeability using several priori ranges and global sigma, the input files for the simulation is ready and the best fit of all the iterations from RAVEN are selected for each sample. The best fit outcome is imputed into @tNavigator to ascertain the actual

permeability and porosity values for each sample. And from the @tNavigator simulations, the evolution of the pressure and saturation over time is also determined. Below is the parameterization for the homogenous reservoir model for the four (4) core plugs under study. For the learning Algorithm, the Particle swarm optimization algorithm (PSO) was used alongside the Random Forest (RF) as shown below

Table 2 : The parameters used in the Stochastic Adaptive History Matching with the particle swarm Optimization algorithm.

| Samples | Permeability Priori range (mD) | Porosity Priori Range [-] | Global Sigma (cm) | Distribution Used | Learning Algorithm |
|---------|--------------------------------------|------------------------------------|-------------------------|----------------------|-----------------------|
| K1 | 0.01- 1.0 | 0.01 – 0.3 | 1.0 | Uniform | PSO + RF |
| K2 | 0.01 -1.0 | 0.01 – 0.5 | 2.0 | Uniform | PSO+RF |
| K3 | 0.001 – 1.0 | 0.001 – 0.5 | 3.0 | Uniform | PSO+RF |
| K4 | 0.001 -0.5 | 0.001 - 0.5 | 2.0 | Uniform | PSO+RF |

3.4.2 Heterogeneous Reservoir Model:

The model description for the heterogeneous reservoir model is same as that of the homogeneous model and every step of the workflow in homogeneous reservoir model is same except for the defined parameters under the History Matching for permeability and porosity which has ten (10) different values each. This is one distinctive difference between the homogeneous and the heterogeneous reservoir model - the parameter set up which are defined in the model itself. So the values in the models are represented with “\$a1, \$a2..... and \$a10 for porosity while for the permeability, the values in the model are represented as \$b1, \$b2, \$b3.....\$b10” A minimum of 1500 iterations was used with a particle size of twenty (30). Several trials were

done on each sample with different parameters but only the best results are represented here in this study.

Table 3: The parameters used in the Stochastic Adaptive History Matching with the particle swarm Optimization algorithm.

| Samples | Permeability (\$b1-\$b10) Priori Range (mD) | Porosity (\$a1- a10) Priori Range [-] | Global Sigma (cm) | Distribution Used | Learning Algorithm |
|---------|--|--|-------------------------|----------------------|-----------------------|
| K1 | 0.001- 1.0 | 0.001 -0.3 | 1.5 | Uniform | PSO + RF |
| K2 | 0.001 – 1.0 | 0.001 – 0.3 | 2.0 | Uniform | PSO+RF |
| K3 | 0.001 – 0.5 | 0.001 – 0.3 | 2.0 | Uniform | PSO+RF |
| K4 | 0.001 -1.0 | 0.001 – 0.3 | 2.0 | Uniform | PSO+RF |

Results of the best fit from each sample was use extracted and run on @tNavigator for the proper estimated values of permeability and porosity of each samples for the heterogeneous reservoir model. Also, the propagation of pressure and water saturation was also simulated over the entire time step.

CHAPTER FOUR (4)

4.0 Results and Discussions

The results of this work are presented in four (4) sections. In Section 4.1, we show the results of the production history of the different samples from the laboratory experiments, in section 4.2, we show results of the Model description and simulation, and the 4.3 shows results of the assisted History Matching for the homogeneous reservoir models and lastly the 4.4 shows results of the Assisted History Matching for the heterogeneous Reservoir Model.

4.1 Laboratory Experiments Results

The results from the laboratory experiment include the production rate of oil and the water, and the plots of volume produced versus time, pressure versus time for all samples and also the result of the recovery factor for each sample with their respective permeability and porosity calculated values.

4.1.1 Pressure versus time plot for all samples

This section will only show results of the final flooding with brine for the oil recovery stage and the pressure versus time plot is shown below

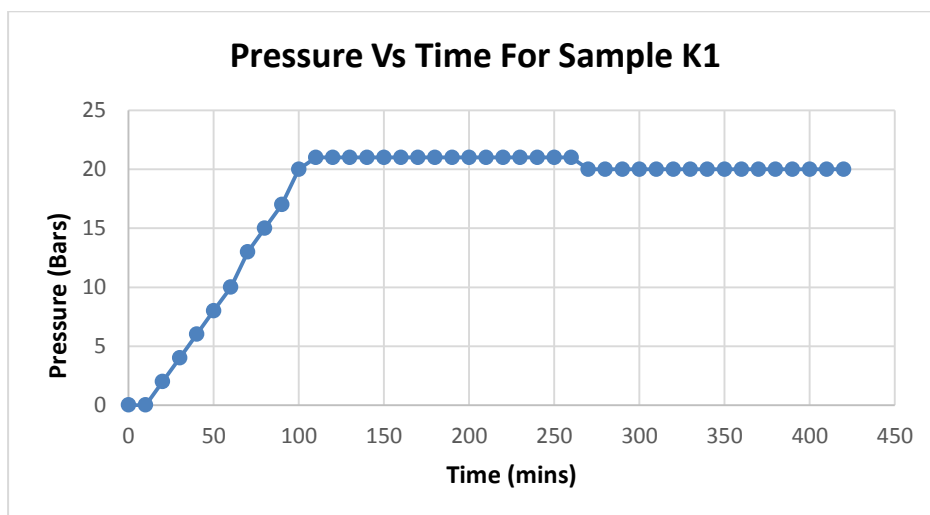


Figure 28: Pressure versus time plot from Laboratory Experiment

Looking at the plot, pressure is building up to provide energy for the reservoir for recovery, at a certain time, the pressure stabilizes and becomes constant

therefore the experiment was stopped and this shows that the system has attained a steady state condition during the experiment.

4.1.2 Results of the production rate versus time

This section presents results of the Production rate over time for the coreflooding experiment. Since this is the recovery stage of the oil (Isooctane), at the beginning of the flooding, the isooctane was produced (collected at the effluent) first before the brine is produced. Below is the graphical representation of the production rate versus time.

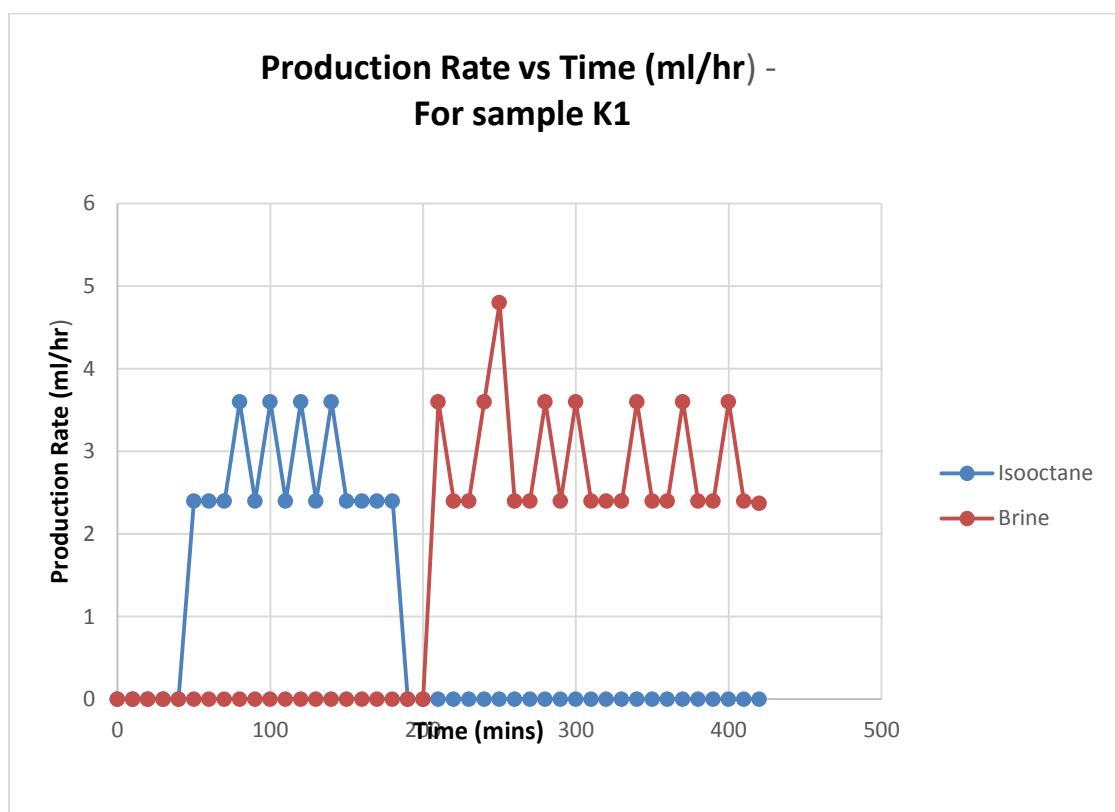


Figure 29: Production rate versus time from laboratory experiment

4.1.3 Recovery Factor

In this section, the results from mathematical calculation which the ratio between the oil produce to the original oil in place and these calculations were based on the laboratory experiment are presented in the table below

Table 4: Calculated Parameters from Routine Core Analysis (RCAL)

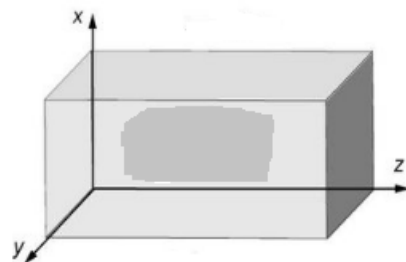
| | K1 | K2 | K3 | K4 |
|---------------------|-------------|-------------|------------|------------|
| Swi at stage 3 [-] | 0.36034115 | 0.476944253 | 0.3956044 | 0.46394384 |
| Pore volume (cm3) | 14.07 | 14.53 | 18.2 | 15.67 |
| Recovery Factor (%) | 42.22222222 | 38.33333333 | 31.8181818 | 42.4778761 |
| Porosity [-] | 0.128172323 | 0.124764314 | 0.12976484 | 0.11940562 |
| Permeability (mD) | 1.46E-01 | 1.46E-01 | 1.81E-01 | 1.70E-01 |

4.2 MODEL DESCRIPTION

This section shows the description of the static model and the dynamic model description of the reservoir under study.

4.2.1 STATIC MODEL

The Static model is developed by approximating cylindrical plug into cuboidal rock sample. Then the cuboid is divided into 10 layers as shown in the figure below



The core plug with dimensions

Diameter: 3.779cm

Length: 10.107cm

The Cartesian Model (1D) 10x1x1

DX: 1.0107cm

DY=DZ= 3.779cm

Figure 30 : Static model representation of the cylindrical core

We have a single layer for the static model and for all the XYZ direction grid cells are assigned average porosity and permeability values obtained from the Routine core analysis in the laboratory experiments. The density values are the values for the Isooctane and brine used in the laboratory experiment.

4.2.2 Dynamic Model

Under the dynamic model, results of the model are represented here with the specific initial and boundary conditions for the model.

4.2.2.1 Dynamic Simulation Constraints.

For the dynamic model, two constraints were put in place as per the laboratory experiment. The confinement pressure was set at 50bar and also we had a constant inlet flow rate for every sample mostly 6ml/hr. All active grid cells are set at initial saturation in the simulator. Below is the graphical representation of the static model of sample K1.

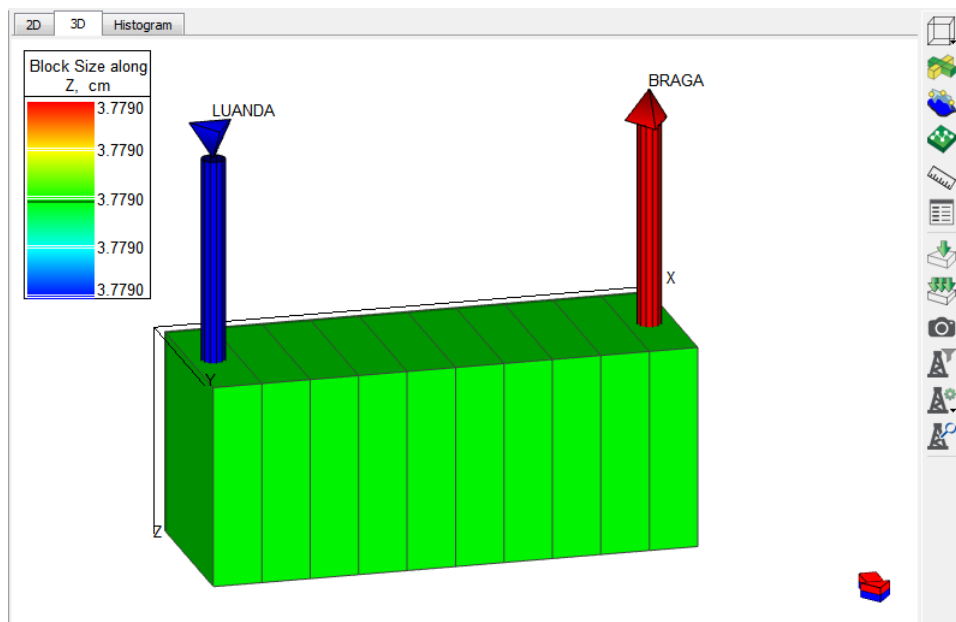


Figure 31: A graphical representation of the Model.

We also have results from the fluid flow simulation that gives a representation of the laboratory experiment being translated into a real reservoir scenario. This result of the simulation is from Eclipse where the Field Oil Production Rate, Field Pressure and the Field Water Production are all represented.

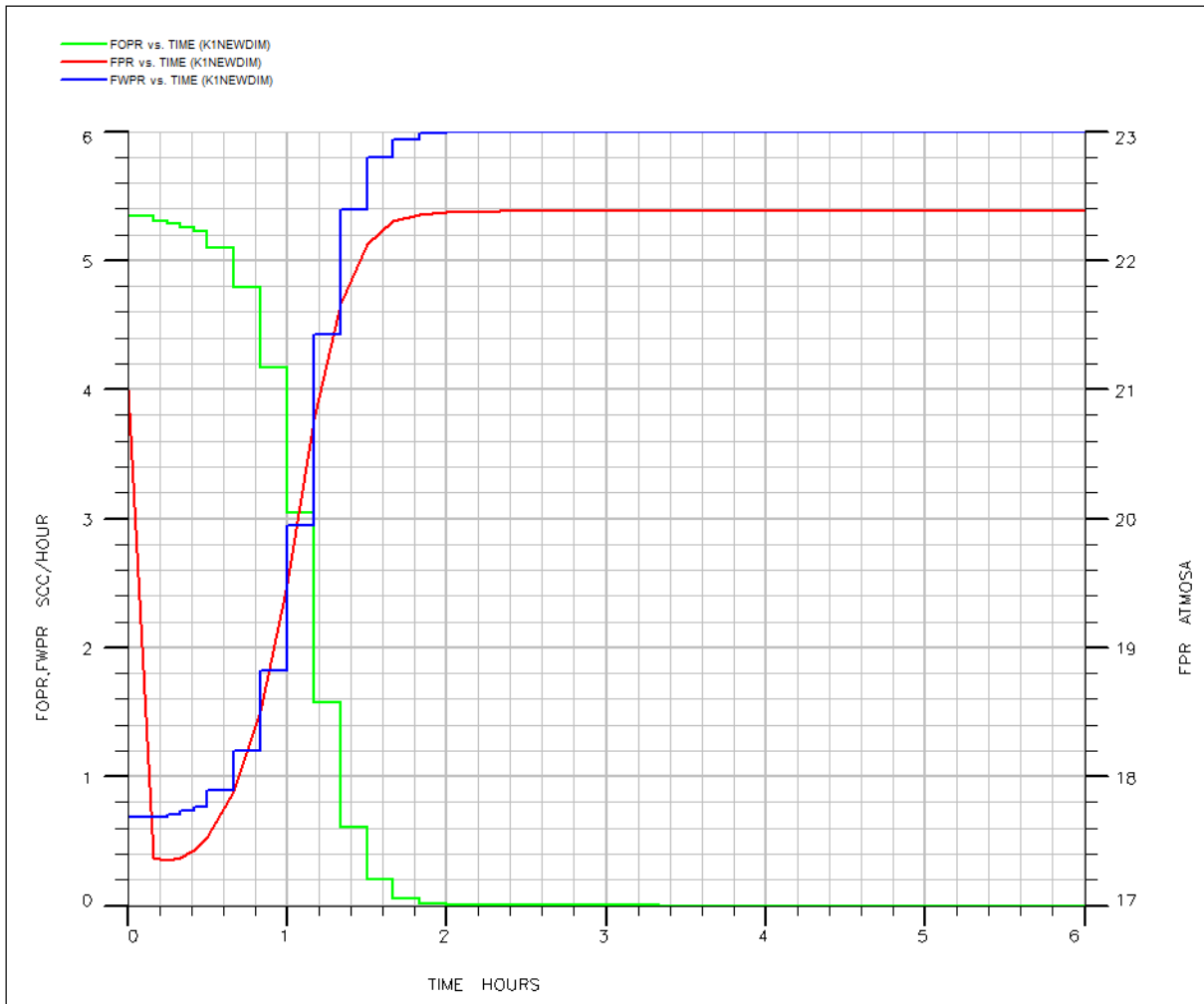


Figure 32: Production History of the sample K1

Form the graph it is evident that at the start of the recovery process, the depleted pressure start building until it attain a constant pressure where we have water breakthrough. The aim of the waterflood is to increase the pressure of the reservoir and in these experiment, we can see that the results proved the Waterflooding with Brine achieve this successfully. During the laboratory experiment, the production of water was not evident but in the simulation, we can see very negligible volume of water was produced alongside the production of brine. This proves that in real life scenario, oil production always is accompanied by a minute volume of water. Also, at breakthrough, we have a constant pressure.

4.3.0 History Matching of the Homogeneous Reservoir Model.

The dynamic reservoir model is modified to match the response of the field production phase and further extrapolation to predict future response of the

reservoir and also to reduce the uncertainty in permeability and porosity in the model. Results of the History Matching are presented below in the figure

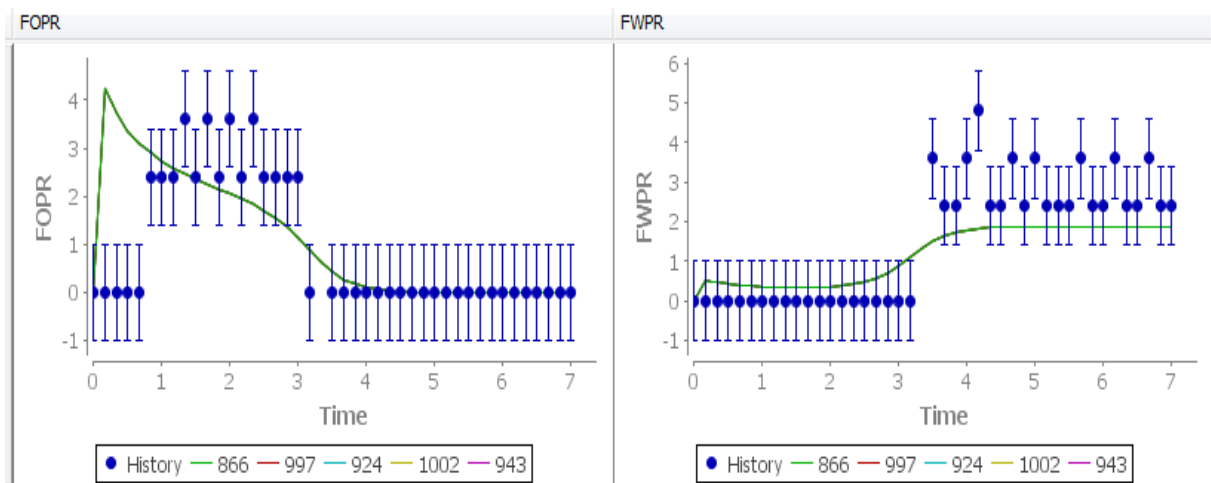


Figure 33: A good History Match for the K1 sample.

represent the History of production with the exact value as the dot and the range of what the minimum value and maximum values can be and it is represented by the length of the

For the model to be a good History Match, the iterations must pass within the range of the sigma (blue vertical line) while a perfect match is the one that passes through the production history (blue dots). Out of the numerous simulations, this was the best simulations for Sample K1. Results for the remaining samples are located in the appendix. Below is the result for the Misfit component for the Field Oil Production Rate (FOPR) and the Field Water Production Rate (FWPR).

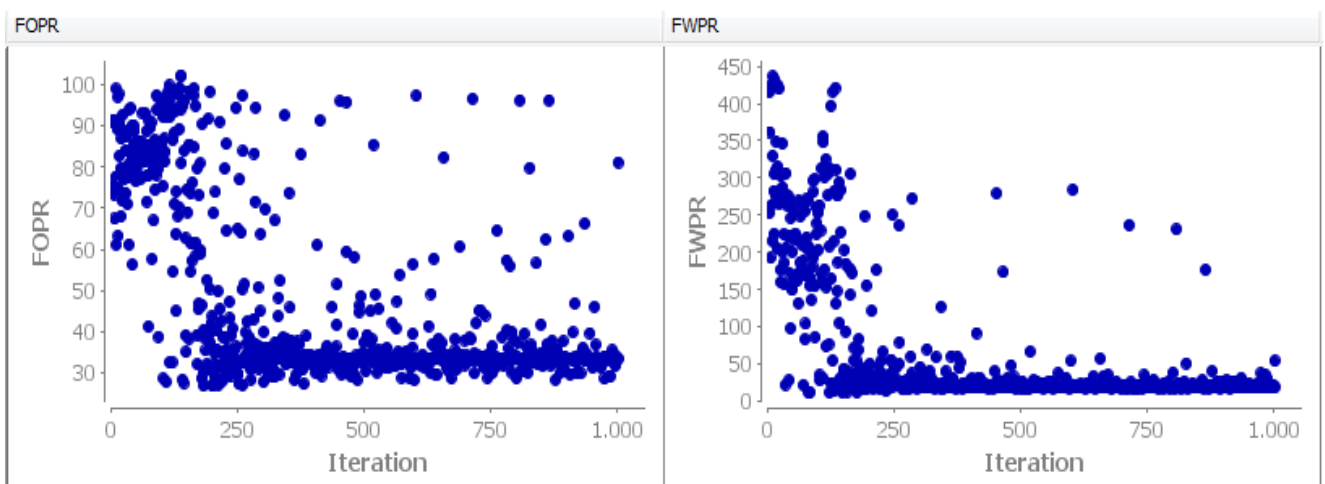


Figure 34: Results of the misfit component for both the FOPR and the FWPR

For the Misfit Component, the plot of the FOPR versus Iteration can be seen that at the beginning of the iteration, the FOPR is at 100 and as the iteration increases the misfit decrease until it got to around 30 where we see points converging and that show that maximum difference between the simulated and the production history is around 30. It can conclude that the lower the misfit, the closer is the simulation to the right Match.

For the FWPR, the misfit started very high at 450 but it decreases as the iteration increases and then convergence occurs at a much lower value of around 20 to 25. Below is a plot of the parameter versus the iteration for a homogenous reservoir.

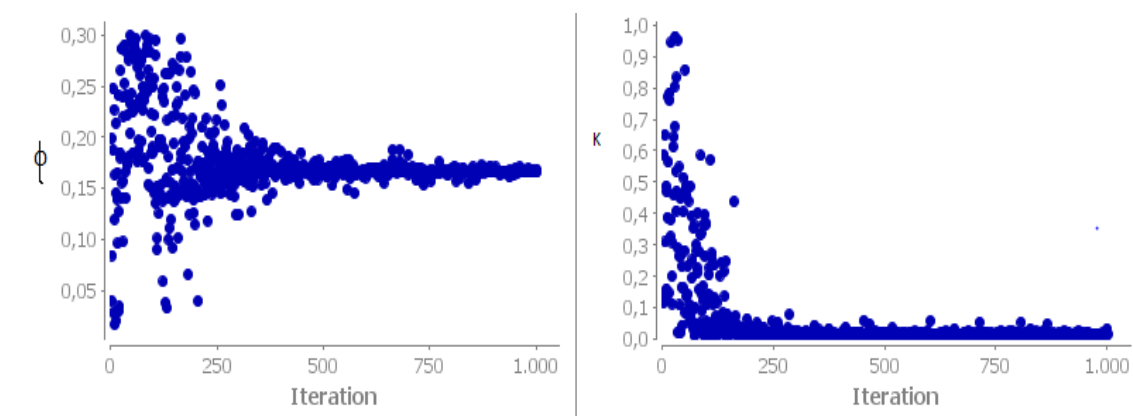


Figure 35: A plot of parameter (porosity and Permeability) versus Iteration

For the porosity versus iteration, the misfit also decreases from 0.3 to around 0.18 as the iteration increases and we can see a complete convergence around 1000 iteration. It is very important to have as much iteration as possible as it helps in giving more clear results. For the permeability versus iteration, the misfit started from 1.0 scantily and begin converging with iteration around 100 and the convergence become great and 1000 iteration at a point of almost zero (~ 0). The true permeability could be 0.028.

4.4 History Matching of the Heterogeneous Reservoir Model.

The heterogeneous reservoir model is modified to match the response of the field production rate and further extrapolation to predict future response of the reservoir, also to reduce the uncertainty in permeability and porosity in the model. In this model, we are interested in finding ten (10) different values

of permeability and porosity each. Results of the History Matching for the heterogeneous model is presented below in the figure

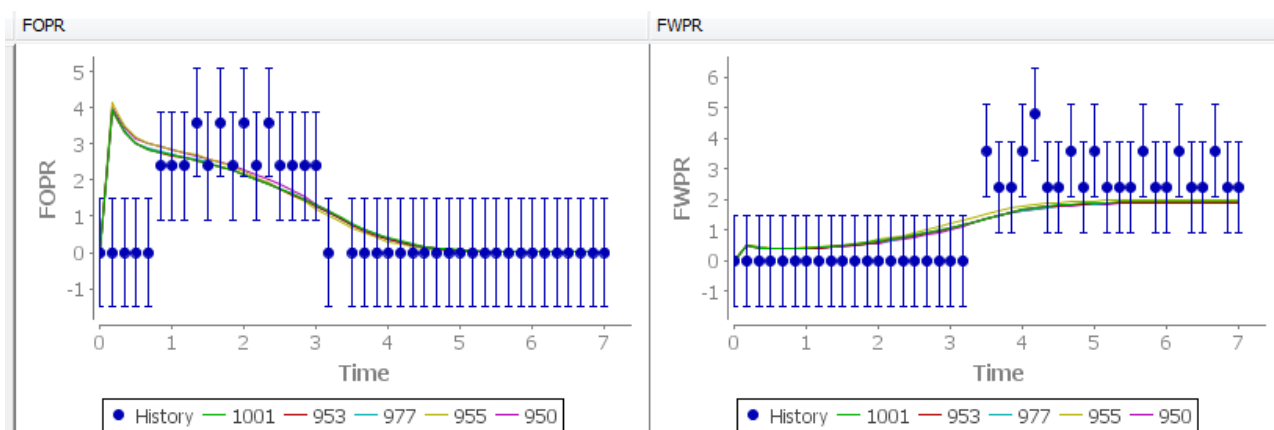


Figure 36: A good History Match for the K1Heterogeneous Mode.

For the model to be a good History Match, the iterations must pass within the range of the sigma (blue vertical line) while a perfect Matches are the ones that passes through the production history (blue dots). Out of the numerous simulations, this was the best simulations for Sample K1. In the heterogeneous we have several iterations matching the Production history since we are looking for about ten (10) values for the accurate permeability and porosity. Results for the remaining samples are located in the appendix. Below is the result for the Misfit component for the Field Oil Production Rate (FOPR) and the Field Water Production Rate (FWPR).

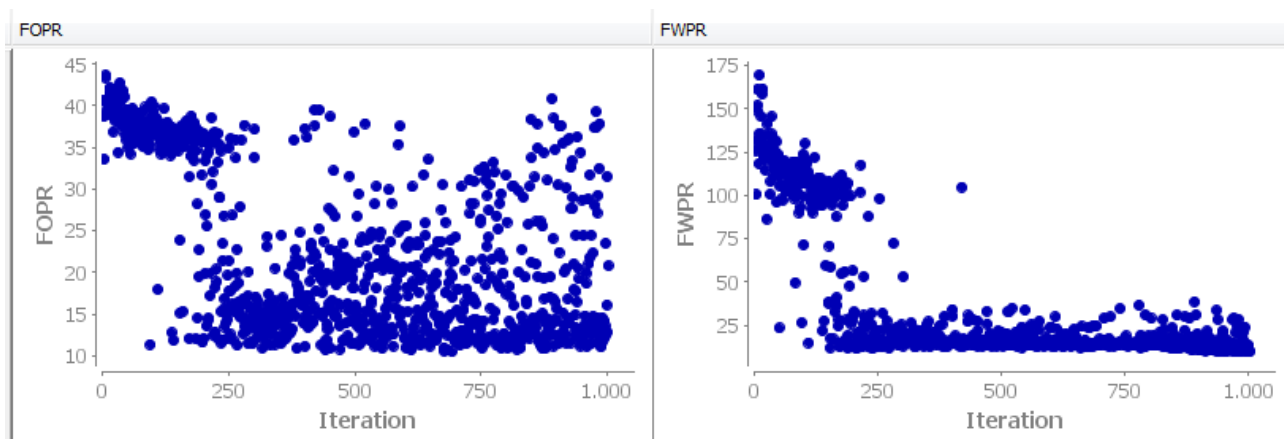


Figure 37: Results of the misfit component for both the FOPR and the FWPR

For the Misfit Component, the plot of the FOPR versus Iteration can be seen that at the beginning of the iteration, the FOPR is at 45 and as the iteration increases the misfit decrease until it got to around 12 where we see points

converging (although it is not a complete convergence) and that show that maximum difference between the simulated and the production history is around 12. It can conclude that the lower the misfit, the closer is the simulation to the right Match. For the FWPR, the misfit started very high at 175 but it decreases as the iteration increases and then convergence occurs at a much lower value of around 20 to 25. It can be seen that with the heterogeneous reservoir model, the misfit is reduced from 100 to 45 for the FOPR and from 450 to 175 for the FWPR.

Since the heterogeneous reservoir model is not uniform, the misfit versus the parameter produced 10 different results for porosity and permeability.

Below is a plot of the parameter versus the iteration for a homogenous reservoir.

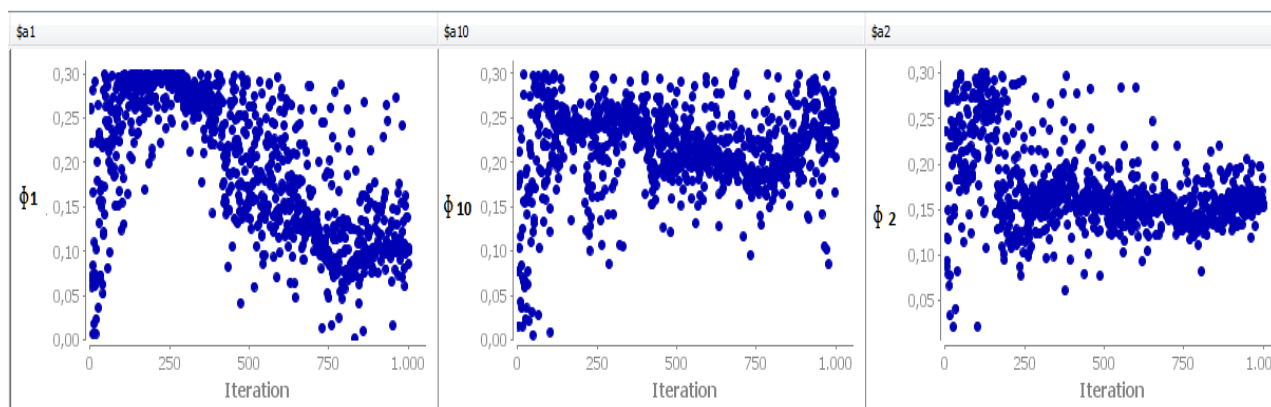


Figure 38: Porosity versus iteration for the first 3 values

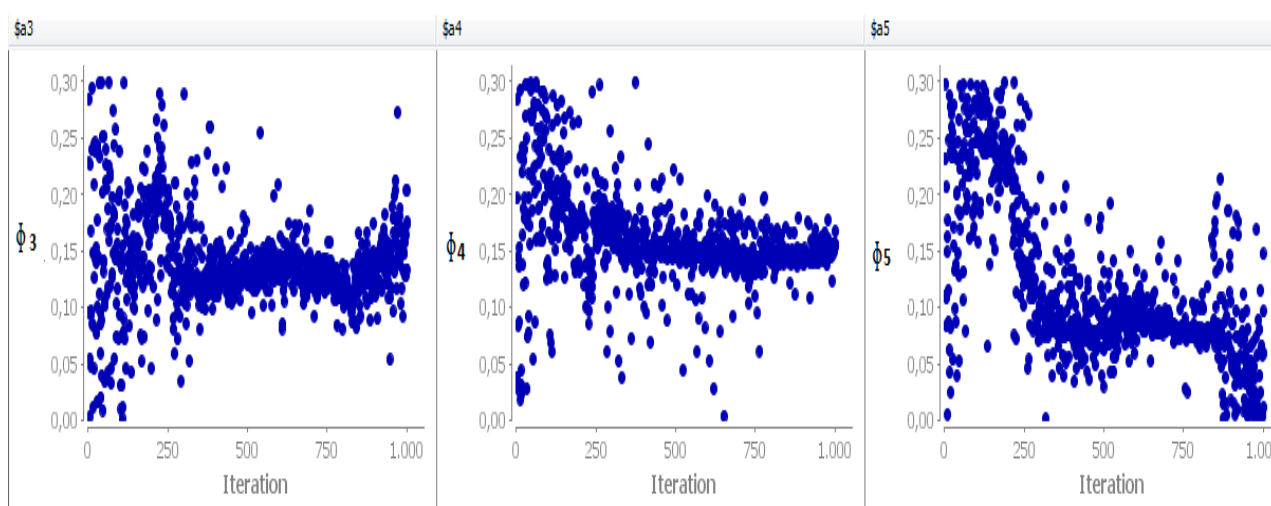


Figure 39: Porosity versus iteration for 3- 5

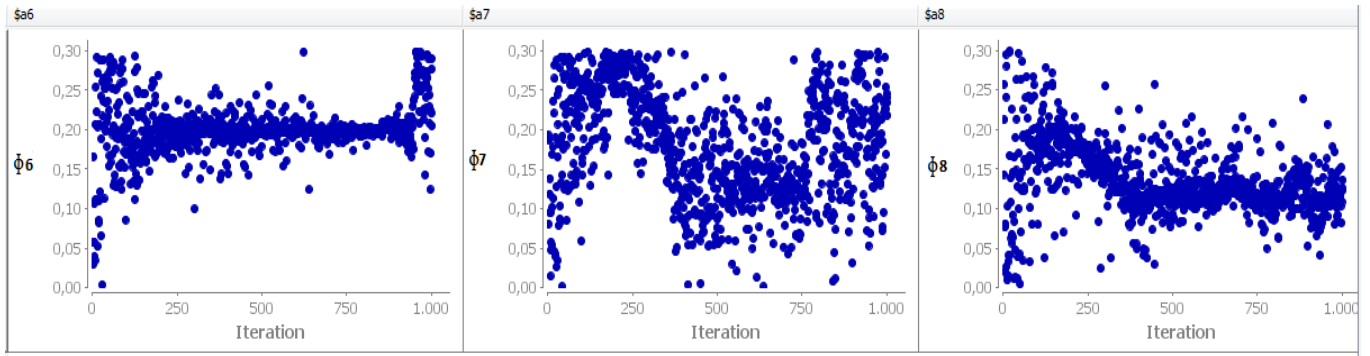


Figure 40: Porosity versus iteration for 6- 5

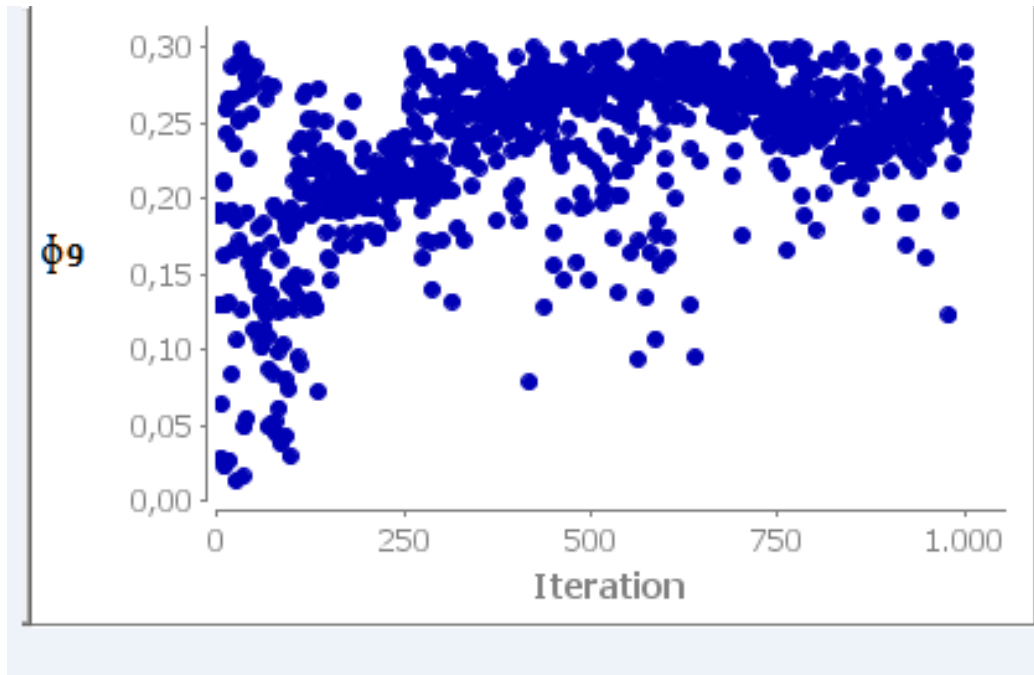


Figure 41: Porosity versus iteration for 9

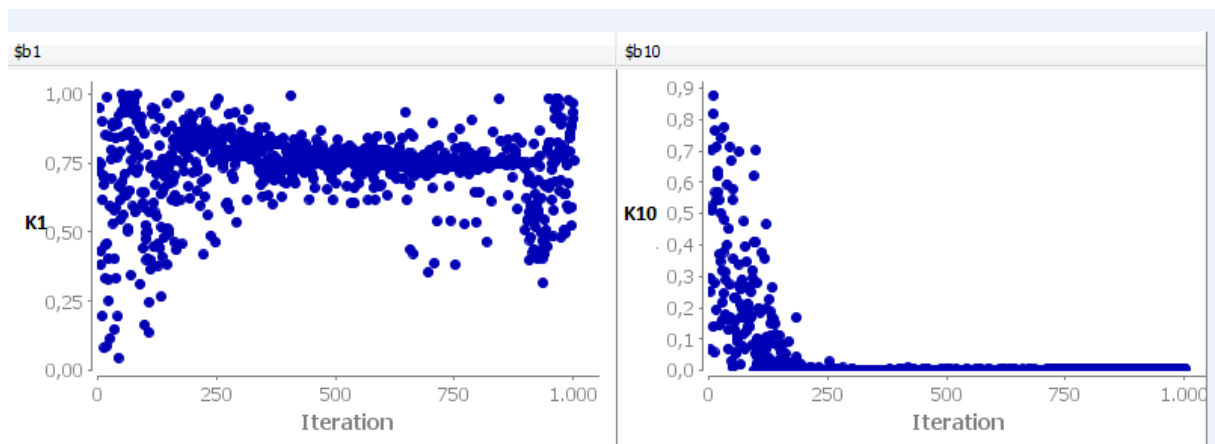


Figure 42: Permeability versus iteration for number 1 and 10

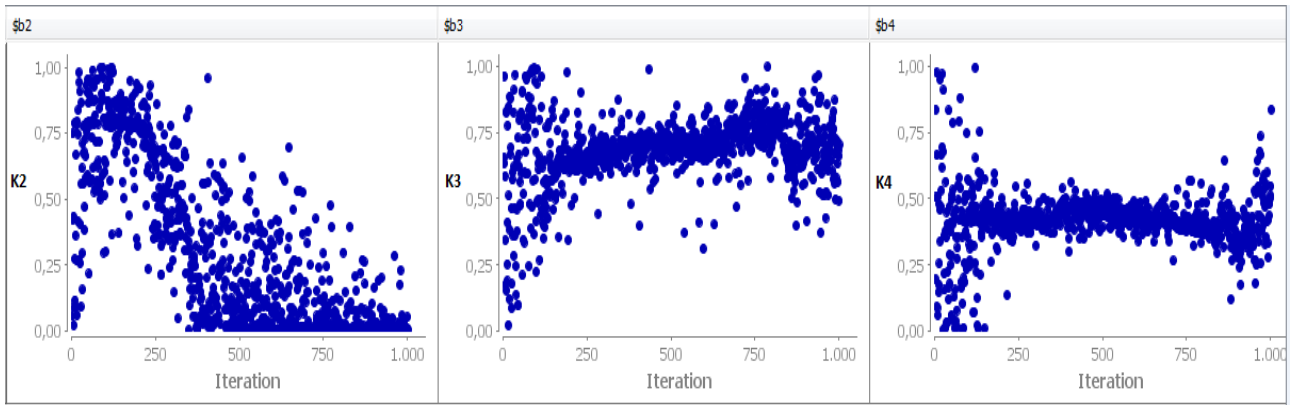


Figure 43: Permeability versus iteration for 2-4

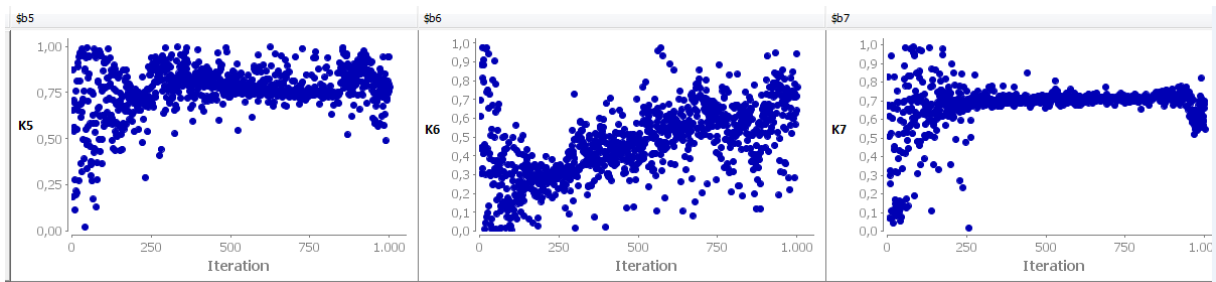


Figure 44: Permeability versus iteration for 5 – 7

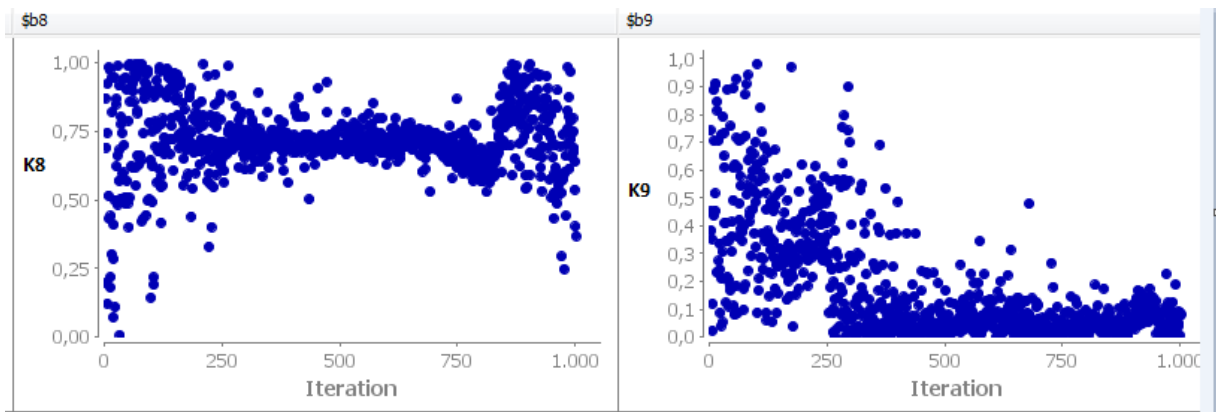


Figure 45: Permeability versus iteration for 8- 9

For the heterogeneous model, it is observed that at iterations around 500, the misfit are still at the barrier of 0.3 (which I place due to laboratory result of the porosity value), but as the iteration increases, the particles converges at a certain value for each porosity and same for the permeability. For every value of the porosity and permeability, the lowest misfit is always the selected value representing permeability and porosity.

4.5 Spatial Distribution of Permeability

Upon selecting the lowest misfit, the result is further ran on @tNavigator in order to ascertain the spatial distribution of permeability for the best result which is believed to show the real spatial distribution of the core samples.

Below is a graphical representation of Sample K1.

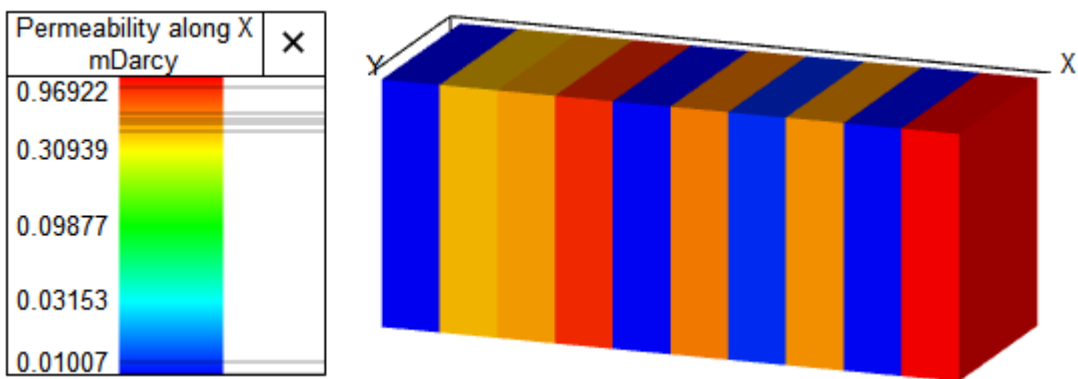


Figure 46: Spatial Distribution of Porosity in Sample K1

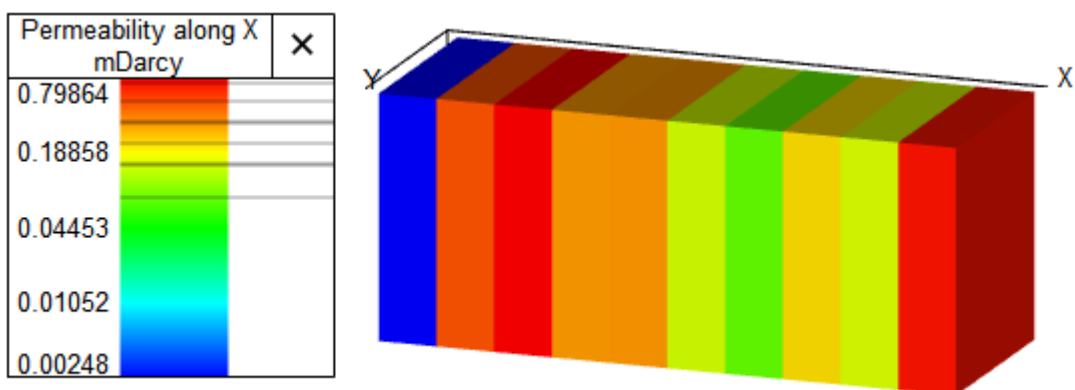


Figure 47: Spatial Distribution of Permeability in Sample K2

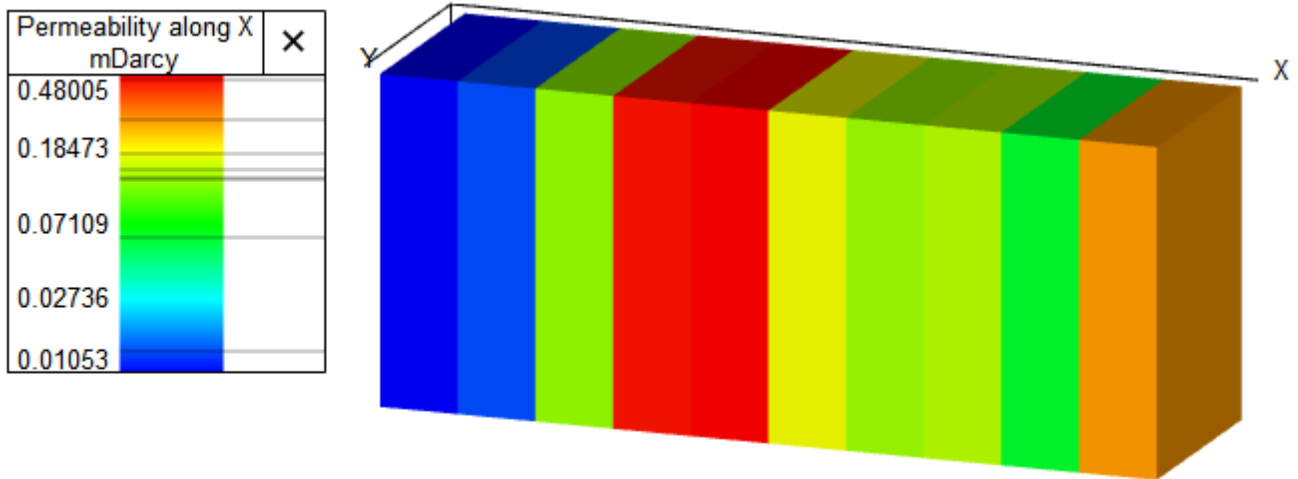


Figure 48: Spatial Distribution of Permeability in Sample K3

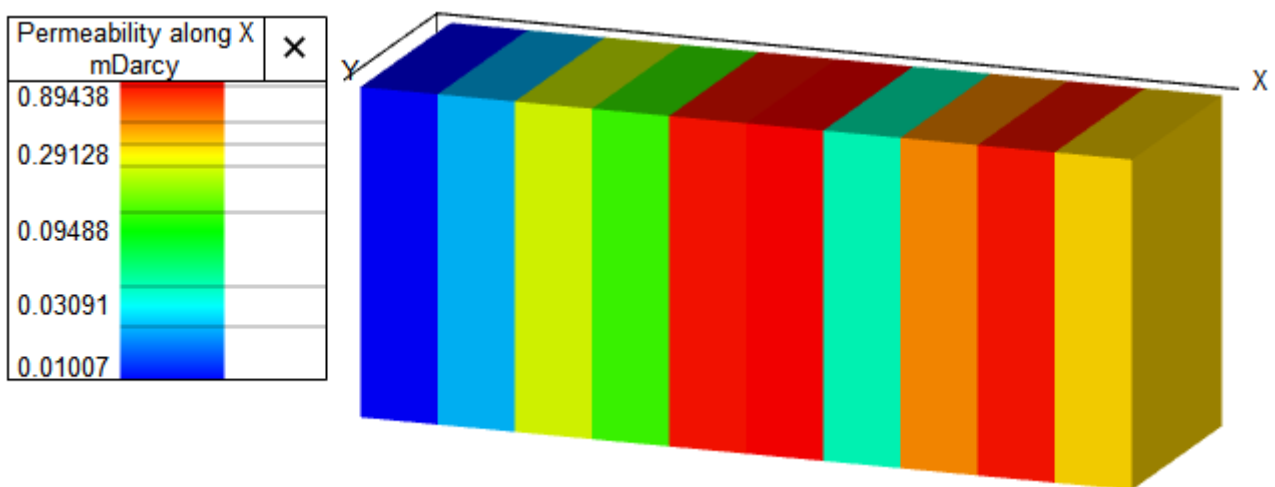


Figure 49: Spatial Distribution of Permeability in Sample K4

4.6 Spatial Distribution of Porosity

Upon selecting the best misfit for each sample for the heterogeneous Model, the result is further ran on @tNavigator in order to ascertain the spatial distribution of porosity for the best result with the minimum uncertainty which is believe to be the real spatial distribution of the core Samples.

Below are the graphical representations of the core samples.

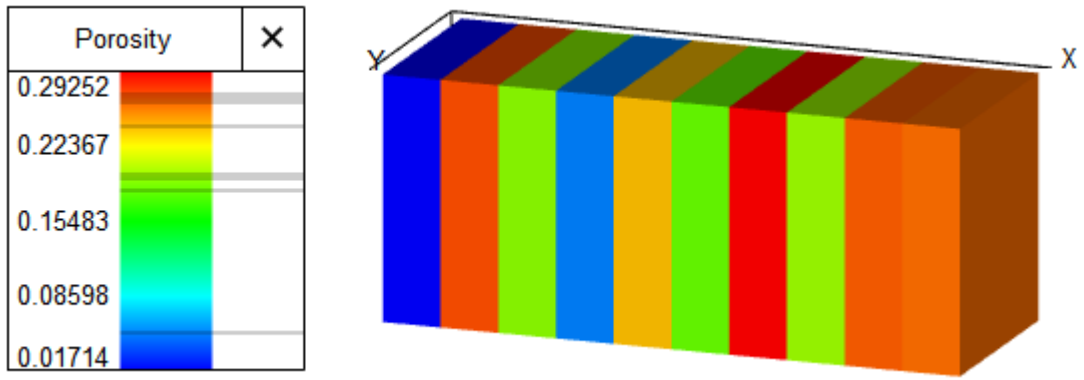


Figure 50: Spatial Distribution of Porosity in Sample K1

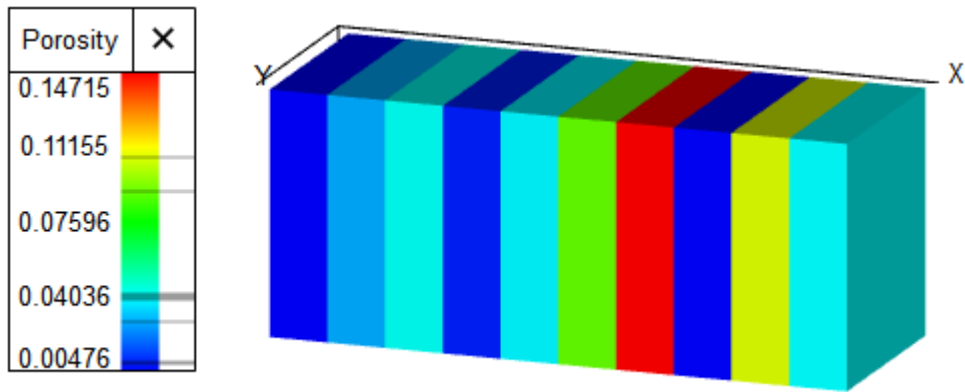


Figure 51: Spatial Distribution of Porosity in Sample K2

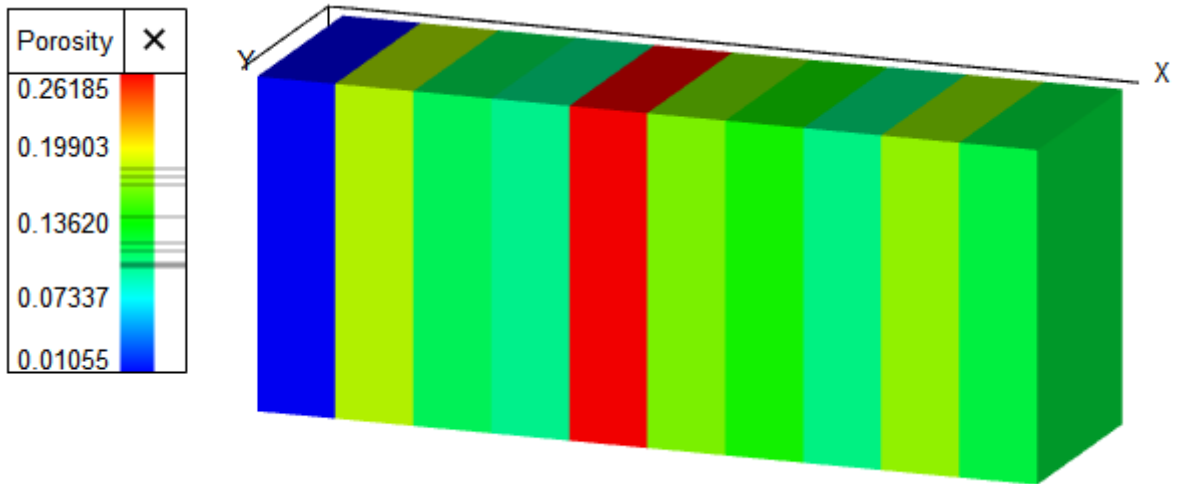


Figure 52: Spatial Distribution of Porosity in Sample K3

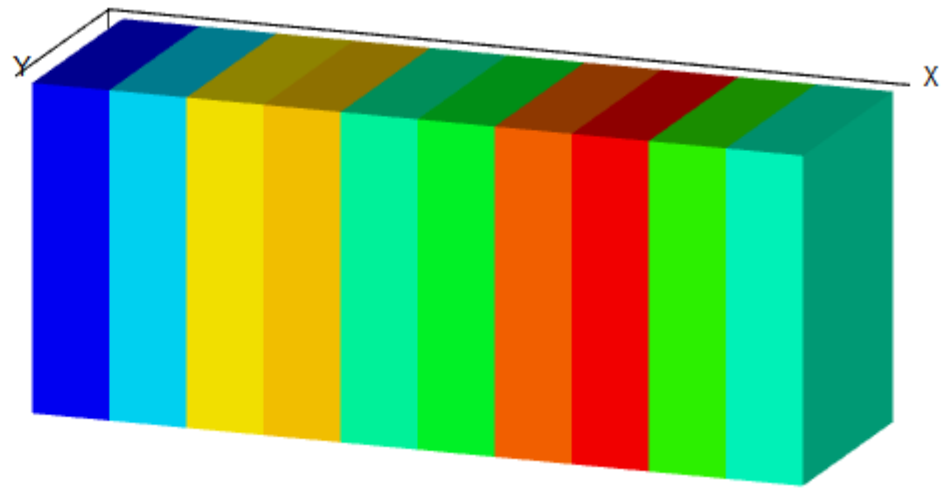
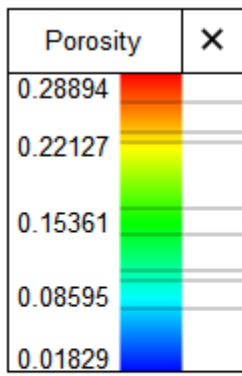


Figure 53: Spatial Distribution of Porosity in Sample K4

CHAPTER FIVE (5)

5.0 Conclusion and Recommendation

The main issues discussed/addressed in this thesis are improving Oil recovery in carbonate samples, translating the laboratory experiment done on carbonate core plugs to a reservoir scale and doing the stochastic History Matching using Particle Swarm Optimization Algorithm. Four carbonate rock samples were tested in the laboratory to evaluate the permeability, porosity and the recovery of the oil. From the experimental results in this thesis, the following conclusions can be drawn:

- The potential of Improved Oil Recovery (IOR) on carbonate rock samples by low salinity (brine) coreflooding has been investigated through both the laboratory measurement and the fluid flow simulation. Results show that both investigations indicate that the potential is high as it can be seen from the Oil Recovery which was between 38% - 42% percentage and this is reasonable for a secondary recovery coreflooding with brine.
- Ageing done on sample K4 shows that ageing increases the oil recovery during water coreflooding.
- Eclipse 100 (Black Oil Simulator) gives a reliable simulation results for water coreflooding experiment; this can be seen from the accurate representation of the real life scenario using the laboratory results in the simulator.
- The History Match parameters for the production history from numerical modelling and from the laboratory experiments of hours of pressure build up test produces nearly identical effective reservoir permeability of 0.01 - 0.02mD and 0.146mD. We can conclude that there is a presence of interconnected micro-fractures as the main contributing factors.
- The simulated waterflood indicates that only the interconnected micro-fractures can provide a flow paths and the oil volume to be produced as the incremental Improved Oil Recovery contribution

- Using the Particle Swarm Optimization Algorithm, a lower misfit provides a better match of the production history and also, the sampling behavior of the optimization algorithm has a direct impact on the prediction/forecast.
- For a heterogeneous Model, using higher particle number and a higher iteration provides more realistic results and gives a better understanding of the result because the convergence can occur at a higher iteration.
- Uncertainty Quantification using stochastic - Particle Swarm Optimization Algorithm seems to be a good approach for predicting and forecasting models in the Reservoir modelling field.

5.1 Recommendation

In the future work, I recommend that the coreflooding should be carried out with the use of a back pressure at the outlet or the production well in order to enable an accurate measurement of the pressure difference. Also, looking at the slight disparity in the values of permeabilities measured in the laboratory and that of the simulation, it is imperative to integrate Digital Rock Physics with coreflooding experiment in order to ascertain the actual permeability of the core plugs. In future work, the injected volume should be measured and ensure it is equal to the pore volume calculated of the core plugs in order to be able to ascertain a more accurate injection rate for the coreflooding. Lastly, considering a comparison between geostatistical History Matching and the Assisted History Matching will be an interesting area to consider under the carbonate rock samples in the future.

Works Cited

- [1] F. A. S. A. I. H. Pulok Kanti Deb, "Nonlinearity and Solution Techniques in Reservoir Simulation: A review," *Journal of Natural Gas Science and Engineering* , vol. 46, pp. 845-864, 2017.
- [2] P. K. Deb, "A finite Volume Approach for the Numerical Analysis and Solution of the Buckley-Leverett Equation Including Capillary Pressure," 2018.
- [3] PWC, 2019. [Online]. Available: <https://www.strategyand.pwc.com/gx/en/insights/industry-trends/2018-oil-gas.html>. [Accessed 06 April 2019].
- [4] R. a. K. M. P. Zitha, "Society of Petroleum Engineering," [Online]. Available: <https://www.spe.org/en/industry/increasing-hydrocarbon-recovery-factors/>. [Accessed Saturday April 2019].
- [5] T. Ahmed, *Reservoir Engineering Handbook*, Third Edition.
- [6] J. e. a. Ferreira, "The importance of outcrop Reservoir Characterization in Oil- Industry Facies Modelling workflows - a case study from the Middle Jurassic of the Mecico Calcario Estremenho, Portugal," in *Abu Dhabi International Petroleum Exhibition & Conference* ., Abu Dhabi, 2016.
- [7] A. C. Azerêdo, "Formalização da litostratigrafia do Jurássico Inferior e Médio do Maciço Calcário Estremenho (Bacia Lusitânica)," *Comunicações Geológicas (INETI)*, vol. 94, p. pp. 29–51, 2007.
- [8] M. N. J Adhunandan P.P, "Effects ot wettability on waterflood Recovery for crude oil/Brine/rock systems," in *SPE 66TH Annual Technical Conference and Exhibition* , Dallas, October 6 -9, 1991.
- [9] M. Avasare, "Digital Rock Physics for coreflooding Simulation," Lisbon, 2016.
- [10] Y. Afinogenov, "How the liquid permeability of rock is affected by the pressure and temperature," *SNIGIMS* , pp. 34-42, 1969.
- [11] J. B. J. W. AMYX, *Petroleum Reservoir Engineering*, New York: McGraw - Hill Book Co.,, 1960, pp. 36 - 132.
- [12] B. M. J. e. al, "Pore Scale Imaging and Mmodelling," vol. 51, 2013.
- [13] Okandan E., "PhD Dissertation," Stanford University , California , 1973.
- [14] Mungan N., "Inerfacial effects in immiscible Liquid - Liquid Displacement in Porous Media," *Society of Petroleum Engineering Journal*, pp. 247 - 253, 1966.
- [15] M. B. M. Amro, "Pressure and Temperature Effect on Petrophysical Characteristics: Carbonate Reservoir Case," pp. 5-6, Jan 2009.
- [16] A. D. Owen W.W, "Effects of rock wettability on Oil - Water Relative Permeability Relationship," *Journal of Petroleum Technology*, pp. 873 - 878, July 1971.
- [17] A. R. H. Sinnokret, "Effect of Temperature level Upon Capillary pressure curves," *Society Petroleum Engineering Journal*, p. 13, March, 1971.
- [18] J. S. R. J. S. S. Marsden, "Effect of Temperature on Petro physical Properties of the reservoir rock," *society petroleum engineer journal* , pp. 171-180, June, 1970.

- [19] S. Y. S. H. A. M. , E. I. R. H. J. Poston, "The effect of temperature or irreducible water saturation and relative water Permeability of unconsolidated sands," *Society of Petroleum Engineer Journal*, pp. 171 - 180, June 1970.
- [20] C. F. F, "The Reservoir Engineering Aspect of Waterflooding," *Society of Petroleum Engineers*, vol. 3, 1971.
- [21] W. Anderson, "Wettability Literature Survey _Part 1; Rock/oil/Brine interactions and the effects of core handling on wettability," *Journal of Petroleum Technology*, vol. 38, no. 10, pp. 1125 - 1144, 1986.
- [22] A. H. A. M. I. C. I. Dullien F. A. I, "Wettability and Immiscible Displacement in Pembina Cardium Sand stone," *Journal of Petroleum Tecnology*, pp. 63 - 74, 1990.
- [23] S. B. Ugar Karabakal, "Determination of wettability and its effect on the waterflood performance in Limestone Medium," *Energy & Fuels*, pp. 438 -449, 2004.
- [24] B. J. M. N. Jia D, "CONTROL OF CORE WETTABILITY WITH CRUDE OIL," in *SPE International Symposium on Oil Field Chemistry* , Anaheim, CA, FEBRUARY 20 - 22 1991.
- [25] M. N. Tang G.Q, "Effecct of temperature, Salinity and Oil Composition on Wetting Behaviour and oil Recovery by Water - Flooding," in *SPE Annual Technical Conference and Exhibition*, Denver, CO, October 6 - 9, 1996.
- [26] M. K. K. H. D. H. M. Chang Y.C, "The impact of wettability and Core Scale Heterogeneities on Relative Permeability," *Joint Petroleum Science Engineering* , pp. 1 - 19, 1997.
- [27] T. L. A. D. Raza S.H, "Wettability of Reservoir Rocks and its Evaluation," *Prod Mon*, pp. 2 -7, 1968.
- [28] T. R. D. Donaldson E. C, "Microscopic Observation of oil Displacement in Water- wet and Oil - wet system.," in *SPE Annual Meeting*, New orleans, LA, october 3 - 6, 1971.
- [29] V. B. B. B. A. Graue A, "A reproducible wettability alteration of Low - permeable outcrop Chalk," in *SPE/DOE Improved Oil Recovery Symposium* , Tulsa, Ok, April 19 - 22 1998.
- [30] Z. X. M. N. Z. X. Ma S. M, "Characterization of wettability from spontaneous Imbibition Measurements," *Journal of Petroleum Technology*, p. 38, 1999.
- [31] M. N. R, "Wettability and its effects on Oil Recovery," *Journal of Petroleum Technology*, pp. 1476 - 1484, 1990.
- [32] N. S. M. Xianmin Zhou, "Interrelationship of Wettability, Initial Water Saturation, Aging Time, and Oil Recovery by Spontaneous Imbibition and Waterflooding," *Society of Petroleum Engineers*, vol. 5, no. 02, pp. 199-207, June 2000.
- [33] R. K. P. Somasundaran, "A new streaming potential apparatus and study of temperature effects using it," *Journal of Colloid and Interface Science*, vol. 45, no. 3, pp. 591-600, December 1973.
- [34] S. M. T. Kittaka, "Surface conductance of silica in electrolyte solutions," *Journal of Colloid and Interface Science*, vol. 55, no. 2, pp. 431-439, May 1976.
- [35] P. P.Jadhunandan, "Effect of Brine composition, crude oil, and ageing conditions on wettability and oil recovery," New Mexico, 1990.
- [36] F. N. D.M. Grist, "The Dependence of Water Permeability On Core Cleaning Methods In the Case of Some

Sandstone Samples," *Journal of Canadian Petroleum Technology*, vol. 14, no. 2, April 1975.

- [37] H. W. Jr., *The Reservoir Engineering Aspect of Waterflooding*, Second edition, Society of Petroleum Engineers, 2015.
- [38] W. O. L.E.Treiber, "A Laboratory Evaluation of the Wettability of Fifty Oil-Producing Reservoirs," *Society of Petroleum Engineers Journal* , vol. 12, no. 06, pp. 531-540, December 1972.
- [39] K. T. N. M. J.S Buckley, "Influence of Electrical Surface Charges on the Wetting Properties of Crude Oils," *Society of Petroleum Engineers*, vol. 4, no. 03, pp. 332-340, August 1989.
- [40] A. S. Khalid Aziz, *Petroleum Reservoir Simulation*, London: Applied Science Publishers LTD, 1979.
- [41] M. E. H. & M. R. Islam, "Knowledge – Based Reservoir Simulation – A Novel Approach," *International Journal of Engineering* , vol. 3, no. 6, pp. 622-638, 2010.
- [42] C. H. B., *Modern Reservoir Engineering: A simulation Approach*, Englewood Cliffs N.J: Prentice-Hall, 1977.
- [43] S. M. & M. R. Islam, "State-of-the-art Petroleum Reservoir Simulation," *Petroleum Science and Technology*, vol. 26, no. 10 -11, pp. 1303 -1329, 2008.
- [44] V. D. L. M. a. M. A. C. Yasin Hajizadeh, "Comparison of Elvolutionary and Swarm Intelligence Methods for History Matching and uncertainty quantification in Petroleum Reservovir Models," in *Intelligent Computational Optimization In Engineering.Studies in Computational Intelligence*, vol. 366, M. K. e. al, Ed., Berlin, Springer-Verlag Berlin Heidelberg, 2011, pp. 209-240.
- [45] A. O. S. D. J. S. a. C. M. Goncalo Soare Oliveira, "Reducing uncertainty in reservoir parameters combining history matching and conditioned geostatistical Realizations," *Journal of Petroleum Science and Engineering*, vol. 156, pp. 75-90, July 2017.
- [46] G. S. a. A. A. Mario Koppen, *Intelligent Computational Optimization in Engineering: Techniques and Applications*, Verlag Berlin Heidelberg: Springer, 2011.
- [47] I. S. Methods, "Suggested Methods for Determining water content, porosity, density, absorption and related properties and swelling and slake-durability index properties," ISRM, 1977.
- [48] A. B. Pinto, "An integrated approach based on coreflooding and digital rock physics techniques to rock porosity and permeability characterization," Lisbon, Portugal, May 2019.
- [49] L. A. S. K. M. V. R. N.Hadia, "Experimental and numerical investigation of one dimensional waterflood in porous reservoir," *Experimental Thermal and Fluid Science*, vol. 32, no. 2, pp. 355 - 361, 2007.
- [50] H. M. Lo, "Effect of temperature on water - wet systems," in *48th Annual Fall Meeting of Society of Petroleum Engineers* , Las Vegas, Nevada, Sept - Oct., 1973.
- [51] W. A. D. owens, "Effect of Rock wettability on oil - wet relative Permearbility Relationship," *Journal of Petroleum Technology*, pp. 873 - 878, JULY, 1971.
- [52] G. Willhite, *Water Flooding*, Texas: Society of Petroleum Engineers Textbook series, 1986.
- [53] S. R.A, "Oil Recovery byt the surface Fim drainage in mixed - wettability rocks," *JPT*, .
- [54] H. P. K., "omputed Tomography as A core Analysis Tool: Applications, Instrument Evaluation and Image

Improvement Techniques," *Journal of Petroleum Technology*, vol. 40, p. 88, 1988.

- [55] H. e. al, "Introduction to Digital Rock Physics and Predictive Rock Properties of Reservoir Sandstone.," in *IOP Conference Series: Earth and Environmental Science*, 2017.
- [56] R. L. O.R. Wager, "Improving Oil Displacement Efficiency by Wettability Adjustment," *Society of Petroleum Engineers*, vol. 216, no. 01, pp. 65-72, 1959.
- [57] P. K. Deb, "A finite Volume Approach for the Numerical Analysis and Solution of Buckley-Leverett Equation Including Capillary Pressure," Newfoundland, October 2018.

APPENDIX A: Laboratory experiment results:

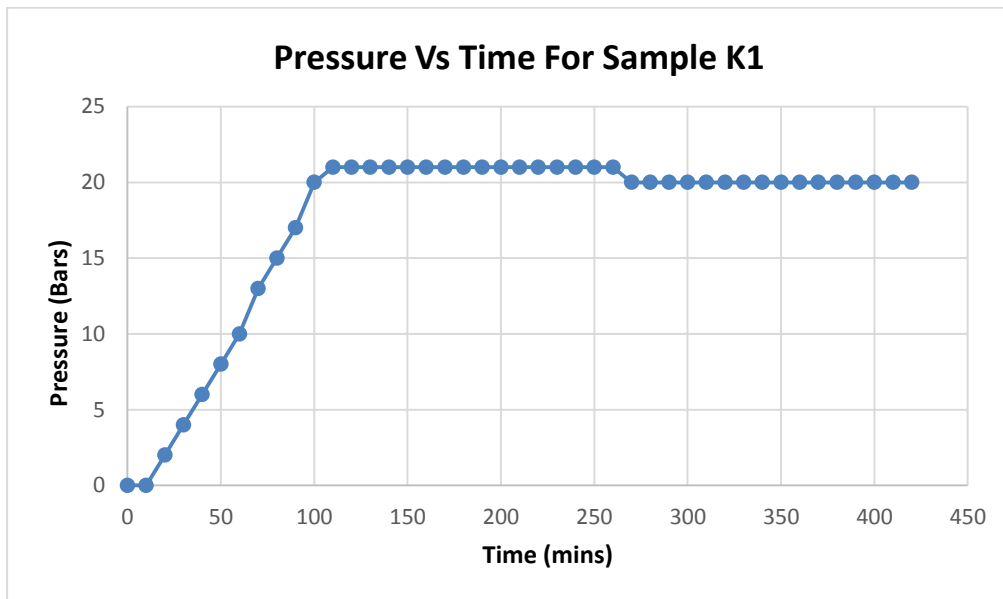


Figure A 1: Pressure versus time plot for samples

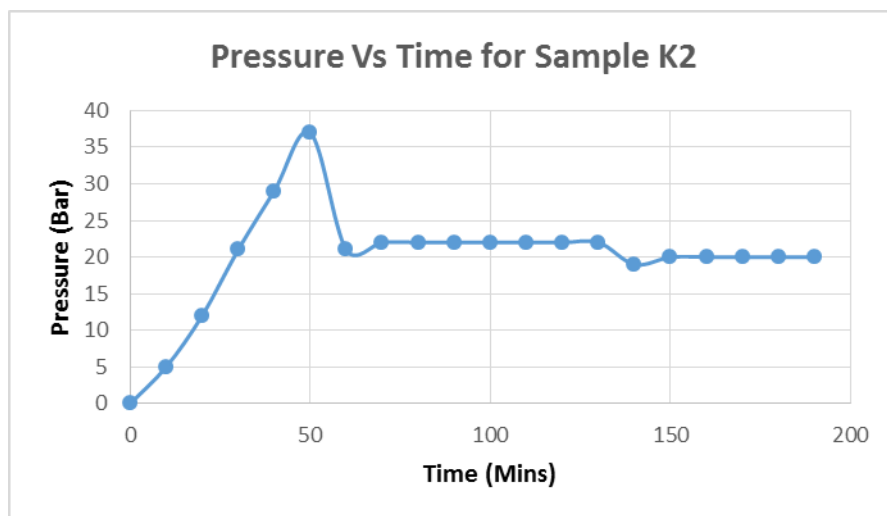


Figure A 2: Pressure versus time plot for K2 sample

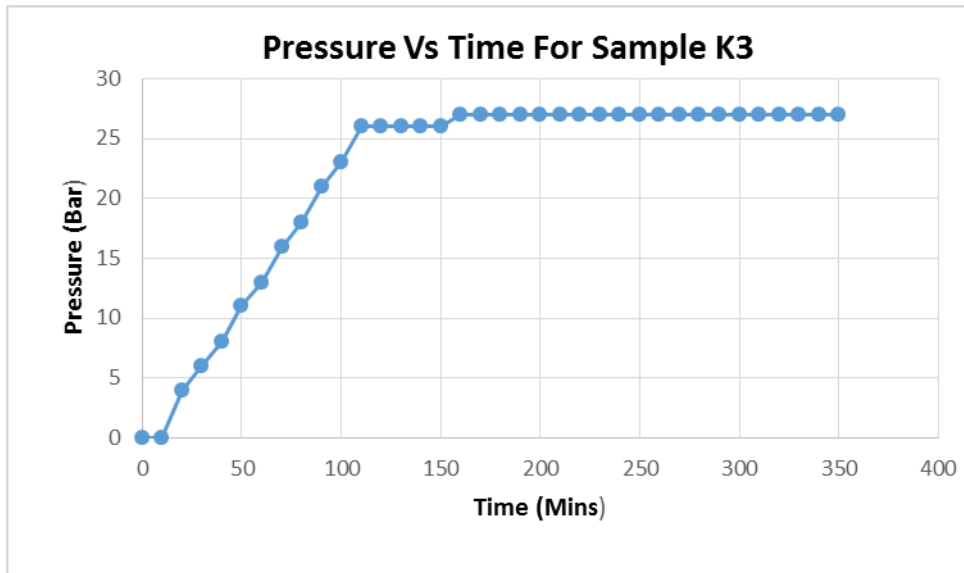


Figure A 3: Pressure versus Time

APPENDIX B: Production Rate for all the samples

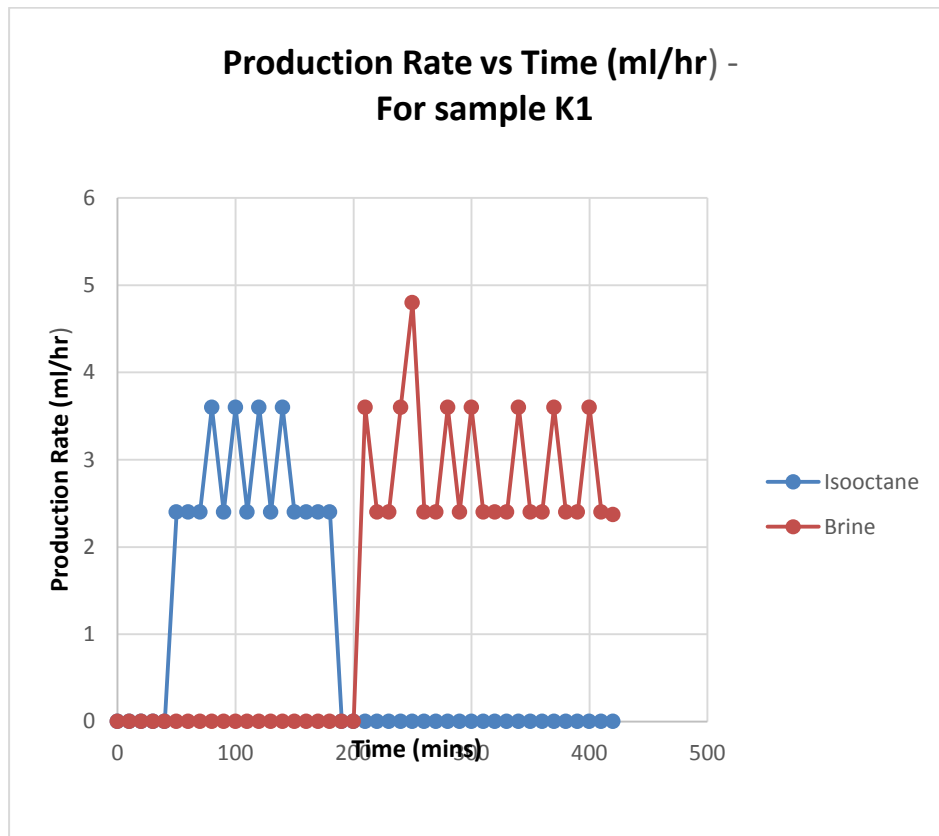


Figure B 1: Production rate versus time for K1 Samples

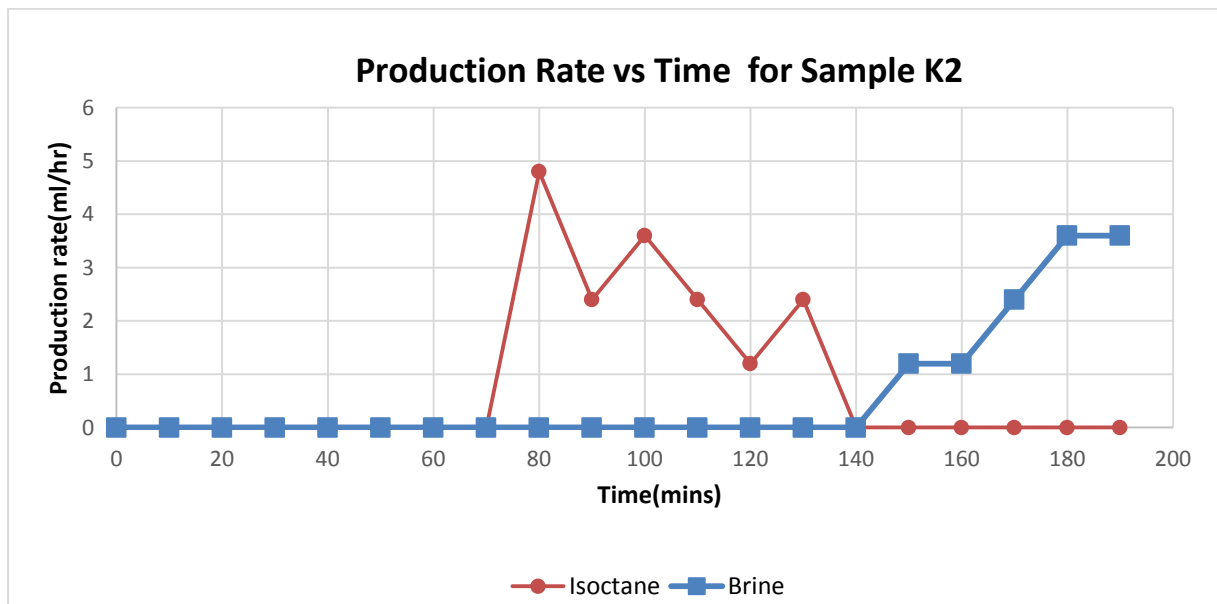


Figure B 2: Production rate versus Time for K2 Sample

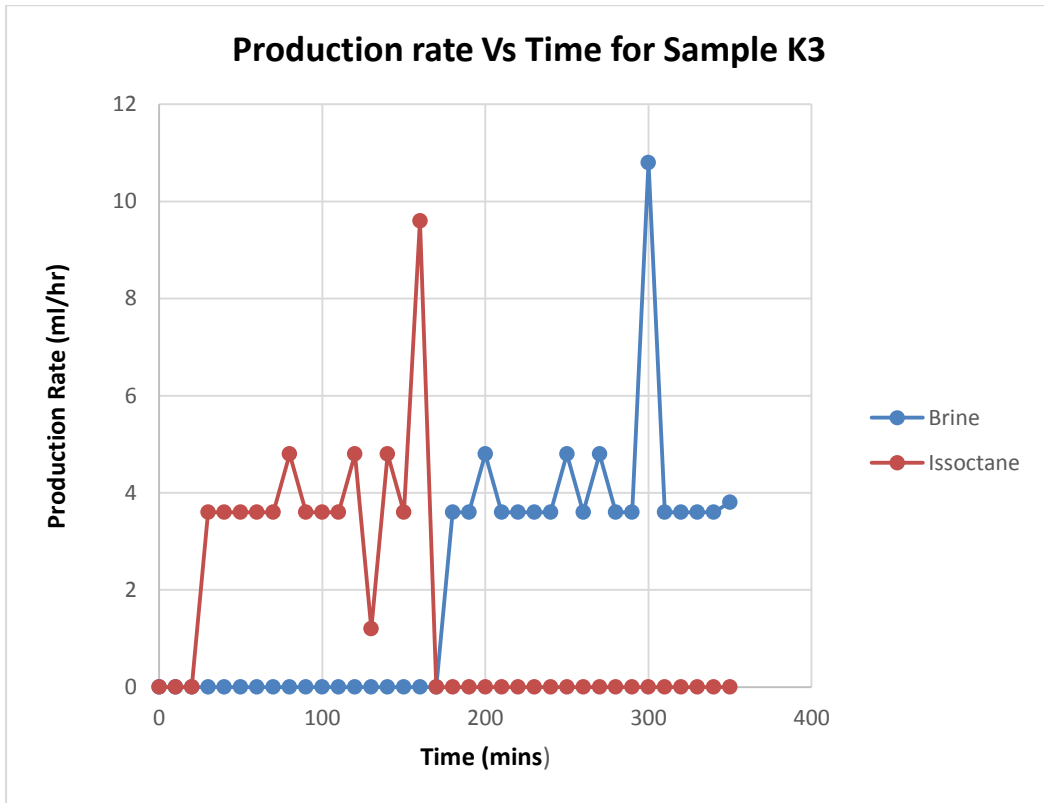


Figure B 3: Production Rate Versus Time for K3 SAMPLE

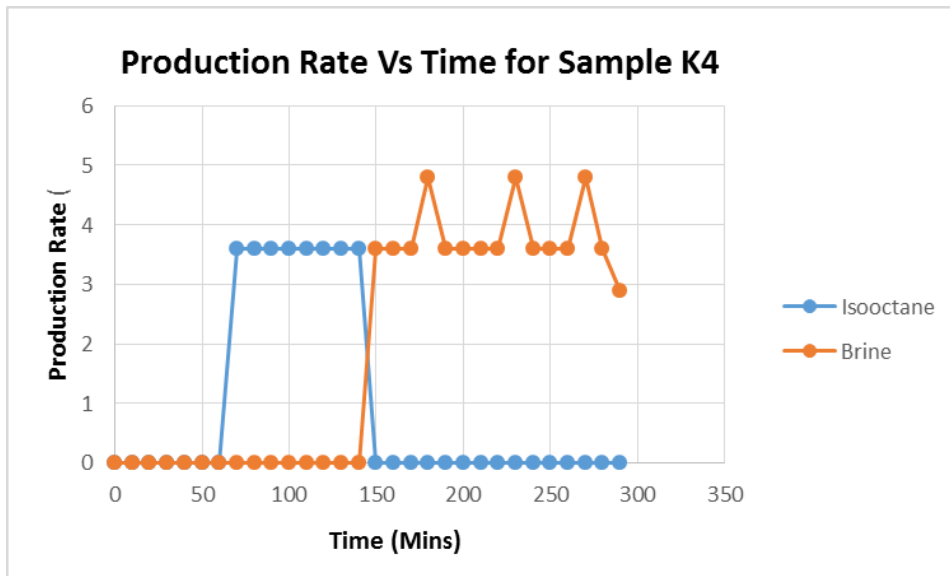


Figure B 4: Production rate versus Time for sample K4

APPENDIX C: FLUID FLOW SIMULATION PLOTS

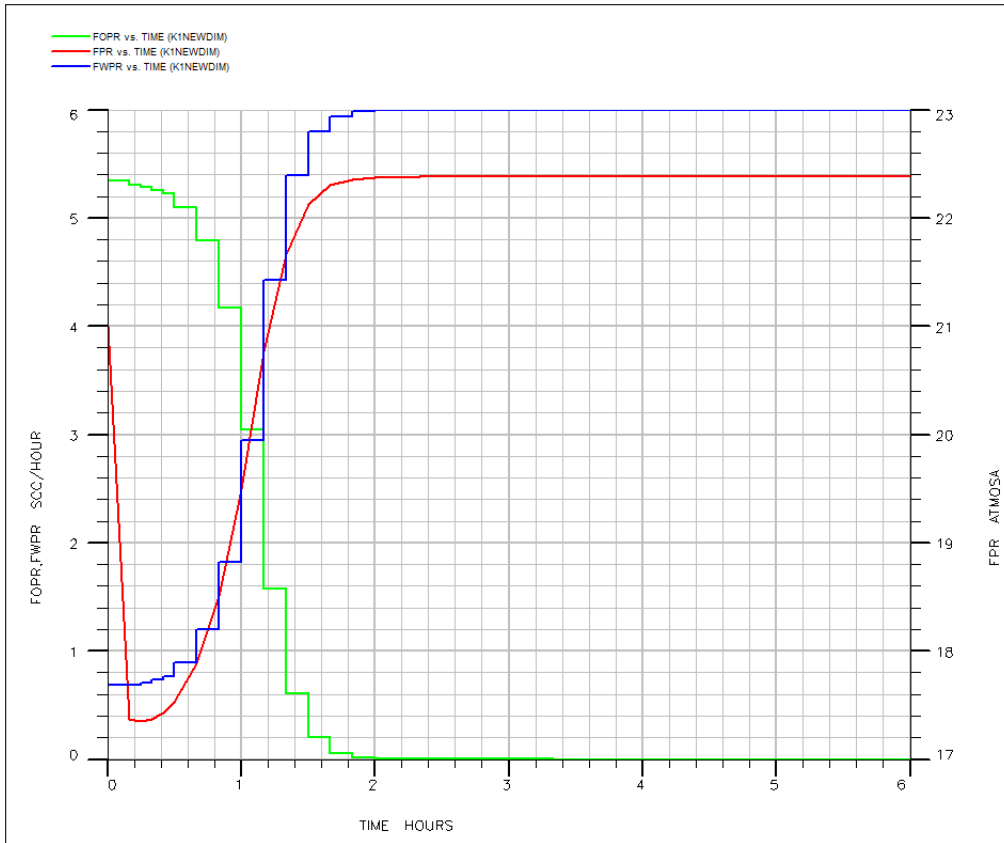


Figure C 1; Production History plot over time (FOPR, FPR and FWPR) FOR K1 sample

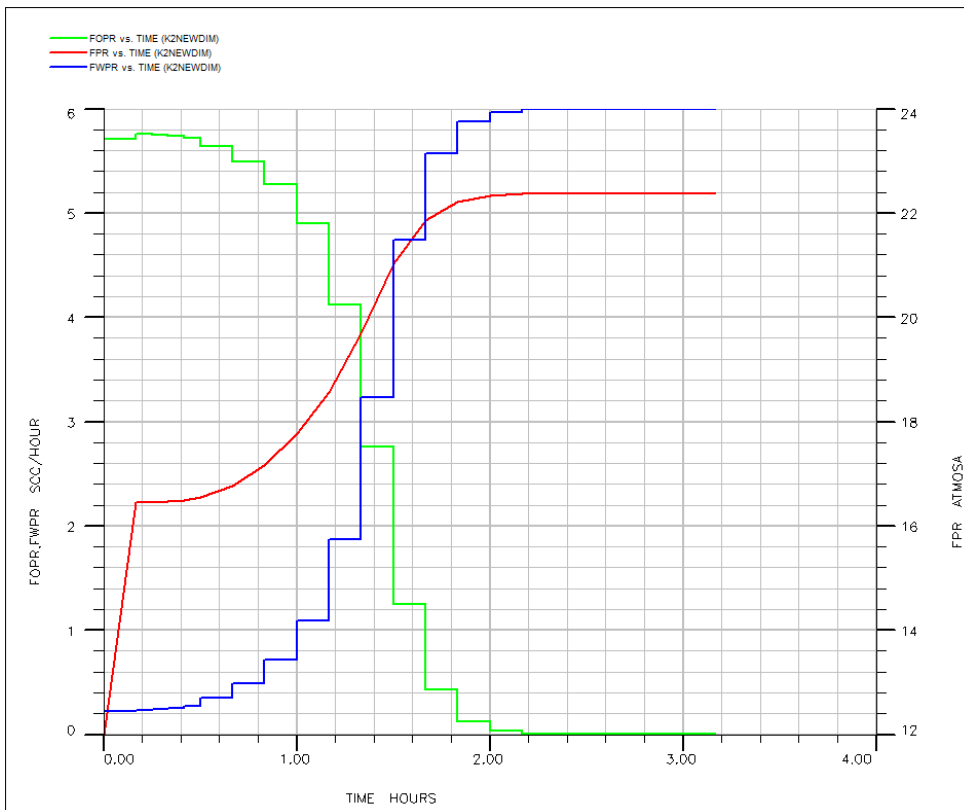


Figure C 2: Production History plot over time (FOPR, FPR and FWPR) FOR K2 sample

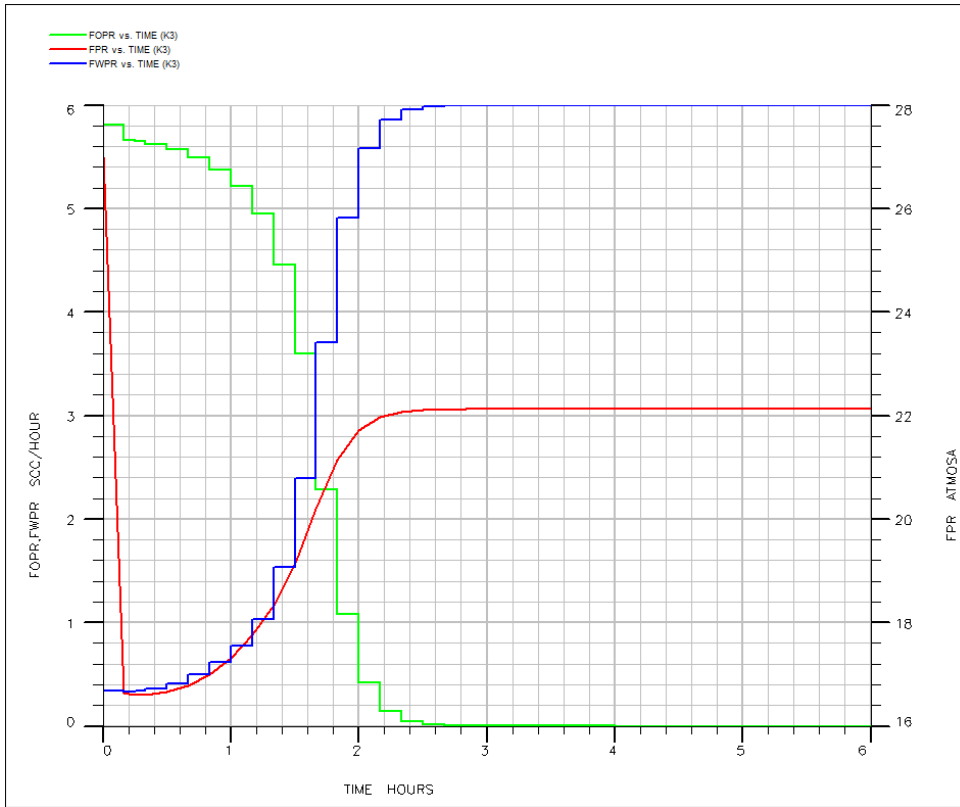


Figure C 3: Production History plot over time (FOPR, FPR and FWPR) FOR K3 sample

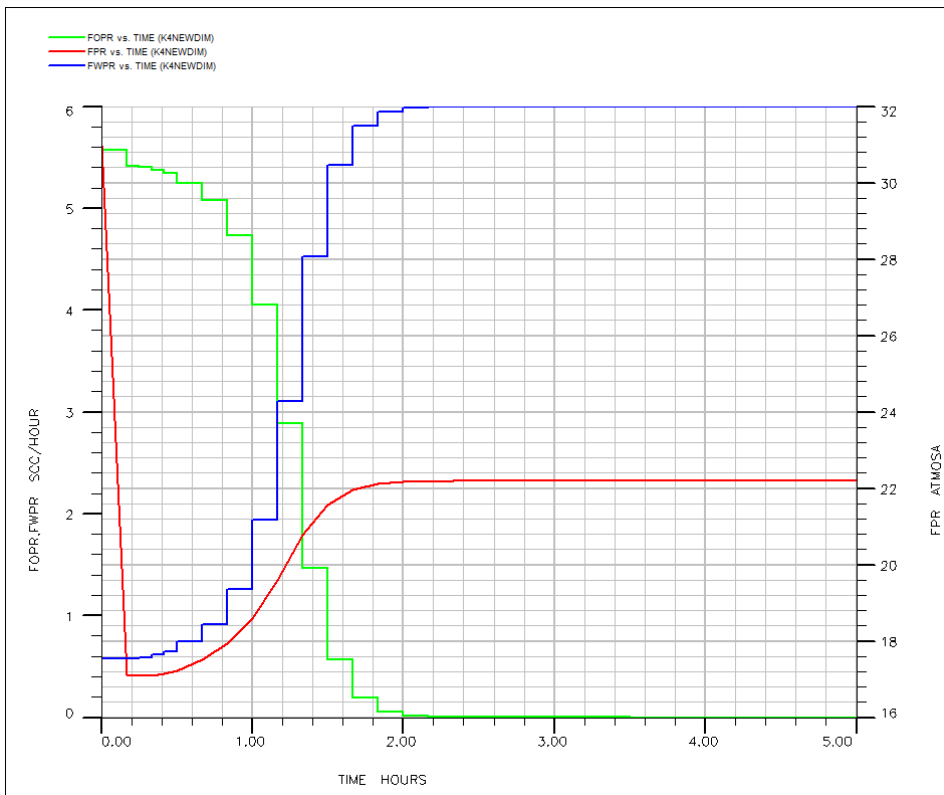


Figure C 4: Production History plot over time (FOPR, FPR and FWPR) FOR K4 sample

APPENDIX D: History Matching Results for Homogeneous system

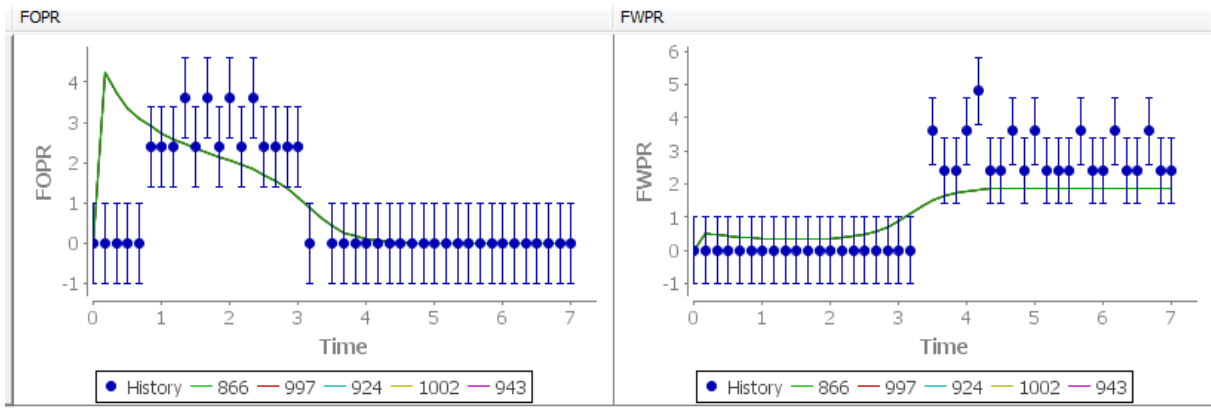


Figure D 1: Best fit Match for sample K1

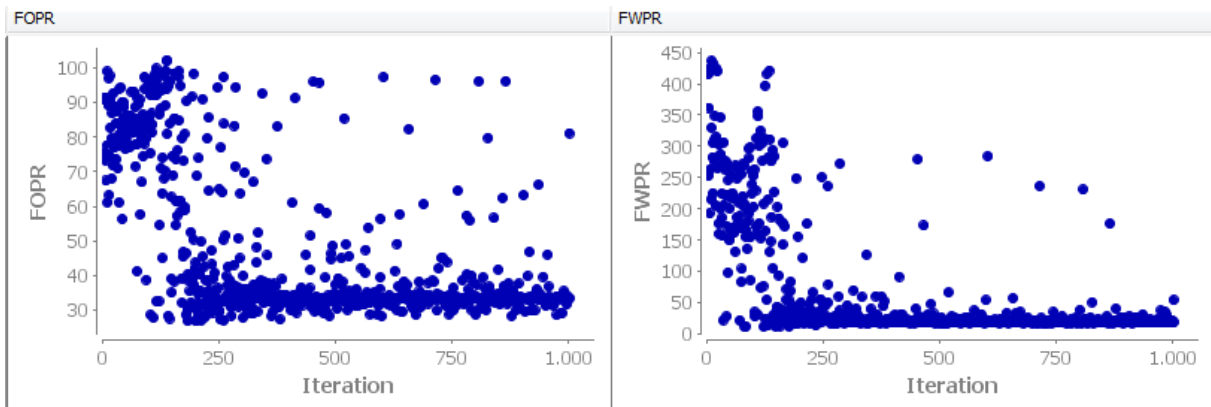


Figure D 2: Misfit Component of the FOPR and FWPR For Sample K1

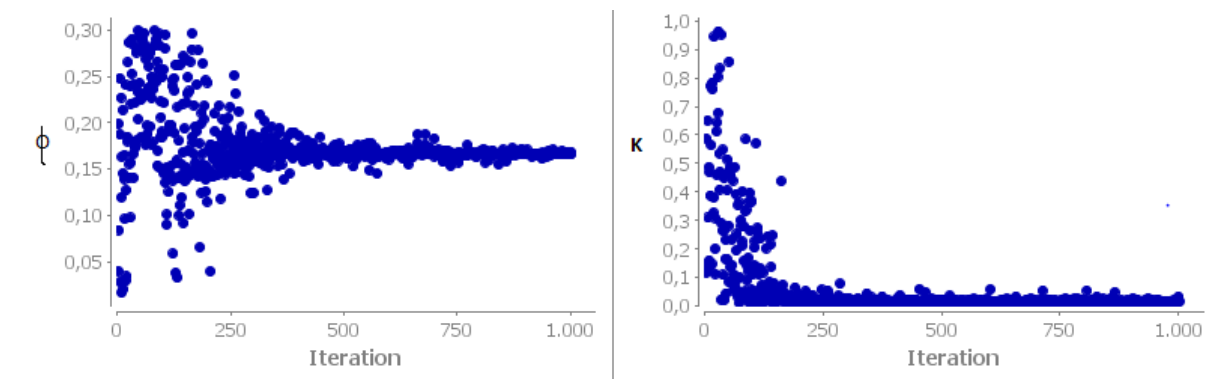


Figure D 3: Parameter (porosity and permeability) versus Iteration for sample K1

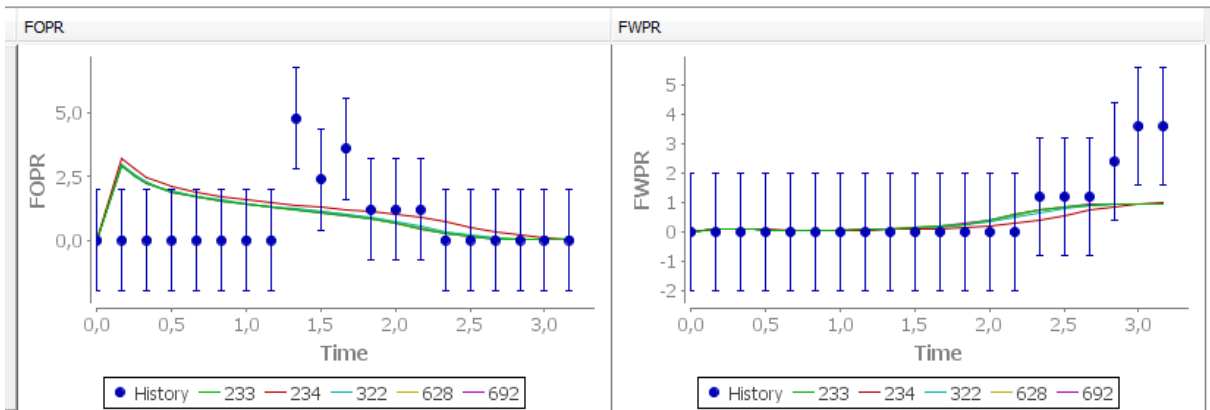


Figure D 4: Best fit History Match for sample K2

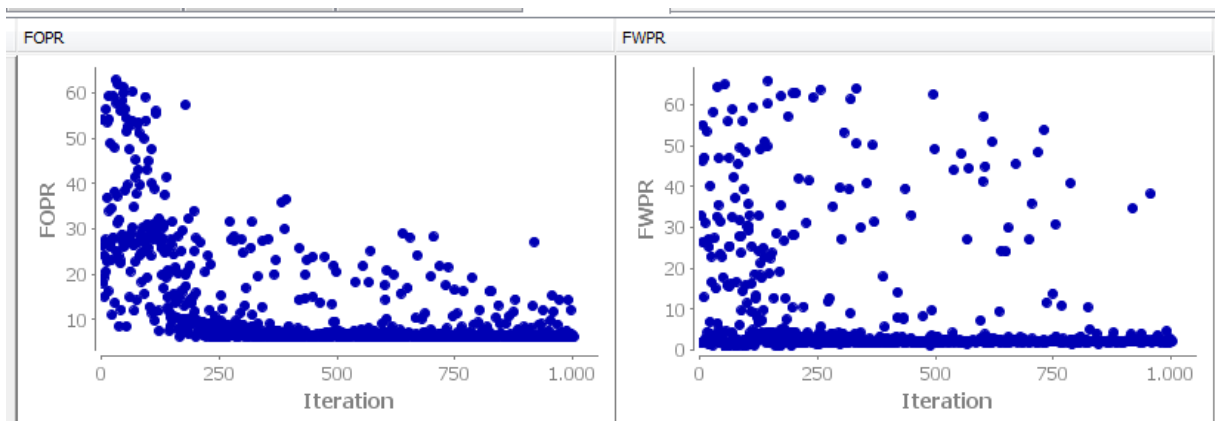


Figure D 5: Misfit Component for Sample K2

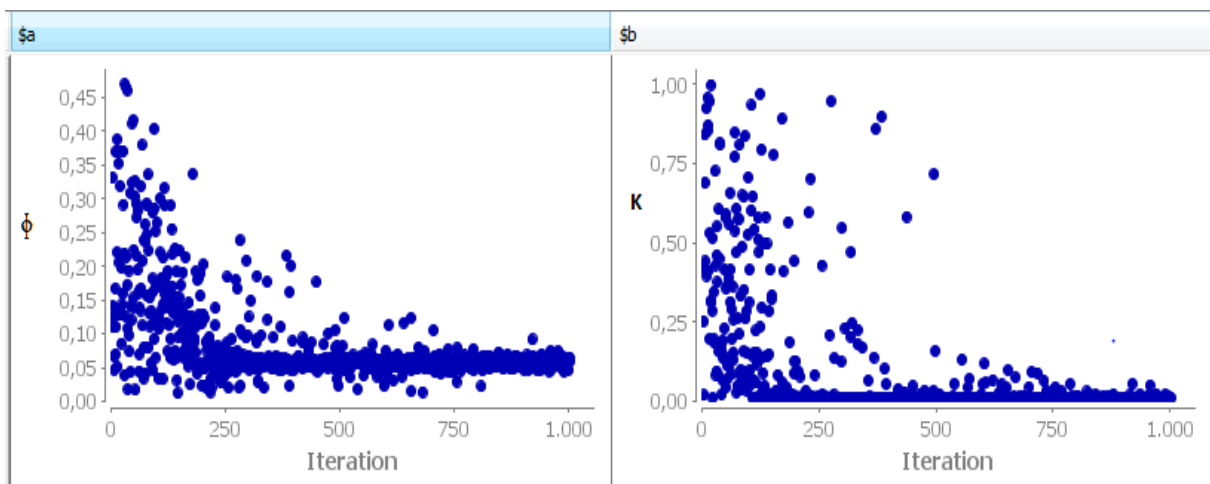


Figure D 6: Parameter (porosity and permeability) versus Iteration for sample K2

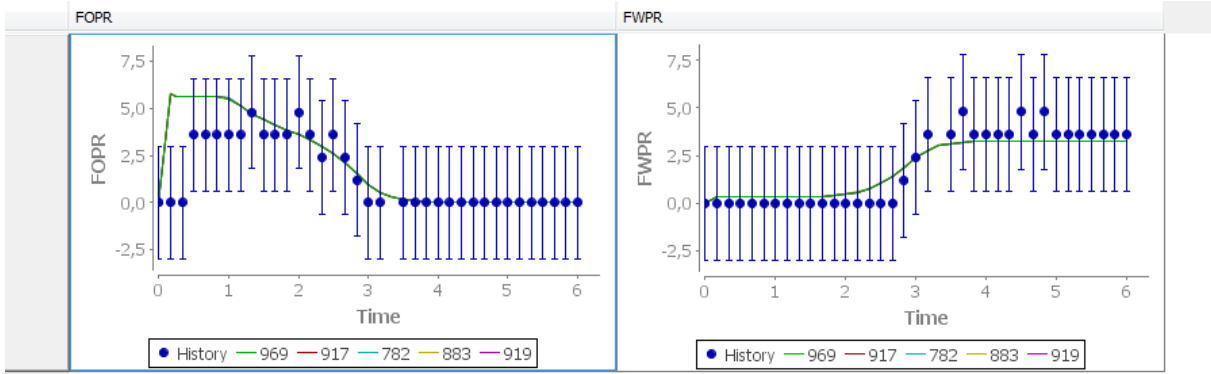


Figure D 7: Best Fit History Match for Homogeneous K3 sample

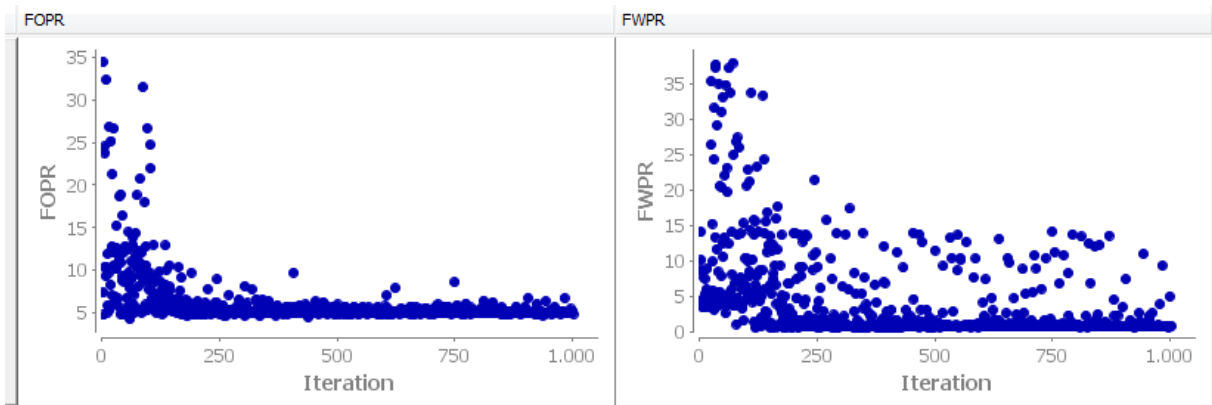


Figure D 8: Misfit component versus Iteration for homogeneous K3 sample

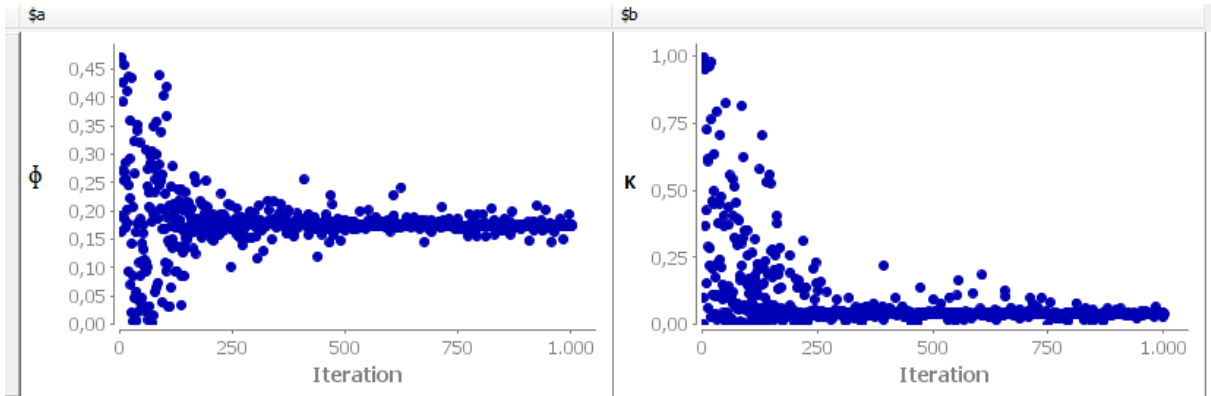


Figure D 9: Parameter (porosity and permeability) versus Iteration for Homogeneous K3 sample

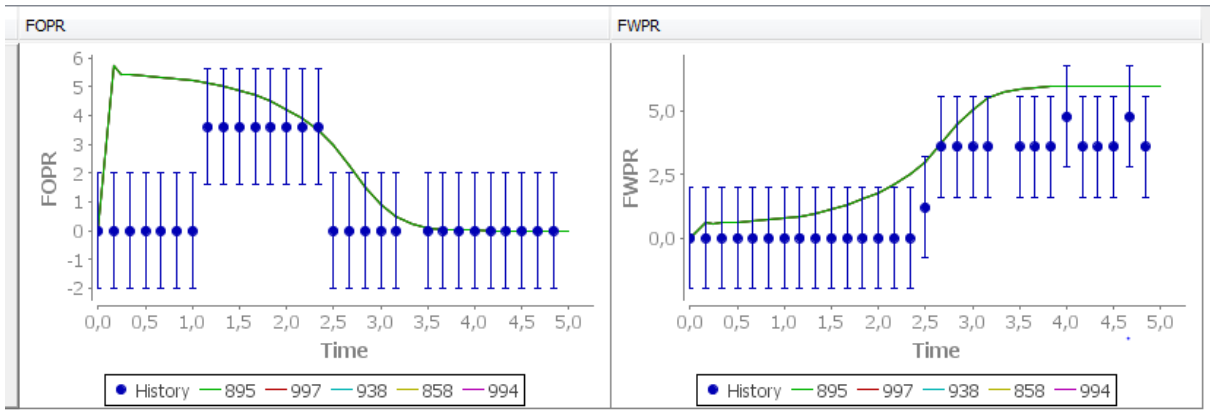


Figure D 10: Best fit History Matching for Homogeneous K4 Sample

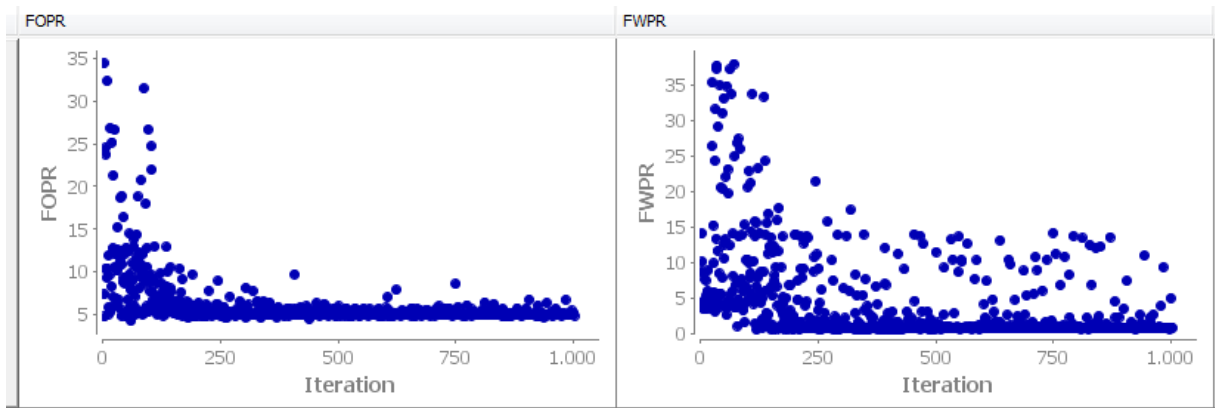


Figure D 11: Misfit component for Homogeneous K4 sample

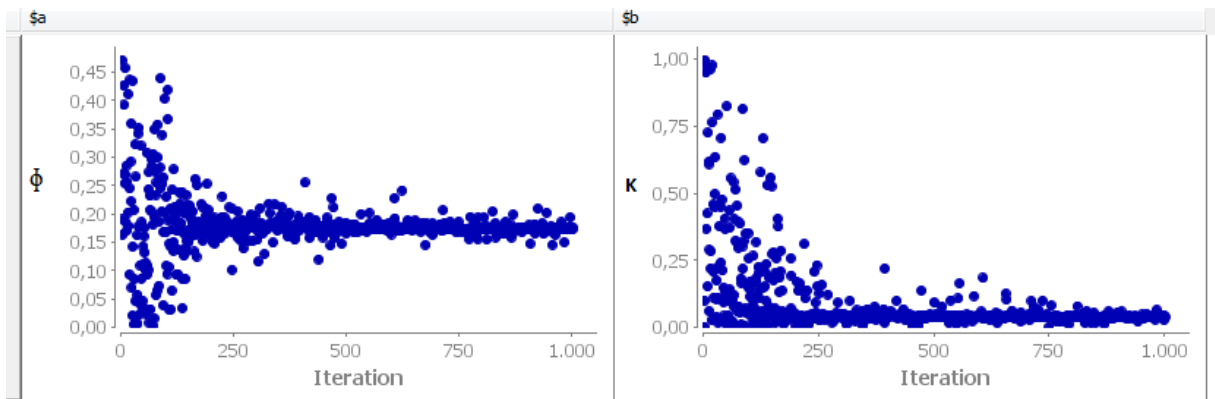


Figure D 12: Parameter (porosity and permeability) versus Iteration for Homogeneous K4 sample

APPENDIX E: History Matching Results for Heterogeneous System

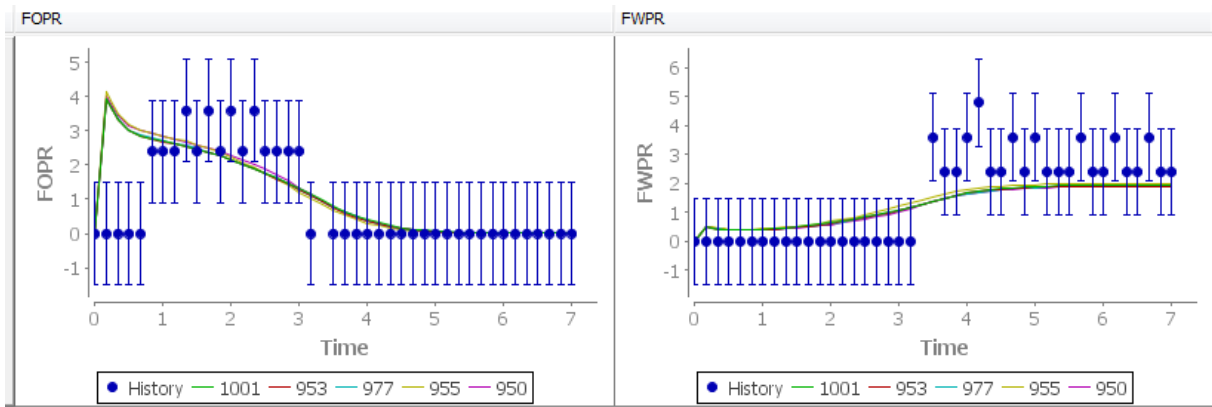


Figure E 1: Best fit History Matching for Heterogeneous K4 SAMPLE

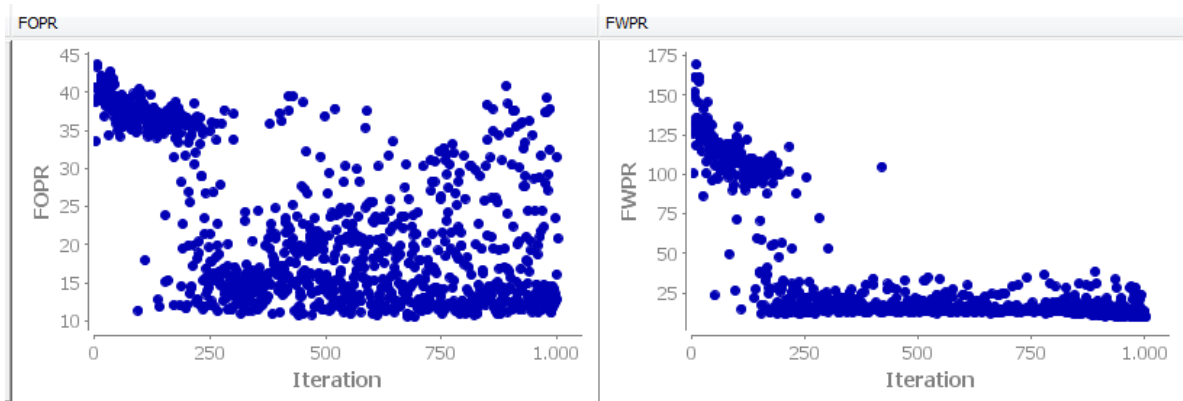


Figure E 2: Misfit Component for Heterogeneous K4 sample

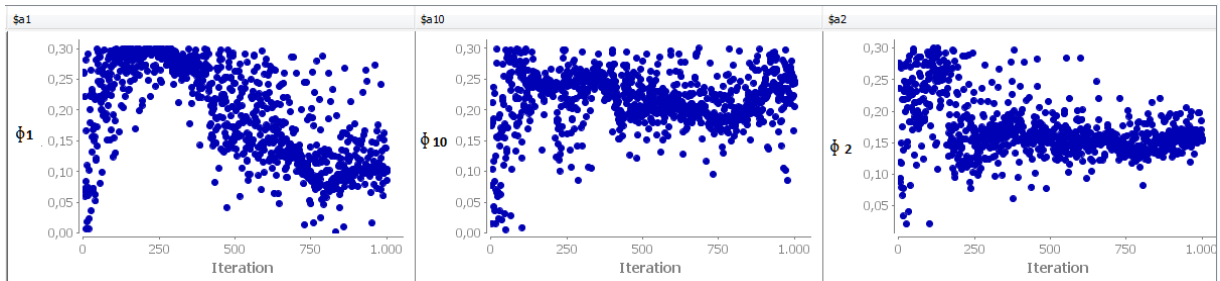


Figure E 3: Parameter (Porosity) versus Iteration for Heterogeneous K4 Sample

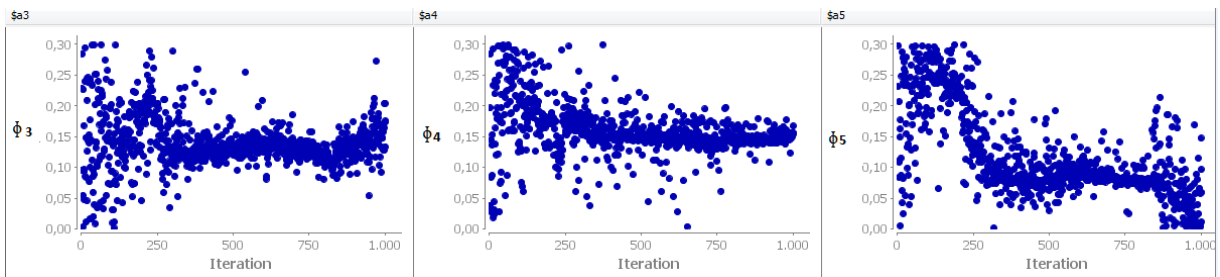


Figure E 4: Parameter (Porosity) versus Iteration for Heterogeneous K4 Sample

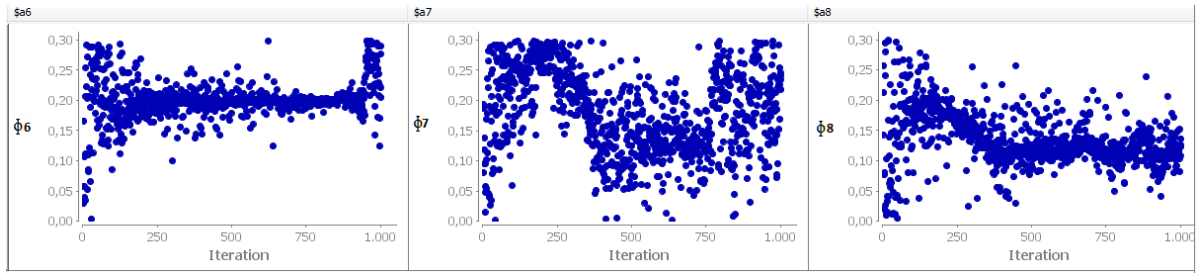


Figure E 5:Parameter (Porosity) versus Iteration for Heterogeneous K4 Sample

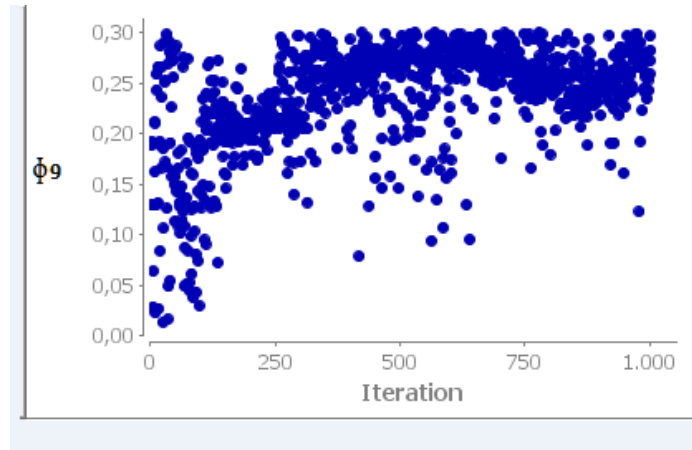


Figure E 6: Parameter (Porosity) versus Iteration for Heterogeneous K4 Sample

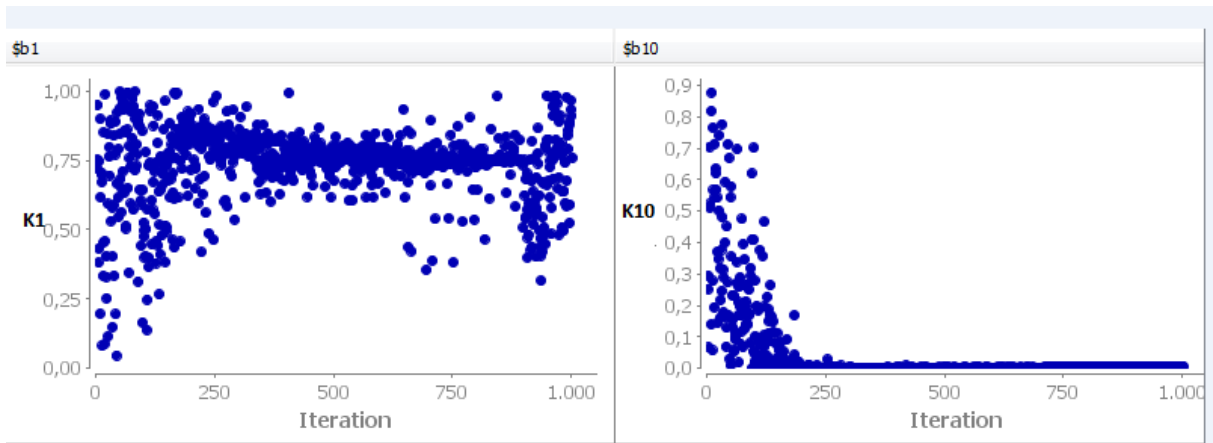


Figure E 7: Parameter (Permeability) versus Iteration for Heterogeneous K4 Sample

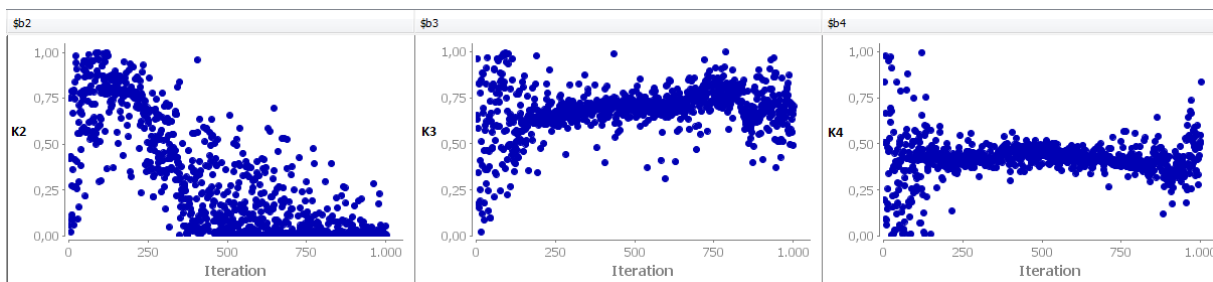


Figure E 8: Parameter (Permeability) versus Iteration for Heterogeneous K4 Sample

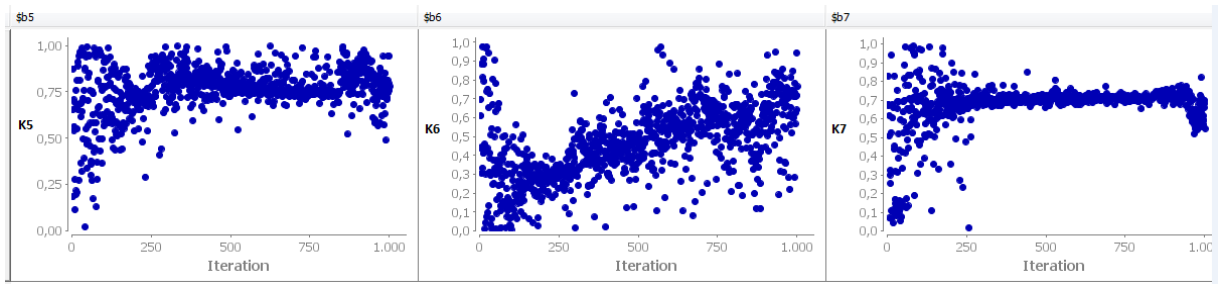


Figure E 9: Parameter (Permeability) versus Iteration for Heterogeneous K4 Sample

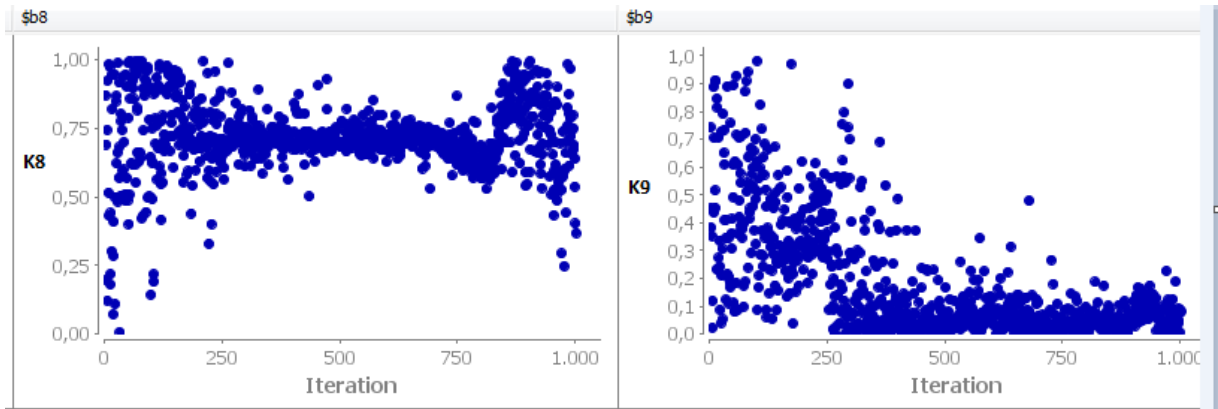


Figure E 10: Parameter (Permeability) versus Iteration for Heterogeneous K4 Sample